Climate Adaption of Rubble Mound Breakwaters

A study to the accuracy of overtopping formulas for combination of solutions

K.P.J. Hogeveen

Technische Universiteit Delft

TU Delft Deltares

Climate Adaption of Rubble Mound Breakwaters

A study to the accuracy of overtopping formulas for combination of solutions

by

K.P.J. Hogeveen

to obtain the degree of Master of Science
at the Delft University of Technology,

In cooperation with:

Deltares
Enabling Delta Life

Student number:	4390199	
Project duration:	December, 2020 – October, 2021	
Thesis committee:	prof. dr. ir. M.R.A. van Gent,	TU Delft and Deltares
	dr. ir. A. Antonini,	TU Delft
	dr. ing. M.Z. Voorendt,	TU Delft
	ir. J.P. den Bieman,	Deltares

TU Delft

Abstract

Rubble mound structures are often constructed to prevent severe wave damage to ships. By constructing the crest at a certain level, the waves are reduced such that safety is ensured. However, a large increase in sea level rise is expected in the next century due to climate change. Because of this, multiple adaptations might be necessary to meet the required lifetime of a rubble mound structure. In current guidelines, the influence of these adaptations is already included. However, for a combination of solutions the empirical equations are not always accurate enough (van Gent, 2019). Accurate guidelines are necessary to correctly predict the overtopping rates for a combination of solutions. In this research, the accuracy of current guidelines is investigated.

The research performed in this thesis is divided into two parts. First, multiple solutions are derived to adapt a breakwater and ensure safety for a rising sea level based on existing empirical equations. Safety is ensured if the mean overtopping rate remains less than 50 l/s/m. Beyond this point, the ships behind the structure might become prone to large wave attacks. Secondly, the accuracy of current guidelines (i.e. the empirical overtopping equations) is tested in an OpenFOAM model. OpenFOAM is a so-called open-source Computational Fluid Dynamics (CFD) software that can solve complex fluid flows.

Several solutions are possible to ensure safety against severe wave overtopping. The four solutions applied in this thesis are the addition of a berm, the addition of a crest wall, an increased foreshore and the implementation of a low-crested structure. By combining these solutions, the overtopping rate remains below the maximum of 50 l/s/m. The combination of solutions forms a path, all paths together form a pathway. The adaptation pathways are a guideline for the moment in time at which a certain solution should be implemented. Therefore, a structure is not unnecessarily expensive and can be managed easily. The paths are rated based on the implementation costs of the combination of solutions.

In total two empirical equations are applied to derive an adaptation pathway. The first pathway is based on the overtopping equation proposed by the TAW (2002). The TAW is a Dutch advisory committee on flood defences. Based on the applied theory, the economically most attractive solution consists of a low-crested structure, a foreshore and a berm. As this equation does not account for the influence of a berm in non-breaking waves, an adapted TAW equation is applied as well. The adapted equation was proposed by Krom (2012) and includes the influence of a berm. Based on the adapted equation, the economically most attractive solution consists of a foreshore, a crest wall and a berm.

Once the economically most attractive solution is derived, the accuracy of current guidelines is reviewed in a phase-resolving model. It is found that, there is a large discrepancy between the results calculated with the empirical equations and the results from the model. As no physical data is applied in this research it is hard to interpret and analyze the exact numbers. Therefore, the relative effect of an adaptation is compared. It is found that in contrast to the TAW overtopping equation for non-breaking waves, a berm decreases the overtopping rate by at least 30% for the case study applied. Furthermore, the current method to account for a crest wall proposed by the TAW overestimates the reduction (73% compared to 40% in OpenFOAM). Finally, it is concluded that the addition of a low-crested structure decreases the overtopping rate by a larger value than based on the applied guidelines (74% in OpenFOAM compared to 35% in theory).

Based on the performed research a realistic combination of the adaptation measures consists of a combination of a berm, a crest wall and a shallow foreshore. Therefore, it is advised to focus further research on the combination of these measures. It is necessary to improve the guidelines for combinations of these adaptation measures since the existing ones seem to be either incorrect (TAW, 2002) or require a better validation (Krom, 2012).

Preface

This thesis has been written as final work for the Master of Science in Hydraulic Engineering at the Delft University of Technology, with a specialisation in Coastal Engineering and Hydraulic Structures. The research that I conducted in the last 9 months is a collaboration between Deltares and the TU Delft. I'm very thankful for the opportunity to write my thesis at such an innovative company as Deltares. The online meetings that I could join were very inspiring.

I would like to thank the people who helped me during this period. First of all, the committee members who were very helpful both in the progress meetings and the personal meetings. I want to thank Joost den Bieman as my daily supervisor. I really appreciate the help during this project. Especially, in the knowledge on OpenFOAM and of course the weekly meetings which were very joyful. I want to thank Marcel van Gent for being chair of this committee and this very relevant subject on climate adaptation. Further I would like to thank Mark Voorendt for his extensive feedback after the progress meetings. This feedback really helped me out in improving the structure of the report. Also, I would like to thank Alessandro Antonini for his knowledge and input during the meetings.

Further, I would like to thank my family for their support during my period at the Delft University of Technology. Last but not least, I would like to thank my friends. Especially Daniel and Jesse, who helped me out with the last details in this report.

I hope all the readers find this such a relevant and interesting research as I did. Enjoy!

K.P.J. Hogeveen
Delft, October 2021

Contents

Abstract i

Preface ii

List of Symbols v

1 Introduction 1
- 1.1 Thesis motivation . . . 1
- 1.2 Problem analysis . . . 2
- 1.3 Objective and scope . . . 3
- 1.4 Research questions . . . 3
- 1.5 Methodology . . . 4
- 1.6 Outline of the thesis . . . 5

2 Theoretical background 6
- 2.1 Failure mechanisms of a rubble mound breakwater . . . 6
- 2.2 Adaptive approach . . . 7
- 2.3 Hydraulic boundary conditions . . . 9
- 2.4 Wave overtopping of a rubble mound breakwater . . . 11
- 2.5 Stability of rubble mound structures . . . 16
- 2.6 Effects climate change on a rubble mound structure . . . 18
- 2.7 Conclusion on applied theory . . . 18

3 Description of the Academic Case 20
- 3.1 Academic Case study . . . 20
- 3.2 Summary of the main dimensions . . . 24

4 Adaptive Pathways for Rubble Mound Breakwaters 26
- 4.1 Selection of adaptation pathways . . . 26
- 4.2 Tipping points different adaptations . . . 27
- 4.3 Cost estimation different solutions . . . 29
- 4.4 Results of the adaptation pathways . . . 30
- 4.5 Application of a machine learning tool . . . 35
- 4.6 Conclusion on the adaptation pathways . . . 36

5 Set-up OpenFOAM model 39
- 5.1 Description of the OpenFOAM model . . . 39
- 5.2 Theoretical aspects of the OpenFOAM model . . . 40
- 5.3 Model set-up . . . 44
- 5.4 Set-up adaptation measures . . . 46
- 5.5 Calibration of the numerical model . . . 47
- 5.6 Conclusions on the applied and configured OpenFOAM model . . . 51

6 Application of adaptive pathways in OpenFOAM 53
- 6.1 OpenFOAM . . . 53
- 6.2 Evaluated combination of solutions in OpenFOAM . . . 54
- 6.3 Solution: Berm - Crest wall - Low-crested structure . . . 54
- 6.4 Effect of adaptations . . . 59
- 6.5 Accuracy Adapted TAW . . . 60
- 6.6 Conclusion on the OpenFOAM computations . . . 62

7 Discussion **64**
7.1 Applied theory . . . 64
7.2 Hydraulic and structural assumptions . . . 64
7.3 Applied case study . . . 65
7.4 Applied data . . . 65
7.5 Applicability adaptation pathways . . . 65
7.6 Applicability on different structures . . . 66

8 Conclusions and Recommendations **67**
8.1 Conclusions . . . 67
8.2 Recommendations . . . 69

References **73**

Appendices **74**

A Individual Adaptation Pathways **75**

B OpenFOAM results case study 2 **83**

List of Symbols

B_{berm}	Width of the berm	[m]
C	Courant number	[-]
C_m	Added mass coefficient	[-]
D_{n50}	Median nominal diameter	[m]
d	Water depth	[m]
d_b	Height berm relative to still water level	[m]
g	Gravitational acceleration=9.81m/s^2	[m/s^2]
H	Wave height	[m]
$H_{2\%}$	Significant wave height exceeded by 2% of the incoming waves	[m]
H_{m0}	Spectral significant wave height	[m]
$H_{m0,t}$	Transmitted spectral significant wave height	[m]
H_s	Significant wave height	[m]
h	Water depth	[m]
KC	Keulegan-Carpenter number	[-]
K_t	Transmission coefficient (H_t/H_i)	[-]
k	Wave number ($2\pi/L$)	[rad/m]
L_0	Deep water wave length	[m]
L_{berm}	Length of the berm	[m]
N	Number of waves	[-]
n	Porosity	[-]
q	Mean overtopping discharge	[l/s/m]
q_{max}	Maximum allowed mean overtopping discharge	[l/s/m]
R_c	Crest height	[m]
$R_{u,2\%}$	Run-up exceeded by 2% of the incoming waves	[m]
r_b	Influence berm width	[-]
r_{db}	Influence berm depth	[-]
S	Damage number≈2	[-]
s_0	Wave steepness	[-]
$T_{m-1,0}$	Spectral mean period (m_{-1}/m_0)	[s]
T_s	Peak period	[s]
α	Slope of structure	[degree]
α	Laminar closure coefficient porous media	[-]
β	Angle of incident of the waves	[degree]
β	Turbulent closure coefficient porous media	[-]
γ	Peak enhancement factor	[-]
γ_b	Influence factor berm	[-]
γ_f	Influence factor roughness	[-]
$\gamma_{f,surging}$	Influence factor roughness for surging waves	[-]
γ_v	Influence factor crest wall	[-]
γ_β	Influence angle of wave attack	[-]
Δ	Relative buoyant density ((ρ_s-ρ_w)/ρ_w≈1.58)	[-]
η	Surface elevation	[m]
ρ_s	Density rock layer ≈2650 kg/m^3	[kg/m^3]
ρ_w	Density water ≈1025 kg/m^3	[kg/m^3]
$\xi_{m-1,0}$	Breaker parameter	[-]
ω	Wave frequency ($2\pi/T$)	[rad/s]

1 Introduction

1.1. Thesis motivation

One of the challenges in the civil engineering world for coastal protections in the coming century is to cope with sea level rise. Some structural adaptations might be required to ensure their functionality and fulfill the expected lifetime. For example rubble mound structures, many port areas depend on these structures and significant damage due to wave attack could occur if too many waves transmit or overtop the rubble mound breakwater. In Figure 1.1 an example of wave overtopping for a breakwater structure is presented.

Figure 1.1: Wave overtopping of a breakwater (credits: Liz Mackney)

Figure 1.2 presents the predicted sea level rise for the next century. Notably, the uncertainty included in the predictions increases over time. At the end of the century, the bandwidth of the most extreme case is more than two meters. Due to the large uncertainty, sea level rise is a difficult parameter to include in the design of structures. Costs might be unnecessarily high if a much lower sea level rise occurs than designed for. The increase of uncertainty in the predictions after 2050 is partly due to the melt process of the ice in Antarctica. This process depends among others on the emission rates. The most extreme case in the figure refers to the highest Representative Concentration Pathway (RCP) scenario adopted by the IPCC (2014), which happens if emissions do not stop rising before the end of the century. The milder RCP4.5 scenario requires the emissions to stop rising after 2050 to limit the effects on nature. The Deltascenario is currently applied in The Netherlands and is based on the KNMI'14 predictions with a maximum sea level rise of 1 meter in 2100. However, this prediction does not include the latest predictions on the melting of ice in Antarctica (Deltares 2018). In 2023 new predictions of the KNMI are expected that include the faster melt of ice in the Arctics based on the IPCC rapport. Besides the melting process on the Arctics as an uncertain factor, many different models predict climate change based on different input parameters. All things considered, sea level rise is a difficult parameter to include in the design phase of structures.

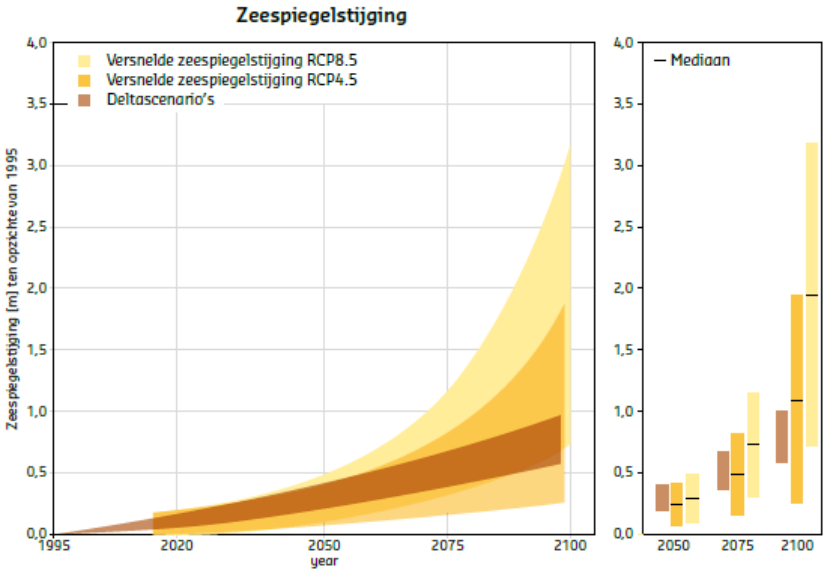

Figure 1.2: Predicted sea level rise until the year 2100 (Deltares 2018)

Several solutions are possible to account for sea level rise in the design and maintenance of coastal structures in the next decades. Due to the large uncertainty in sea level rise, an adaptive approach is required as costs for flood defences might be unnecessarily high if the sea level rise is not as high as expected (van Gent, 2019). In this research, this adaptive approach is applied to rubble mound breakwaters. Breakwaters are used for several purposes, but the main function is damping waves for navigation routes and port areas. This function is lost or decreases if the sea level rise is larger than currently designed for.

1.2. Problem analysis

The main issue caused by sea level rise for rubble mound breakwaters is the increased overtopping discharge such that the effectiveness of the breakwater decreases. To adapt and protect such a structure several solutions that limit the overtopping discharge are possible, for example: create a shallow foreshore, add a crest wall or add a berm. For each of these solutions, a guideline already exists and can be found either in the Rock manual (Rock Manual 2007) or in a technical report of the TAW (Dutch advisory committee on flood defence) (TAW 2002). However, an individual solution is limited by certain dimensions to prevent cost-inefficient designs. In extreme cases where one solution is not sufficient to protect against climate change or at the point from which a combination of solutions is economically more beneficial, the solutions should be combined to ensure the functionality of the breakwater. In recent research conducted by Deltares, the combination of these solutions were applied on coastal dikes (Deltares 2019). The different solutions were combined into an adaptive pathway scheme to see until which amount of sea level rise the individual solution is possible. Subsequently, for different amounts of sea level rise, the economically most attractive combinations were estimated. The rubble mound structure assessed in this thesis is very similar to the coastal dike. Therefore, almost the same solutions apply. Possible adaptation methods against sea level rise for rubble mound structures:

- *The addition of a berm*
- *The addition of a crest wall*
- *The addition of a shallow foreshore*
- *The addition of a low-crested structure in front of the breakwater*
- *Increasing the roughness*

All the possible solutions that are summed up previously influence the overtopping rate. A crest wall limits the amount of overtopping by increasing the crest height but, without increasing the footprint. To

limit the wave impact on a crest wall, the wall should not be too high. Also, from an aesthetic point of view, this is not attractive as it blocks the view. Due to the shallow foreshore or the addition of a berm, the waves start to break. Consequently, the wave overtopping decreases. The roughness of a rubble mound breakwater is more or less given by its stability requirement and therefore not elaborated further in this thesis. Low-crested structures in front of the breakwater decrease the wave height by transmitting a fraction of the offshore wave height.

The previous described adaptations influences the wave overtopping. However, these adaptations separately are only feasible until a certain amount of sea level rise, depending among others on costs or constructability. For example, the wave load on a crest wall should not be too big. If a certain solution is no longer feasible, solutions are combined. For these combinations of solutions, empirical formulas are available with corresponding influence factors. However, due to a lack of research, these empirical formulas are not always able to deal with such a combination of adaptation methods and therefore further research is necessary. For example in the research of Chen (2020), in which the berm and increased roughness for a dike were combined and validated against empirical formulas proposed in the TAW 2002 and EurOtop 2007. These manuals state that the equations are valid for such combinations, but seem not to be accurate enough for these combinations and Chen proposed a new equation to deal with such combinations.

1.3. Objective and scope

1.3.1. Objective

The objective of this research is to elaborate on several relevant combinations of adaptation solutions that limit wave overtopping at rubble mound breakwaters, where the sequence of solutions with lack of validation in current guidelines is computed in a numerical model to enhance insight into the accuracy of those combinations.

1.3.2. Scope

The hydraulic conditions applied in this thesis remain constant during a rising sea level. Theoretically, the wave height might increase for a large water depth (i.e. decrease of depth limited conditions). For the design of a rubble mound structure multiple criteria should be checked. As this research investigates solutions that limit the amount of overtopping, the stability of the structure is assumed as sufficient for different wave heights and water levels. With this assumption, the focus of this study is completely on the wave overtopping and corresponding theoretical guidelines.

1.4. Research questions

The research questions elaborated in this thesis, taken the objective and scope into account, are formulated as:

1. *What sequence of solutions is economically beneficial according to the adaptation pathways by limiting wave overtopping of rubble mound breakwaters against sea level rise?*
2. *How do the relevant combinations of solutions perform in the numerical model if the outcome is compared to the current guidelines?*

Together, these two research questions sum up the main purpose, the objective, of this research. The next section explains the methodology used to answer the objective and research questions in more detail.

1.5. Methodology

This section describes the structure of the thesis and how the previous stated research questions are answered in the next chapters. The first two steps describe the background information required to answer the research questions. At step three, the first research question is answered. At step five, the second research question is answered.

1.) Describe the theory of rubble mound breakwaters regarding functionality and possible adaptation methods.
The used literature to obtain results on the stated research questions is described in Chapter 2. First, a brief introduction to the functionality of a breakwater is given, where the functionality in this thesis depends on the overtopping rate. Additionally, some literature on an adaptive approach is studied. Multiple adaptation possibilities could be implemented to reduce the wave overtopping and preserve the functionality of the breakwater. These individual solutions and their empirical formulas are explained as well. The applied guidelines form the basis of this thesis and are used to derive adaptation pathways in Chapter 4.

2.) Describe academic case studies
The academic or fictive case study to apply and test the accuracy of current guidelines is explained in Chapter 3. The application of current guidelines is performed in Chapter 4 and the accuracy is evaluated in Chapter 5 and 6. The description of the academic case study includes hydrodynamics, bathymetry and a stability assessment. As the case study is an academic one, the location does not represent a real structure. However, the derived conditions are based on realistic values. In total two different case studies are evaluated. Both case studies are based on the applied theory and are derived such that the overtopping rate is 50 l/s/m. The case studies are required to derive adaptation pathways in Chapter 4.

3.) Evaluate possible adaptation pathways
Chapter 4 elaborates the adaptation pathways based on the empirical equations, the academic case studies and the amount of sea level rise. As the sea level rise has a large uncertainty, especially for predictions far in time, such an adaptive approach is necessary to enhance management strategies during the lifetime of a rubble mound structure. To derive the optimal solution based on the adaptive pathways, the costs for the different solutions are compared. Finally, based on these costs, the first research questions is answered.

4.) Set-up OpenFOAM model for the verification of relevant solutions
In Chapter 5, the set-up of the numerical model to verify the accuracy of current guidelines is described, including some configuration and theoretical aspects. The correct configuration of hydrodynamics is important as no experimental data is available. Once the model is configured for the prevailing wave conditions, one by one the adaptations according to the most interesting path are implemented in the model.

5.) Verify the accuracy of current guidelines for the relevant solutions in a numerical model
Subsequently, in Chapter 6, the most interesting adaptation strategy is computed in the OpenFOAM model. The results are compared with the results from the empirical formulas. Depending on the accuracy of those equations, a certain strategy can become more or less economically attractive. Finally, the second research question is answered in this chapter.

1.6. Outline of the thesis

The previous is combined into the following flowchart (Figure 1.3). This flowchart gives an overview of the outline of the thesis.

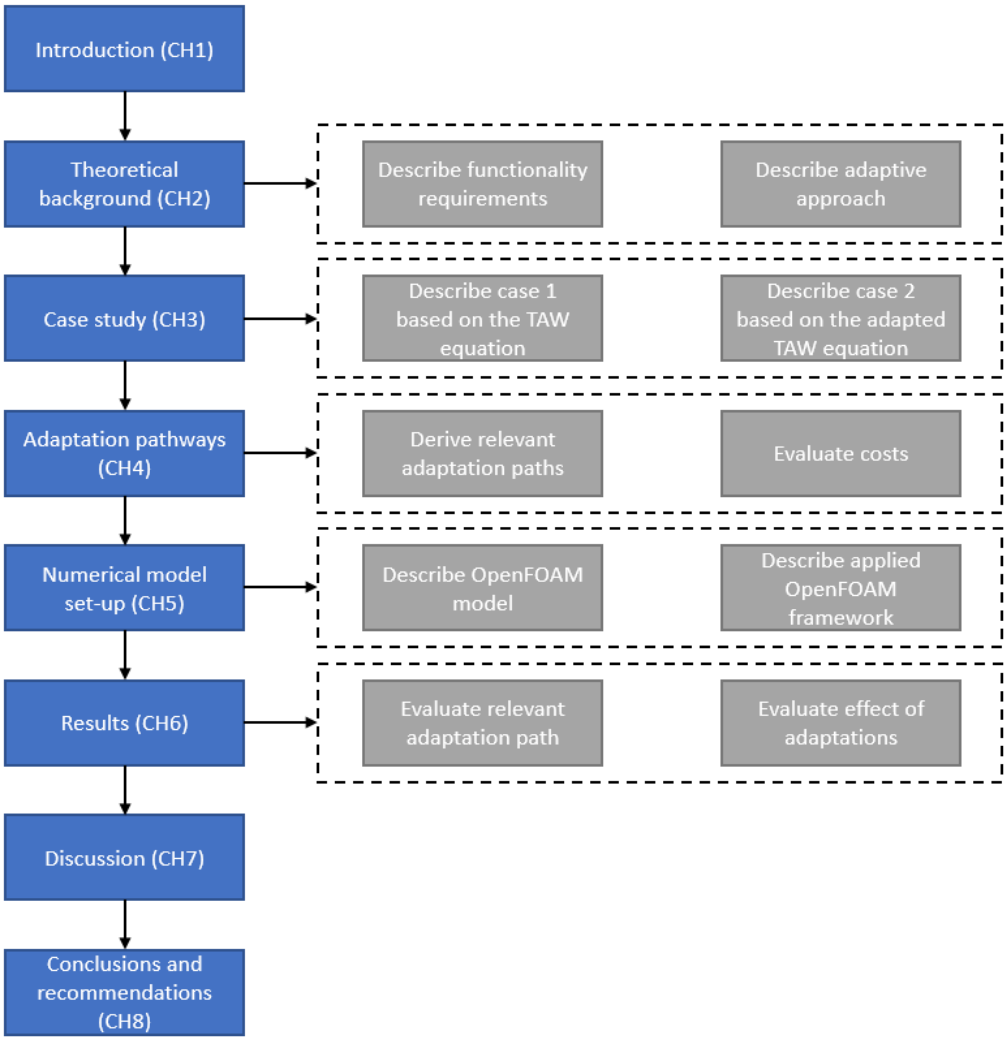

Figure 1.3: Flowchart overall overview thesis

2

Theoretical background

In this chapter, the first step of the methodology is performed. The step includes a literature review that describes the basic conditions for the remaining part of this report. First, the functionality of a rubble mound structure and the adaptive approach are described. Additionally, the type of hydraulic conditions that influence the functionality of a breakwater is briefly investigated. Subsequently, the possible adaptations which can be implemented to reduce wave overtopping are investigated. With the empirical overtopping equations, an adaptation pathway has been made in Chapter 4. Furthermore, the influence of sea level rise on the hydraulic and structural conditions is investigated briefly in the last section.

2.1. Failure mechanisms of a rubble mound breakwater

The stability of a rubble mound structure depends on multiple criteria as can be seen in Figure 2.1. The failure mechanisms are divided into two categories, the geotechnical conditions and the wave conditions (Rock Manual 2007). The latter are considered as normative in this research and particularly wave overtopping as all adaptation measures are tested against wave overtopping in Chapter 4. Only for the assessment of the case study and the low-crested structure, stability is also taken into account. The wave action failure causes toe erosion, wave impact damage, crest erosion and leeside damage due to overtopping. Too much overtopping causes significant damage to vessels in the port protected by the rubble mound structure. The other criteria depend on the stability of the rock protection. The stability of the structure is a ratio between the wave load (H) and the strength, the relative density of the armour layer (ΔD). Typical values for stability ($H/\Delta D$) of the armour layer of a rubble mound structure vary between 1 and 4. Therefore, the structure is statically stable (Rock Manual 2007).

As explained above, the stability for the case study and low-crested structure is calculated later on in the report. For the case study derived in Chapter 3 a stability calculation has been performed to give some realistic values. The derived stone sizes are assumed as stable in the remaining part of the thesis where sea level rise becomes important. To estimate the costs of the low-crested structure a stability calculation is necessary to determine the rock sizes.

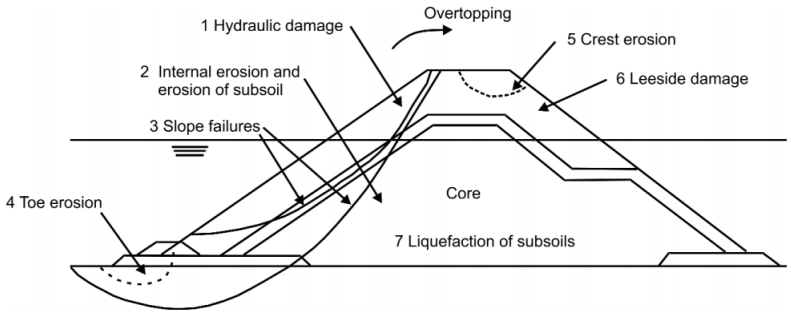

Figure 2.1: Failure modes for a rubble mound breakwater (Rock Manual 2007)

2.2. Adaptive approach

2.2.1. Adaptive approach in general

With the large uncertainty of sea level rise in the future (see Figure 1.2), it is a difficult condition to take into account when designing a structure. An underestimated rise could significantly decrease the design lifetime and as a consequence, the costs increase to meet the safety requirements again (Deltares 2019). Likewise, an over-dimensioned design is not beneficial for the costs. To deal with such difficulties an adaptive approach has been developed (Walker et al., 2001). In Figure 2.2 such an approach can be seen, the first four steps are elaborated in this thesis.

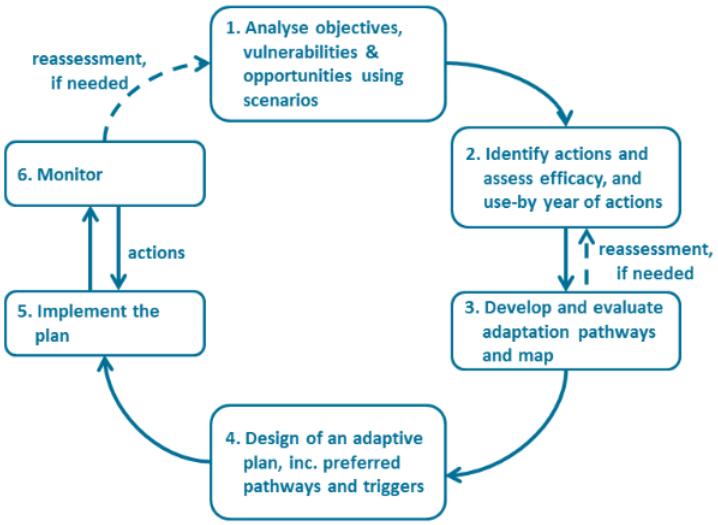

Figure 2.2: Dynamic adaptive policy pathways approach (Haasnoot et al., 2013)

An adaptive approach can deal with large uncertainties in contrast to the classical top-down approach. The top-down approach uses a certain amount of sea level rise according to a scenario. If a type of construction does no longer meets the safety requirements, this cycle is repeated with corresponding adaptation measures. The adaptation tipping point approach, which is more or less a bottom-up approach that starts with how much sea level rise the current strategy can deal with (Kwadijk et al., 2010). If the sea level rise is bigger than currently designed for, other strategies are available in advance to adapt the structure which makes it easier for policymakers. The so-called tipping point is the point at which a certain solution is no longer meeting the objective (Haasnoot et al., 2013). If this happens the next stage is reached and the structure needs adaptation to cope with the increased sea level rise. In Figure 2.3 on the next page, a summary of the above is shown in a scheme.

2.2.2. Application of the Adaptation pathways

Due to the largely uncertain sea level rise, adaptive approaches become much more relevant and the managing process of a certain coastal structure can vary throughout the lifetime of the structure. This decreases the construction costs compared to the classical approach, in which structures can be very expensive if the sea level rise is overestimated.

In the adaptive approach multiple solutions together form a pathway. In total, different paths are elaborated to ensure safety until a maximum defined sea level rise. In Figure 2.4 an example of such an adaptation pathway for dikes is shown, where the vertical lines (|) at the end of a solution represent the point at which the current strategy is no longer feasible. The circles or so-called tipping points represent the point at which other solutions are necessary to preserve the function of the structure.

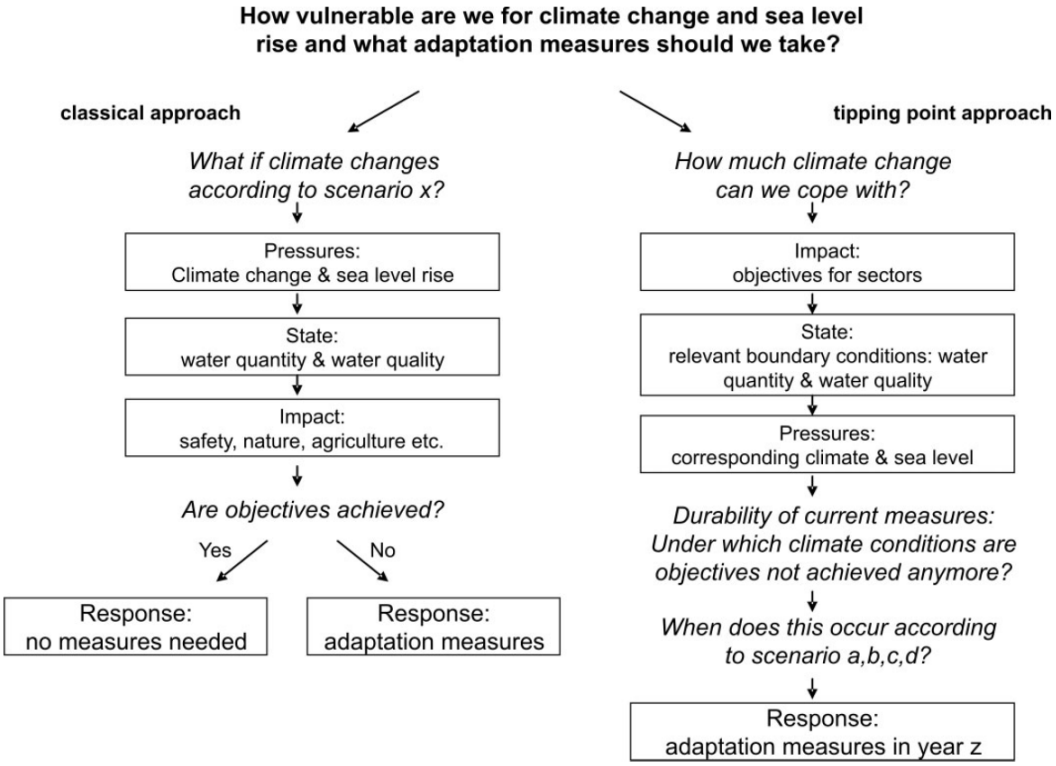

Figure 2.3: The classical approach versus the Tipping point approach (Kwadijk et al., 2010)

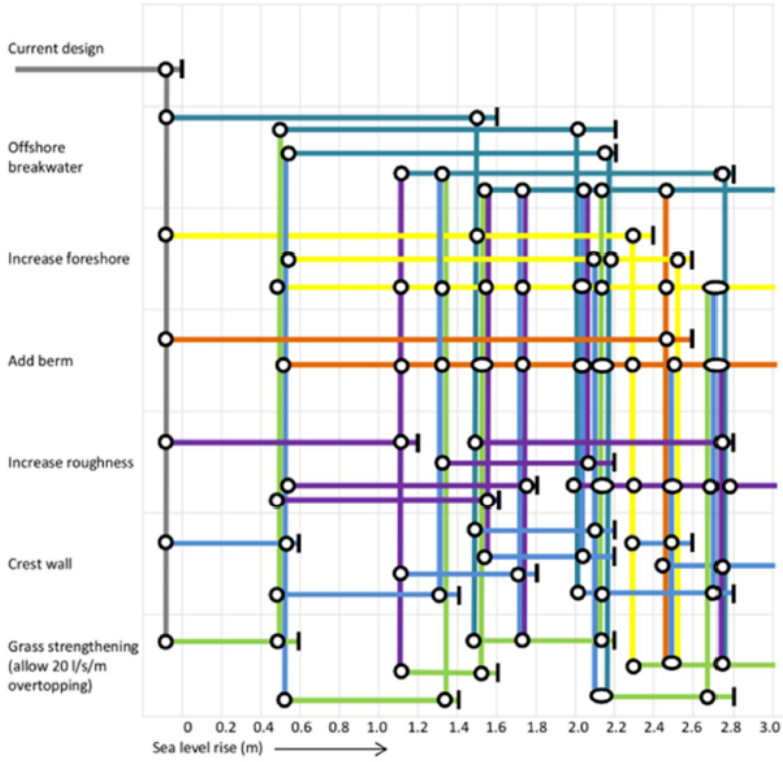

Figure 2.4: Example of possible climate adaptation pathways for dikes (Deltares 2019)

2.3. Hydraulic boundary conditions

The waves that approach the structure depend on multiple factors and thus some basic information on waves is given. For different types of waves, different empirical formulas should be used to correctly predict the overtopping discharge.

2.3.1. Wave spectrum

In a spectral analysis, all amplitudes and phases for each frequency are found by using for example a Fourier analysis. With the amplitudes summed up for each frequency, an energy spectrum is derived corresponding to the sea-state investigated. In the spectrum, the spectral significant wave height is defined as: $H_{m0} = 4\sqrt{m_0}$ such that in deep water: $H_{m0} = H_s$. If the moments are elaborated the spectral period is defined as $T_{m-1,0}$, a commonly used wave period to emphasize the longer waves in design formulas. For single peaked spectra, a relation between the peak period and spectral period exists ($T_{m-1,0} = T_p/1.1$). The peak period corresponds to the highest peak in the spectrum and only defines a certain moment of the wave. To include the complete spectrum often the mean period ($T_{m-1,0}$) is used in design formulas especially when bimodal or very flat spectra occur (Rock Manual 2007).

The two most used spectra are Pierson-Moskowitz and JONSWAP, they both contain amplitudes and frequencies of the waves in their formula based on wind and water conditions. The Pierson-Moskowitz spectrum describes a fully developed deep water sea state. The JONSWAP spectrum, based on the Pierson-Moskowitz spectrum describes a growing or fetch limited sea and includes a peak enhancement factor (γ). If this factor is one, the spectrum describes a Pierson-Moskowitz spectrum, a higher factor gives a higher peak frequency. The average peak enhancement factor for a JONSWAP spectrum is 3.3.

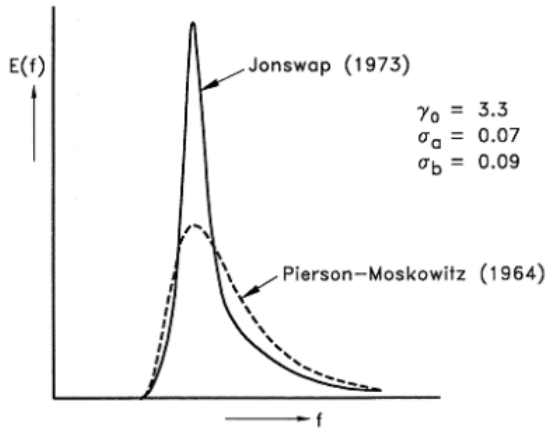

Figure 2.5: Difference between JONSWAP and Pierson-Moskowitz spectrum (Holthuijsen, 2007)

2.3.2. Wave steepness

The wave steepness defines the state of the sea, typical values for swell seas are less than 0.01. For steeper waves, like the wind waves, the steepness varies between 0.04-0.06. It is also called the fictitious wave steepness as the wave height at the toe of the structure and the deepwater wavelength are investigated and thus not the actual wavelength. Subsequently, with the deepwater wavelength the influence of the wave period on the structure is defined and is used in design formulas (EurOtop2007). The wave steepness is elaborated based on Equation 2.1, the deepwater wavelength (L_0) is defined in Equation 2.2.

$$s_0 = \frac{H_{m0}}{L_0} \tag{2.1}$$

$$L_0 = \frac{g \cdot T_{m-1,0}^2}{2 \cdot \pi} \tag{2.2}$$

2.3.3. Breaker parameter

The Iribarren number or breaker parameter is used to evaluate different types of wave breaking, depending on the wave steepness (s_0) and the slope of the structure (α). See, Equation 2.3. Four types of waves are classified using the Iribarren number (Battjes, 1974): Spilling waves ($\xi_{m-1,0} < 0.3$), Plunging waves ($0.5 < \xi_{m-1,0} < 3$), Collapsing waves ($\xi_{m-1,0} = 3$) and Surging waves ($\xi_{m-1,0} > 3$). If the breaker parameter is smaller than a value between 2.0 and 2.5 waves are considered as breaking, for a higher breaker parameter waves are non-breaking (TAW 2002). As the transition between the different types of breaking is gradual, the values for the breaker parameter are indications.

$$\xi_{m-1,0} = \frac{\tan(\alpha)}{\sqrt{H_{m0}/L_{m-1,0}}} \tag{2.3}$$

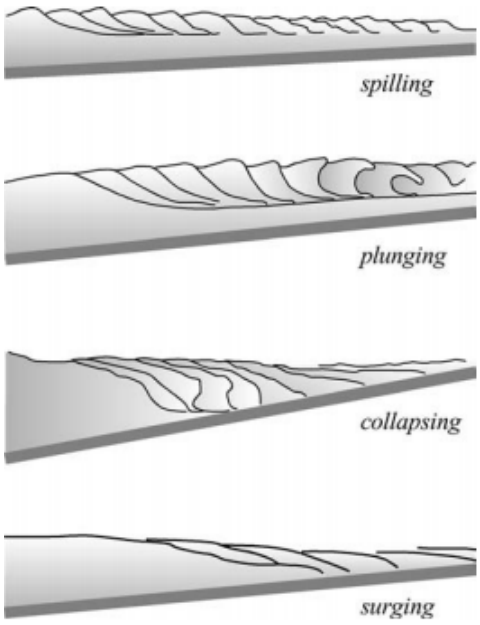

Figure 2.6: Breaker types (Holthuijsen, 2007)

2.3.4. Wave height in shallow water

For the transformation of waves from deep to shallow water, often a model like Swan is used to predict the wave statistics near-shore. For the assessment of the wave height near-shore, some empirical formulas have been derived as well. Like in formulas proposed by Battjes and Goda in which information of water depth and the slope of the foreshore is necessary. In the work presented by Goda (Goda 2000) graphs for different types of wave steepnesses are presented to determine the wave height near-shore. However, as a rule of thumb for mildly sloping foreshores with irregular waves, Equation 2.4 presents as a good estimation of the wave height at the toe of the structure if significant wave data is not available.

$$H_{s,max} = \frac{h_{toe}}{2} \tag{2.4}$$

As waves approach the toe of the structure, the wave height decreases due to depth limited conditions, but for shallow water conditions the wave period ($T_{m-1,0}$) remains more or less the same. If very shallow conditions prevail ($h/H_{m0,deep} < 1$), the wave spectrum is flattening and the spectral period becomes much longer due to wave breaking and the presence of long infra-gravity waves (EurOtop 2007).

2.4. Wave overtopping of a rubble mound breakwater

The overtopping discharge is one of the normative conditions for the design height of the crest. To ensure enough safety during storm conditions this discharge should be limited. At dikes with a good grass slope on the crest and leeside, the overtopping discharge can be larger than 10 l/s/m (TAW 2002) without serious damage. For dikes with poor grass protection erosion is easily possible. Consequently, this value should be much lower to prevent damage due to wave overtopping. Impermeable dikes also experience more load due to an increasing water level. Because of better stability at rubble mound breakwaters, overtopping discharges until 200 l/s/m are possible. However, this overtopping rate would not ensure safety to the vessels behind and therefore an overtopping discharge of 50 l/s/m is the maximum. Beyond this point, significant damage to smaller vessels has been observed (EurOtop 2007).

2.4.1. TAW and EurOtop 2007

The TAW manual proposes Equation 2.5 as overtopping formula for the assessment of rubble mound structures. The mean equations are used to compare the empirical formulas with the results computed in OpenFOAM later on in this thesis as the deterministic equations already contain some conservatism. While EurOtop 2018 is available as well at the moment, the older version (EurOtop 2007), which is based on TAW is used. In recent research (den Bieman et al., 2020) the EurOtop 2018 proved to be less accurate than the TAW for different data sets. The difference between EurOtop 2007 and 2018 is mainly in the part for a low R_c/H ratio. In which the older formula predicts a larger overtopping.

$$\frac{q}{\sqrt{g \cdot H_{m0}^3}} = \frac{0.067}{\sqrt{\tan\alpha}} \cdot \gamma_b \cdot \xi_{m-1,0} \cdot \exp\left(-4.75 \frac{R_c}{\xi_{m-1,0} \cdot H_{m0} \cdot \gamma_b \cdot \gamma_f \cdot \gamma_\beta \cdot \gamma_v}\right)$$
$$\text{With a maximum of: } \frac{q}{\sqrt{g \cdot H_{m0}^3}} = 0.2 \cdot \exp\left(-2.6 \frac{R_c}{H_{m0} \cdot \gamma_f \cdot \gamma_\beta}\right) \tag{2.5}$$

With:

$q =$	Overtopping discharge	[l/s/m]
$g =$	Gravitational acceleration (=9.81)	[m/s^2]
$H_{m0} =$	Spectral wave height	[m]
$R_c =$	Crest height	[m]
$\gamma_f =$	Influence factor roughness (≈ 0.40)	[-]
$\gamma_\beta =$	Influence angle of wave attack	[-]
$\gamma_b =$	Influence factor berm	[-]
$\gamma_v =$	Influence factor wave wall	[-]

The roughness for a rubble mound structure with two layers and a permeable core is defined as 0.4 (EurOtop 2007). The influence of oblique waves is described as:

$$\gamma_\beta = 1 - 0.0063 \cdot \beta \tag{2.6}$$

Equation 2.6 is used for wave angles (β) $\leq 80°$. For more oblique waves between 80°and 110°an obliqueness of 80°should be used. For even larger wave angles the waves will not reach the structure and thus is the influence factor one.

Yet, a simple breakwater construction is not always sufficient to reduce wave overtopping without extremely high crest heights as sea level rise should be taken into account. For this purpose, several adaptation measures are possible to reduce the overtopping rate as is presented later on in this chapter. Figure 2.7 shows the conceptual design of a two-layer rubble mound breakwater.

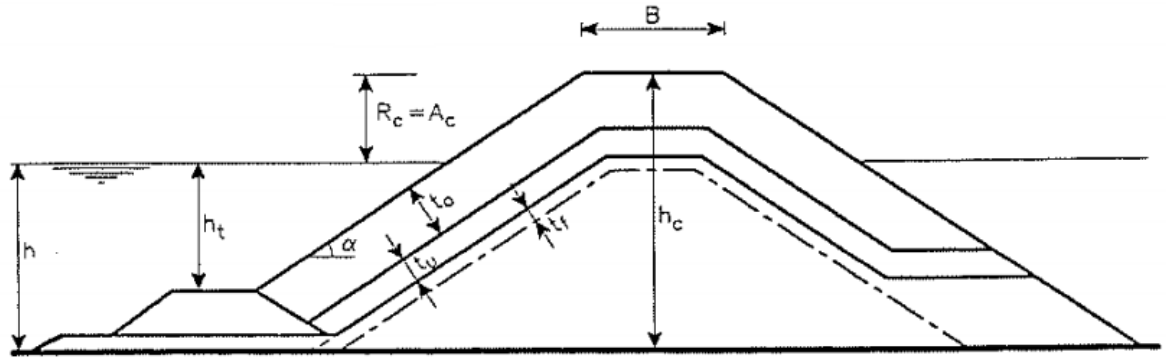

Figure 2.7: Cross-section rubble mound breakwater (van der Meer, 1995)

2.4.2. Adapted TAW equation

Often the slope of the rubble mound breakwaters is steep enough such that the maximum equation for non-breaking waves should be used. According to the equation as stated in the TAW or EurOtop (2.5) there is no influence of a berm in front of the breakwater. Also, the steepness of the structure and the waves is not accounted for in the equation as the breaker parameter ($\xi_{m-1,0}$) is missing. The latter was investigated by Lioutas (2010,2012), in the MSc thesis, the influence of different steepnesses for both the structure and waves were investigated. Because the steepness indeed had an influence on the outcome of the tests and differed from the TAW equation an adapted version of the TAW equation was proposed to include the steepness (See Equation 2.7).

$$\frac{q}{\sqrt{g \cdot H_{m0}^3}} = (0.2 - 0.133 \cdot k) \cdot \left(\frac{\gamma_b \cdot \xi_{m-1,0}}{\sqrt{\tan \alpha}} \right)^k \exp\left(-(2.6 + 2.15 \cdot k) \frac{R_c}{H_{m0}} \frac{1}{\gamma_f \cdot \gamma_\beta \cdot (\gamma_b \cdot \gamma_v \cdot \xi_{m-1,0})^k} \right) \quad (2.7)$$

If k is zero the equation is the same as the one for non-breaking waves (Equation 2.5). Likewise, if k is 1 the equation above is the same as the one for breaking waves in the TAW. A value of 0.6 seemed a good fit for the results from the physical model.

However, it was not clear if the influence of the berm is accounted for correctly (to the power k) as there was no berm included. Therefore, in a subsequent MSc thesis by Jan Krom (Krom, 2012) the adapted TAW equation was investigated further in combination with a berm. The adapted TAW equation indeed was a better fit than the original TAW equation for non-breaking waves. However, still some scatter was present. To overcome this, a new expression was proposed as stated in Equation 2.8. This equation is referred to as the adapted TAW expression in the remainder of this thesis.

$$\frac{q}{\sqrt{g \cdot H_{m0}^3}} = 0.2 \cdot \exp\left(-2.6 \cdot \frac{R_c}{H_{m0}} \frac{1}{\gamma_b \cdot \gamma_{f,surging} \cdot \gamma_\beta} \right) \quad (2.8)$$

In the equation above, the influence for both the wave steepness and slope of the structure is included in the influence of the roughness. Because of the limitation of the TAW equation this expression is investigated as well to verify if berms indeed have an influence. Figure 2.8 presents the experimental data used for the fit of the adapted TAW equation.

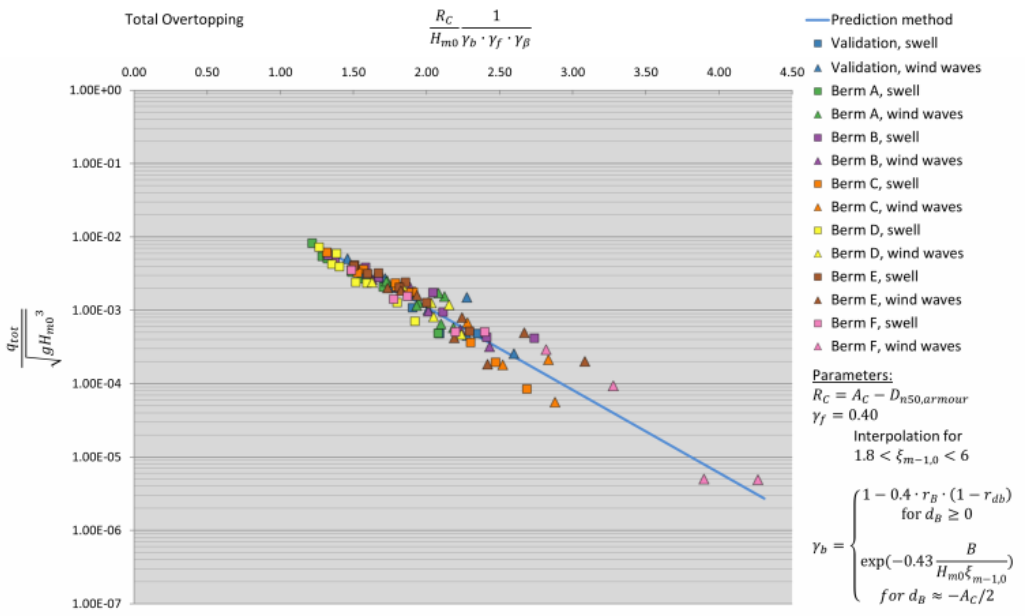

Figure 2.8: Comparison experimental data with the adapted TAW equation (Krom, 2012)

2.4.3. XGB-overtopping

Besides the current guidelines for overtopping, machine learning has become an important tool for the prediction of mean wave overtopping as well. Important data for the prediction of the overtopping consists of more than 10.000 physical model tests obtained in the Clash database (Steendam et al., 2005). Van Gent et al (2007) used this data to develop a neural network tool. This tool is trained to generate the overtopping of a structure in the conceptual design stage. The output overtopping consists of the mean overtopping, including the confidence intervals to give some information about the reliability. More recently, den Bieman et al., 2020 developed a tool that predicts wave overtopping even better than the neural network tool, using the machine learning tool XGBoost. Compared to the current empirical equations the machine learning tool predicts the wave overtopping with higher accuracy.

The XGB-overtopping tool is briefly applied on the elaborated adaptation paths in Chapter 4 to compare the accuracy of current guidelines with a machine learning prediction tool.

2.4.4. Influence roughness

TAW and EurOtop 2007

The roughness of a construction depends on the type of protection used and the porosity of the construction. For a rubble mound structure with 2 layers of rock and a permeable core the influence factor for roughness (γ_f) is proposed as 0.40 in the EurOtop 2007.

Influence roughness Adapted TAW equation

In the equation proposed by Krom, the roughness included is almost the same as the one described in the TAW for surging waves and is repeated here in Equation 2.9.

$$\gamma_{f,surging} = \begin{cases} \gamma_f & \text{for } \xi_{m-1,0} < 1.8 \\ \gamma_f + (\xi_{m-1,0} - 1.8) \cdot \frac{1-\gamma_f}{4.2} & \text{for } 1.8 < \xi_{m-1,0} < 6.0 \\ 1.0 & \text{for } \xi_{m-1,0} > 6.0 \end{cases} \tag{2.9}$$

By applying the equation above, the influence of steepness is included in the overtopping equation for non-breaking waves. For very long waves the roughness does not lead to a reduction of overtopping.

2.4.5. Influence berm

TAW and EurOtop 2007

Berms are often placed to create a more gentle equivalent slope and are placed around the still water

line. Due to this gentler slope, waves are slowed down and can break before the crest of the rubble mound structure has been reached (EurOtop2007). Because rubble mound structures often have a steep slope, the overtopping equation for non-breaking waves is used. Equation 2.5 does not include the influence of a berm. Therefore, the same overtopping discharge is calculated as for the situation without berm. The average slope should be gentle enough such that Equation 2.5 for breaking waves becomes normative for the berm to become influential. The part for breaking waves of Equation 2.5 is repeated here as:

$$\frac{q}{\sqrt{g \cdot H_{m0}^3}} = \frac{0.067}{\sqrt{tan(\alpha)}} \cdot \gamma_b \cdot \xi_{m-1,0} \cdot \exp\left(-4.75 \frac{R_c}{\xi_{m-1,0} \cdot H_{m0} \cdot \gamma_b \cdot \gamma_f \cdot \gamma_\beta \cdot \gamma_v} \right)$$

With:

$\gamma_b =$ Influence factor berm [-]

The influence factor of the berm is described as (TAW 2002):

$$\gamma_b = 1 - r_B(1 - r_{db}) \qquad \text{With } 0.6 \leq \gamma_b \leq 1.0 \tag{2.10}$$

Where r_B is the influence of the berm width and is defined in Equation 2.11. Likewise, the influence of the berm depth (r_{db}) is defined in Equation 2.12

$$r_B = \frac{B_{berm}}{L_{berm}} \tag{2.11}$$

$$r_{db} = \begin{cases} 0.5 - 0.5\cos\left(\pi \frac{d_b}{R_{u2\%}}\right) & \text{for berm above still water line, with: } 0 \leq d_b \leq R_{u2\%} \\ 0.5 - 0.5\cos\left(\pi \frac{d_b}{2 \cdot H_{m0}}\right) & \text{for berm below still water line, with: } 0 \leq d_b \leq 2H_{m0} \end{cases} \tag{2.12}$$

Where:

$B_{berm} =$ Width of the berm [m]
$L_{berm} =$ Length of the berm [m]
$d_b =$ Height berm relative to still water level [m]
$R_{u2\%} =$ Wave run-up height exceeded by 2% of the incoming waves [m]

The maximum run-up is calculated according Equation 2.13. For a first estimation the influence of the berm (γ_b) is one (without berm).

$$\frac{R_{u2\%}}{H_{m0}} = 1.00 \cdot \gamma_b \cdot \gamma_f \cdot \gamma_\beta \left(4.0 - \frac{1.5}{\sqrt{\xi_{m-1,0}}} \right) \tag{2.13}$$

The influence of a berm is maximum ($\gamma_b = 0.6$) if the width is equal to 40% of the length ($B_{berm} = 0.4 \cdot L_{berm}$) and a berm height around still water level ($d_b = 0$). The equations above are applicable for $B < 0.25L_0$, for a longer berm a foreshore is created and therefore interpolation between a berm and a foreshore is advised (TAW 2002).

Influence berm Adapted TAW equation

The influence factor required for the proposed overtopping equation (Equation 2.8) is slightly different than proposed by the TAW. For berms below SWL an extra factor is included. If the berm is above SWL an exponential function was found (Equation 2.14).

$$\gamma_b = \begin{cases} 1 - f_{dB \geq 0} \cdot r_B \cdot (1 - r_{db}), & \text{for } d_B \geq 0 \\ \exp\left(\frac{f_{dB<0} \cdot B}{H_{m0} \cdot \xi m-1,0} \right), & \text{for } \frac{d_B}{A_c} \approx -0.5 \end{cases} \tag{2.14}$$

As only limited research was performed for berms above SWL, linear interpolation between these values is advised if a berm is applied in the adaptation pathways in Chapter 4. The extra factor (f_{dB}) had a value of 0.4 for good fitting (Krom, 2012). The remaining parameters are the same as used in the TAW and are described at the beginning of this section.

2.4.6. Influence crest wall

A crest wall or crown wall is a vertical wall on top of the breakwater and can reduce the overtopping discharge. It is important to realize a crest wall should not be much higher than the crest height as wave impact increases significantly for higher walls. It is advised to use Equation 2.5 again since no empirical formulas for a crest wall are available in the TAW. In this formula, the extra height of the crest wall is included in the crest height (R_c). Figure 2.9 gives an example of such a wave wall.

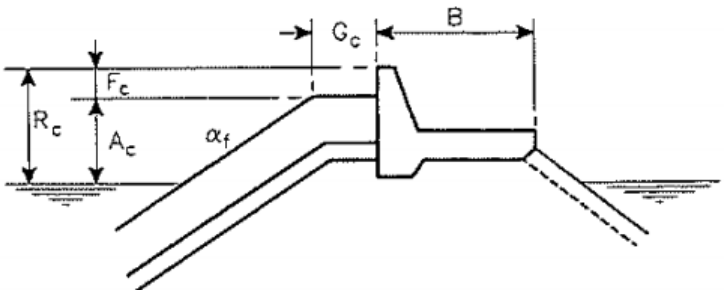

Figure 2.9: Crown wall on top of a rubble mound structure (van der Meer, 1995)

2.4.7. Influence shallow foreshore

When waves approach the foreshore, depth-limited conditions start to play a role. Due to shoaling the wave height increases. On the other hand, waves start to break at a certain depth, the breaking depth (h_B). From this point on waves start to dissipate and lose height, the condition at which waves start to break according to the solitary wave theory is described as follow:

$$h_b = \frac{H_{m0}}{0.78} \tag{2.15}$$

For irregular waves and a lack of wave data the rule of thumb in Equation 2.4 should be used to estimate the significant wave height. As can be seen in Equation 2.15 the wave height reduces significantly for smaller water depths (h). Subsequently, due to a smaller wave height, the overtopping discharge reduces as well. For the transition from deep to shallow water, the wave height decreases but the spectrum stays more or less the same. When a very shallow foreshore is considered this spectrum will change and almost no peak is found anymore (EurOtop 2007).

For the assessment of the wave overtopping two equations should be evaluated depending on the Iribarren number, where the maximum holds for non-breaking waves. If the breaker parameter($\xi_{m-1,0}$) is smaller than 5 Equation 2.16 should be used. For values larger than 7, corresponding to shallow and very shallow foreshores, Equation 2.17 should be used. Between these values interpolation is recommended (TAW 2002).

For $\xi_{m-1,0} < 5$:

$$\frac{q}{\sqrt{g \cdot H_{m0}^3}} = \frac{0.067}{\sqrt{\tan\alpha}} \cdot \gamma_b \cdot \xi_{m-1,0} \cdot \exp\left(-4.75 \frac{R_c}{\xi_{m-1,0} \cdot H_{m0} \cdot \gamma_b \cdot \gamma_f \cdot \gamma_\beta \cdot \gamma_v}\right)$$
$$\text{with a maximum of: } \frac{q}{\sqrt{g \cdot H_{m0}^3}} = 0.2 \cdot \exp\left(-2.6 \frac{R_c}{H_{m0} \cdot \gamma_f \cdot \gamma_\beta \cdot \gamma_v}\right) \tag{2.16}$$

For $\xi_{m-1,0} > 7$:

$$\frac{q}{\sqrt{g \cdot H_{m0}^3}} = 10^{-0.92} \cdot \exp\left(-\frac{R_c}{\gamma_f \cdot \gamma_\beta \cdot H_{m0} \cdot (0.33 + 0.022 \cdot \xi_{m-1,0})}\right) \tag{2.17}$$

With:

$\alpha =$	Seaward slope of the structure	[°]
$\xi_{m-1,0} =$	Breaker parameter	[-]
$\gamma_b =$	Influence factor for a berm	[-]
$\gamma_v =$	Influence factor for a vertical wall	[-]

The minimum length of a foreshore should be at least one wavelength (L_0) (TAW 2002). For values between the maximum length of a berm ($B = 0.25L_0$) and the minimum length of a foreshore, interpolation is advised.

2.4.8. Influence low-crested structure

Low-crested structures like a submerged breakwater change the wave height. When waves travel towards this structure, wave energy dissipates and the wave height decreases. The average wave energy is determined as: $E = 1/8 \cdot \rho_w \cdot g \cdot H^2$. The new and lower wave is called the transmitted wave and is simply expressed in Equation 2.18, depending on the transmitted energy (Rockmanual 2007).

$$K_t = \frac{H_{m0,t}}{H_{m0,i}} \tag{2.18}$$

With:

$K_t =$	Transmission coefficient	[-]
$H_{m0,t} =$	Transmitted significant wave height	[m]
$H_{m0,i} =$	Incident significant wave height	[m]

The transmission coefficient for rubble mound breakwaters has been investigated in the European DELOS project and Equation 2.19 gives a prediction for the transmission. As can be seen does the amount of transmission depends on the wave steepness. Longer waves are often less steep and will increase the transmitted energy.

$$K_t = -0.4\frac{R_c}{H_{m0}} + 0.64\left(\frac{B}{H_{m0}}\right)^{-0.31} \cdot (1 - \exp(-0.5\xi_{op})) \qquad \text{for: } 0.075 \leq K_t \leq 0.8 \tag{2.19}$$

$B =$	Width of the crest	[m]
$\xi_{op} =$	Breaker parameter	[-]

In Briganti (2003) a slightly different formula was proposed for wide structures (B/H_i>10), also based on d'Angremond's formula in Equation 2.19 (d'Angremond et al., 1996), which is applicable for narrow structures (B/H_i<10). Equation 2.20 gives the relation for the transmission coefficient for wider structures.

$$K_t = -0.35\frac{R_c}{H_{m0}} + 0.51\left(\frac{B}{H_{m0}}\right)^{-0.65} \cdot (1 - \exp(-0.41\xi_{op})) \tag{2.20}$$

With an upper limit for Equation 2.19 and Equation 2.20 of:

$$K_{tu} = -0.006\frac{B}{H_t} + 0.93 \tag{2.21}$$

In Figure 2.10 the concept of wave-transmission is shown.

2.5. Stability of rubble mound structures

Because stability has been assessed for the case study and the low-crested structure, a brief description of the used equations has been given in the next sections.

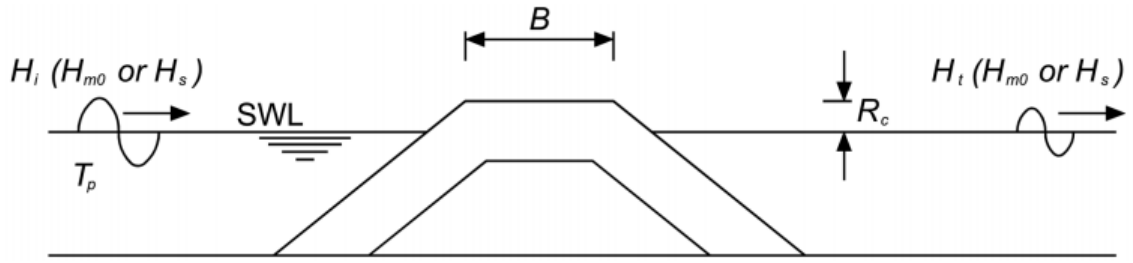

Figure 2.10: Influence low-crested structure on waves (Rock Manual 2007)

2.5.1. Stability of a rubble mound breakwater

As stated in Section 2.1, the stability of a structure depends on the ratio between the load and the strength, (i.e. a higher wave requires a bigger stone size for stability). For rubble mound structures this value is approximately 2 to be statically stable. In the past, different researchers derived empirical formulas for the stability of these structures, all including the ratio between the load and the strength ($H/\Delta D$) on the left-hand side. Hudson (1953) proposed one of the first equations for the stability of the armour layer as:

$$\frac{H}{\Delta D_{n50}} = \sqrt[3]{K_D \cot \alpha} \tag{2.22}$$

With:

$H =$	Wave height at toe of structure	[m]
$D_{n50} =$	Median nominal diameter	[m]
$K_D =$	Damage coefficient	[-]
$\alpha =$	Slope of structure	[-]
$\Delta =$	Relative buoyant density	[-]

Equation 2.22 is tested for non-breaking and non-overtopping waves at the toe of the structure with a slope between $1.5 < \cot \alpha < 4$. As the equation does not include important parameters such as the wave period, permeability and damage level van der Meer (1988) proposed a new empirical equation based on curve-fitting of model tests. One of the limitations for both the Hudson and van der Meer equation is the validation in shallow water. In van Gent et al. 2003 the equations derived by van der Meer were modified such that they are valid for shallow water ($h < 3H_{s,toe}$). As can be seen in Equation 2.23, the required armour layer size depends on the type of wave breaking.

$$\frac{H_s}{\Delta D_{n50}} = c_{pl} \cdot P^{0.18} \left(\frac{S}{\sqrt{N}} \right)^{0.2} \cdot \left(\frac{H_s}{H_{2\%}} \right) \cdot \xi_{m-1,0}^{-0.5} \qquad \text{For plunging waves} \tag{2.23}$$

$$\frac{H_s}{\Delta D_{n50}} = c_s \cdot P^{0.13} \left(\frac{S}{\sqrt{N}} \right)^{0.2} \cdot \left(\frac{H_s}{H_{2\%}} \right) \cdot \sqrt{\cot(\alpha)} \cdot \xi_{m-1,0}^{P} \qquad \text{For surging waves} \tag{2.24}$$

With:

$c_{pl} =$	Fitting parameter plunging waves	[-]
$c_s =$	Fitting parameter surging waves	[-]
$P =$	Notional permeability	[-]
$S =$	Damage level	[-]
$N =$	Number of waves	[-]
$H_{2\%} =$	Wave height exceeded by 2%	[m]

The same research (van Gent et al. 2003) describes a more simplistic equation if significant wave data at the toe is not available. In Equation 2.25 the permeability is defined as the ratio between the core

($D_{n50,c}$) and the armour layer(D_{n50}), the equation has been validated for ratio's between 0 and 0.3.

$$\frac{S}{\sqrt{N}} = \left(0.57 \frac{H_s}{\Delta D_{n50}} \sqrt{\tan(\alpha)} \frac{1}{1 + D_{n50,c}/D_{n50}}\right)^5 \tag{2.25}$$

With:

$D_{n50} =$ Nominal diameter rocks armour layer [m]
$D_{n50,c} =$ Nominal diameter rocks core layer [m]

2.5.2. Stability of a low-crested structure

The stability of a low-crested structure for depth-limited conditions is estimated with a rule of thumb. For depth limited conditions Kramer and Burcharth (2006) provided two estimations. Equation 2.26 is used for emerged structures ($R_c > 0$) and Equation 2.27 for submerged structures ($R_c < 0$). Where the nominal stone size depends on the water depth (h) or the height of the structure relative to the seabed (d).

$$D_{n50} \geq 0.3 \cdot h \tag{2.26}$$

$$D_{n50} \geq 0.3 \cdot d \tag{2.27}$$

In non-depth limited conditions it is assumed that the required stone size is the same as derived for the rubble mound breakwater. For a first estimation these equations provide enough information to determine the costs of a low-crested structure in the adaptive pathway analysis in Chapter 4.

2.6. Effects climate change on a rubble mound structure

As has been explained in Chapter 1 climate change becomes important in the design of many coastal structures. Currently, a safety factor for sea level rise is already included in the design of such structures. However, this value is often high and if the sea level rise does not reach the design level structures are unnecessarily expensive (van Gent, 2019). The rise in water level has also some influence on the hydraulic parameters affecting the rubble mound structure. Due to the rise in water level, the shore becomes less shallow and the maximum wave height possibly increases. For larger wave impact, the required nominal stone size (d_{n50}) to ensure stability could increase as well, depending on the amount of sea level rise and the increase in wave height. For every meter of sea level rise, the wave height could increase by half and thus the overtopping discharge increases too. Likewise, the crest height should also increase proportionally with the increased sea level and wave height. In recent research, these effects of sea level rise on offshore and nearshore wave height are investigated (e.g. Kim and Suh, 2018).

2.7. Conclusion on applied theory

This chapter presents various theory to describe the wave overtopping at rubble mound breakwaters. One of the most famous equations to describe the overtopping was proposed by the TAW (2002). This equation is defined as:

$$\frac{q}{\sqrt{g \cdot H_{m0}^3}} = 0.2 \cdot \exp\left(-2.6 \frac{R_c}{H_{m0} \cdot \gamma_f \cdot \gamma_\beta}\right)$$

Because of the large uncertainty in sea level rise, rubble mound breakwaters possibly need adaptations to ensure safety and limit wave overtopping. Four different adaptations are evaluated in this thesis: a berm, a crest wall, a foreshore and a low-crested structure. The disadvantage of the equation above is the lack of the influence of a berm. Therefore, an adapted TAW equation is investigated as well (Krom, 2012):

$$\frac{q}{\sqrt{g \cdot H_{m0}^3}} = 0.2 \cdot \exp\left(-2.6 \cdot \frac{R_c}{H_{m0}} \frac{1}{\gamma_b \cdot \gamma_{f,surging} \cdot \gamma_\beta}\right)$$

Besides the influence of a berm, the influence of wave steepness is also included in this equation via the roughness coefficient. In both equations, the influence of a crest wall is included by increasing the crest height (R_c) with the height of the wall. Furthermore, the influence of a foreshore is included with a rule of thumb (H/d = 0.5). Finally, the low-crested structure is included based on the transmitted wave height (Briganti et al., 2003).

Based on the empirical equations and adaptations measures described above, an adaptation pathway is derived in Chapter 4. Adaptation pathways are developed to increase the managing strategies of structures under a largely uncertain sea level rise. The tipping points of a solution determine the moment in time at which the next solution should be implemented to ensure safety. By doing so, a structure is not unnecessarily expensive.

3

Description of the Academic Case

This chapter describes the academic case study which is used as starting point for the implementation of the different solutions that decrease the overtopping discharge in Chapter 4. Moreover, the chapter presents the second methodological step. The stability of the structure for the situation without sea level rise is calculated. The stability is assumed as sufficient for the remaining of the report in which sea level rise plays an important role. The academic case is based on hydraulic conditions governing for the Dutch coast and is used to compare the empirical formulas for overtopping defined in Chapter 2 with the numerical model in Chapter 6. A summary of the defined academic case is presented at the end of this chapter. The summary includes a figure and table of all derived parameters. Because two different guidelines for overtopping are investigated, two different case studies are elaborated as well. Both case studies ensure safety until the maximum allowed mean overtopping discharge of 50 l/s/m.

3.1. Academic Case study

The hydraulic conditions derived for the case study are corresponding to conditions for the design lifetime of a breakwater of 50 years. These conditions are derived at Scheveningen, located in the middle part of the Dutch coast. As Scheveningen specifically is not important in this research, this could be any place along the coast. However, a location had to be chosen to define the hydraulic conditions for the academic case. In Figure 3.1, the location used for the derivation of the hydraulic conditions is shown.

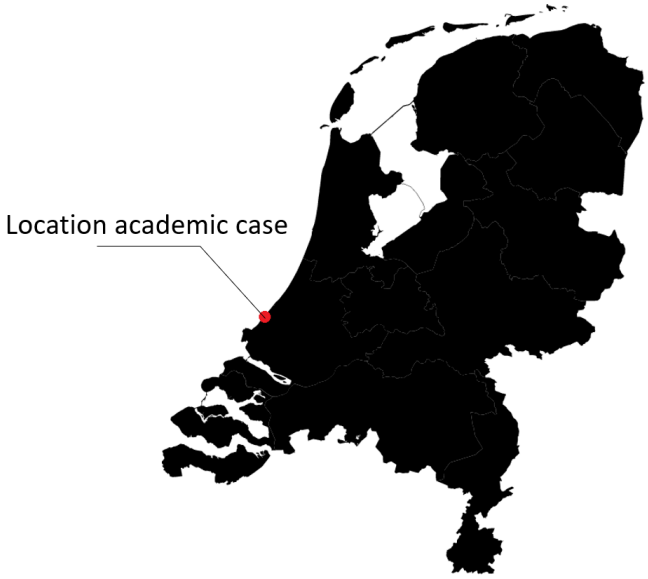

Figure 3.1: Location at which the hydraulic conditions are derived

3.1.1. Hydraulic conditions Scheveningen

For the assessment of the hydraulic conditions in Scheveningen, the probabilistic model HydraNL (HydraNL v2.7) has been used (Input=DEMO_HollandseKust). With this model, some realistic values for the fictive case are found based on a certain return period. If a breakwater fails, the loss of life and economic damage is limited and for this reason a target failure probability ($p_{f,TL}$) of 20% is used (van den Bos and Verhagen, 2018). Subsequently, based on Equation 3.1, the rewritten Poisson distribution, the corresponding return period (R) of 225 years for a design lifetime of 50 years (T_L) is found.

$$R = \frac{T_L}{-\ln(1 - p_{f,TL})} \tag{3.1}$$

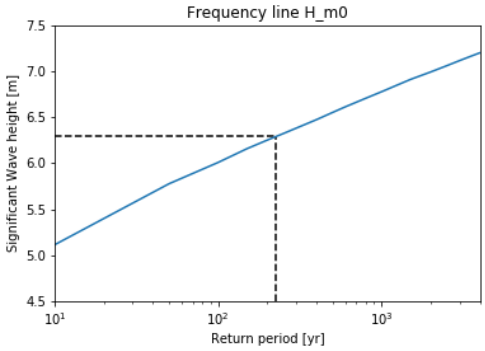

Figure 3.2: Wave height versus return period at Scheveningen

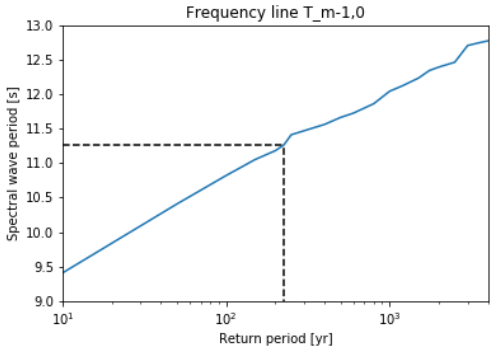

Figure 3.3: Spectral period versus return period at Scheveningen

3.1.2. Deep water conditions

The significant wave height (H_{m0}) and spectral wave period ($T_{m-1,0}$) for a return period of 225 years are respectively, 6.29 meters and 11.26 seconds (Figure 3.2 and Figure 3.3). The data in HydraNL is in correspondence with the WBI2017 (WBI 2017), an assessment criteria tool for hydraulic conditions and structures in the Netherlands. Within HydraNL the wave model SWAN is used to derive the hydraulic conditions for coastal areas. Because at the location investigated no bathymetry data is available in HydraNL for the calculation, it is assumed that the conditions are not depth-limited yet.

Based on the wave data gathered with HydraNL, the deep water wave length ($L_{m-1,0}$) and wave steepness ($s_{m-1,0}$) are calculated according Equation 3.2 and Equation 3.3.

$$L_o = \frac{g \cdot T_{m-1,0}^2}{2\pi} \tag{3.2}$$

$$s_{m-1,0} = \frac{H_{m0}}{L_{m-1,0}} \tag{3.3}$$

On the basis of the derived parameters in HydraNL the wave steepness represents a developed wind sea:

$$L_o = \frac{9.81 \cdot 11.26^2}{2\pi} = 199.4[m]$$

$$s_{m-1,0} = \frac{6.29}{199.4} = 0.032[-]$$

3.1.3. Toe conditions

The conditions at the toe of the breakwater depend on the water depth. In this thesis a wave height (H_{m0}) over depth (d) ratio of 0.2 is applied such that the waves are not breaking too much. With a water depth of 12.5 meters, the corresponding maximum wave height is 2.5 meters. To remain the same conditions as derived in Hydra for deep water, the same steepness is applied. With this assumption,

the wave period and length are calculated.

$$L_0 = \frac{H_{m0}}{s_{m-1,0}} = \frac{2.5}{0.032} = 78.7[m]$$

$$T_{m-1,0} = \sqrt{\frac{L_0 \cdot 2\pi}{g}} = 8.15[s]$$

Note that the notional wave steepness is used, i.e. the actual wave height over the deepwater wavelength. The results are visualized in Figure 3.4.

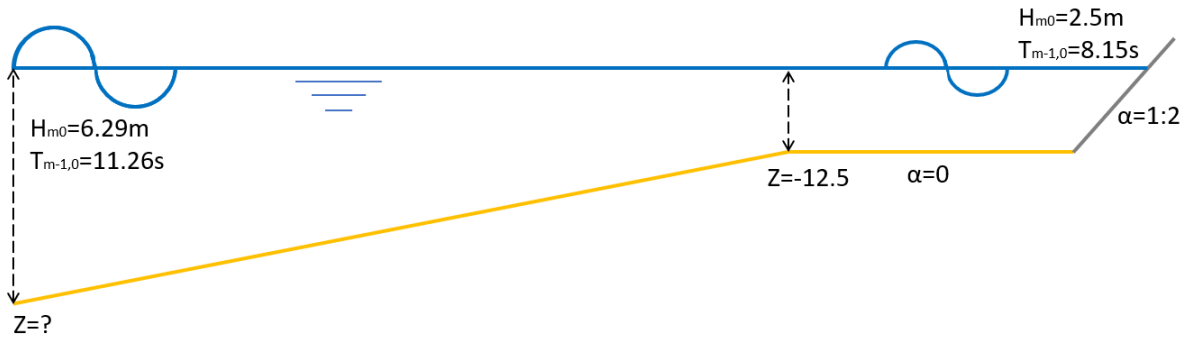

Figure 3.4: Deep water conditions versus toe conditions

3.1.4. Crest height rubble mound breakwater

Because the original TAW equation lacks the influence of a berm, two different guidelines are used. Therefore, two different case studies should be derived as well.

TAW and EurOtop 2007

The crest height for rubble mound structures depends on the acceptable limit of overtopping discharge, defined with a maximum of 50 l/s/m for this structure. At this rate, vessels start to encounter damage due to the overtopping waves (TAW 2002). As stated in Chapter 2, the older guidelines are used because recent research (den Bieman et al., 2020) showed that the EurOtop 2018 seems less accurate than the original TAW equations. The mean overtopping equation according to the TAW is:

$$\frac{q}{\sqrt{g \cdot H_{m0}^3}} = 0.2 \cdot \exp\left(-2.6 \frac{R_c}{H_{m0} \cdot \gamma_f \cdot \gamma_\beta}\right)$$

With:

$q =$	Overtopping discharge	[l/s/m]
$g =$	Gravitational acceleration=9.81m/s^2	[m/s^2]
$H_{m0} =$	Spectral wave height	[m]
$R_c =$	Crest height	[m]
$\gamma_f =$	Influence factor roughness ≈ 0.40 for rubble mound structures	[-]
$\gamma_\beta =$	Influence angle of wave attack	[-]

Subsequently, based on the previously derived significant wave height at the toe, the minimum crest level is determined. With waves approaching normal incident ($\gamma_\beta = 1$) and a roughness of 0.40 (γ_f) the minimum required crest height is:

$$R_c = \frac{H_s \cdot \gamma_f \cdot \gamma_\beta}{2.6} \cdot \left(-\ln\left(\frac{q_{max}}{\sqrt{g \cdot H_s^3 \cdot 0.2}}\right)\right) = \frac{2.5 \cdot 0.4 \cdot 1}{2.6} \cdot \left(-\ln\left(\frac{50/1000}{\sqrt{9.81 \cdot 2.5^3 \cdot 0.2}}\right)\right) = 1.5[m]$$

Crest height Adapted TAW equation
The adapted TAW overtopping equation is almost the same as the original TAW overtopping equation. The equation proposed by Krom (2012) contains a different factor for the roughness and berm. Because the influence of the berm is one at first, the only difference compared to the TAW overtopping equation is the roughness. The roughness includes both the steepness of waves and structure and is calculated with Equation 3.4.

$$R_c = \frac{H_s \cdot \gamma_{f,surging} \cdot \gamma_\beta}{2.6} \cdot \left(-\ln\left(\frac{q_{max}}{\sqrt{g \cdot H_s^3} \cdot 0.2}\right)\right) = \frac{2.5 \cdot 0.6 \cdot 1}{2.6} \cdot \left(-\ln\left(\frac{50/1000}{\sqrt{9.81 \cdot 2.5^3} \cdot 0.2}\right)\right) = 2.26[m]$$

With the influence of roughness:

$$\gamma_{f,surging} = \gamma_f + (\xi_{m-1,0} - 1.8) \cdot \frac{(1-\gamma_f)}{4.2} = 0.4 + (3.22 - 1.8) \cdot \frac{1-0.4}{4.2} = 0.6[-] \tag{3.4}$$

And the breaker parameter:

$$\xi_{m-1,0} = \frac{\tan(\alpha)}{\sqrt{s_0}} = \frac{0.5}{0.032} = 3.22[-]$$

3.1.5. Safety included for sea level rise

In this research, a safety factor for sea level rise is not necessary because the aim is to investigate adaptation possibilities. With a safety factor, the starting point of such a measure is only moved in time. However, as currently designed structures also include a certain safety and to make the design more realistic a safety level according to the Delta scenario has been included. The Delta scenario represents the sea level rise prediction according to the KNMI'14 scenarios (KNMI 2015) and is used in the design of coastal structures in The Netherlands. In Figure 1.2 this prediction and two other predictions based on the emission rates set by the IPCC are shown. The assumed lifetime for the rubble mound structure is approximately 50 years and the average expected sea level rise with the Delta scenario in 2070 is 0.6 meters. From that point on adaptation measures are necessary to ensure safety. Therefore, with the extra safety included the minimum required crest height for the TAW and adapted TAW equations are respectively 2.1 and 2.85 meters.

3.1.6. Stability of the Rubble Mound Breakwater

The stability of the structure only has been assessed for the base case and is assumed as stable for an increased sea level. For the rock stability of a rubble mound breakwater thorough research has been performed by Hudson (1953) and van der Meer (1988) as can be seen in Section 2.5. However, these researches are both validated for deepwater conditions.

More recently van Gent et al (2003) gave a better-fitted equation for shallow water conditions based on the van der Meer equation. In the mentioned research of van Gent, a stability equation was derived for the situation with limited information about the wave heights ($H_{2\%}$). This equation can easily be applied to determine the required rock sizes because for this thesis only information about deepwater wave conditions are derived. In Chapter 2 this equation has been defined, but is stated again for convenience in Equation 3.5. The permeability is defined as the ratio between the core ($D_{n50,c}$) and the armour layer (D_{n50}), with validated ratio's between 0 and 0.3.

$$\frac{S}{\sqrt{N}} = \left(0.57 \frac{H_s}{\Delta D_{n50}} \sqrt{\tan(\alpha)} \frac{1}{1 + D_{n50,c}/D_{n50}}\right)^5 \tag{3.5}$$

Layer	Standard grading	D_{n50} [m]
Armour	HM_a 3-6T	1.18
Filter	HM_a 0.3-1T	0.59
Core	Quarry run	0.21

Table 3.1: Standard grading classes according to NEN-EN 13383-1 (2002) applied on the fictive case study

Where:

$S =$ Damage number [-]
$N =$ Number of waves [-]
$H_s =$ Wave height at toe of structure [m]
$D_{n50} =$ Nominal diameter rocks armour layer [m]
$D_{n50,c} =$ Nominal diameter rocks core layer [m]
$\alpha =$ Slope structure=1:2 [°]
$\Delta =$ Relative buoyant density$(\rho_s - \rho_w)/\rho_w \approx 1.59$ [-]

The damage number (S) is assumed as 2, at this point start of damage has been defined for rubble mound breakwaters. The number of waves is limited to the maximum value of 7500. For a larger number of waves, the construction is assumed in equilibrium. To increase the stability of the layers, a filter layer has been implemented. In the Rock Manual (Rock Manual 2007) a ratio between the two layers of 2.2 is advised ($\frac{D_{n50,a}}{D_{n50,f}} = 2.2$) as rule of thumb. Taking all the layers into account the ratio between the core and armour layer is determined as:

$$\frac{D_{n50,c}}{D_{n50}} = 0.21$$

Applying all parameters in Equation 3.5 gives a nominal armour layer diameter of:

$$\frac{2}{\sqrt{7500}} = \left(0.57 \frac{2.5}{1.59 \cdot D_{n50}} \sqrt{tan(26.6)} \frac{1}{1 + 0.21}\right)^5$$
$$D_{n50} = 1.18[m]$$

According to the NEN-EN 13383-1 (2002), the first standard grading would be HM_a 3-6T with a nominal diameter of 118 centimeters. With the given relation between the layers, the nominal diameters for the remaining layers are calculated as:

$$D_{n50,f} = 1.18/2.2 = 0.54[m] \qquad D_{n50,c} = 1.18/2.2/2.2 = 0.24[m]$$

In correspondence with NEN 13383-1, the layers are divided into standard grading classes summarized in Table 3.1. For the core material often a quarry run is used to decrease construction costs. Quarry run consists of a relatively wide range of material.

3.2. Summary of the main dimensions

In this chapter the defined hydraulic conditions at Scheveningen are used to determine the stability of the rubble mound structure. As the stability of a breakwater is not the objective of this thesis it is not important. However, to give some realistic rock sizes for the governing conditions they are elaborated for the situation without sea level rise. The stability is assumed as sufficient for the remaining part of the report in which sea level rise is taken into account. In Figure 3.5 and Figure 3.6 the important parameters for both case studies are presented. Finally, all derived parameters are presented in Table 3.2. The only difference between both case studies is the difference in crest height (highlighted in the red circle). The wave overtopping is approximately 50 l/s/m at the presented crest heights.

Case study 1

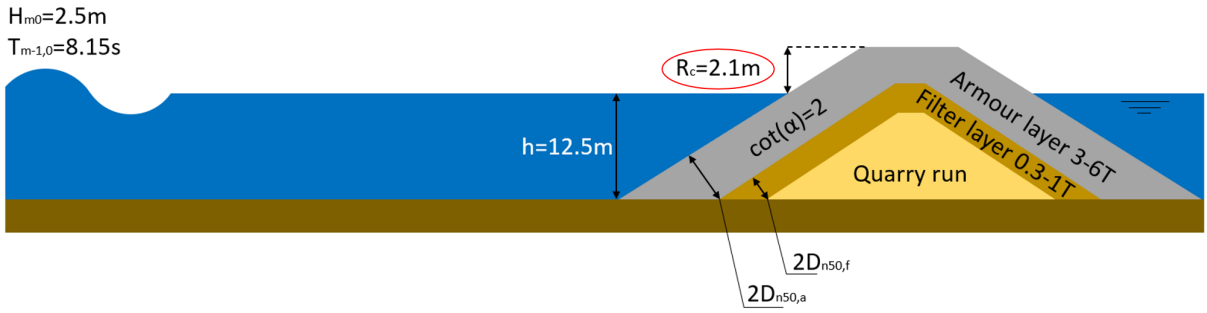

Figure 3.5: Case study 1 based on the original TAW equations

Case study 2

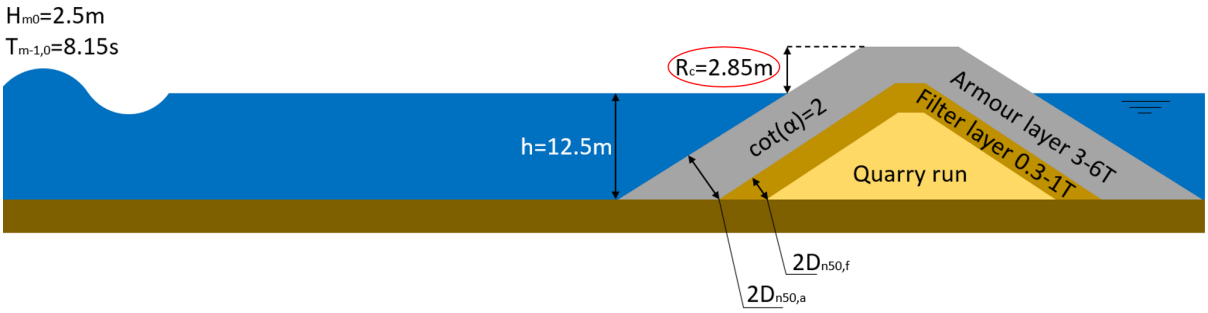

Figure 3.6: Case study 2 based on the Adapted TAW equations

Summary of used parameters

Parameter	Definition	Value	Unit
$H_{m0,offshore}$	Spectral wave height in deep water	6.3	[m]
$T_{m-1,0,offshore}$	Spectral wave period	11.3	[s]
$s_{0,offshore}$	Wave steepness	0.032	[-]
L_0	Deep water wave length	199.4	[m]
h	Water depth at toe of structure	12.5	[m]
α	Slope of structure (1:2)	26.6	[°]
H_{m0}	Significant wave height at toe of structure	2.5	[m]
$T_{m-1,0}$	Wave period at toe of structure	8.15	[s]
$s_{m-1,0}$	Notional wave steepness at the toe	0.032	[-]
ρ_w	Density sea water	1025	[kg/m3]
ρ_s	Density rock material	2650	[kg/m3]
Δ	Relative buoyant density	1.59	[-]
S	Damage number	2	[-]
N	Number of waves	7500	[-]
D_{n50}	Nominal diameter armour layer (HM_a 3-6T)	1.18	[m]
$D_{n50,f}$	Nominal diameter filter layer (HM_a 0.3-1T)	0.59	[m]
$D_{n50,c}$	Nominal diameter core layer (Quarry run)	0.21	[m]
q_{max}	Maximum allowed wave overtopping	50	[l/s/m]
$R_{c,min,1}$	Minimum height crest level TAW	1.5	[m]
$R_{c,1}$	Height crest level TAW including some safety for sea level rise	2.1	[m]
$R_{c,min,2}$	Minimum height crest level adapted TAW	2.25	[m]
$R_{c,2}$	Height crest level adapted TAW including some safety for sea level rise	2.85	[m]

Table 3.2: Summary of parameters used to set-up the fictive cases

4

Adaptive Pathways for Rubble Mound Breakwaters

The third methodological step is performed in this chapter by elaborating an adaptive pathway scheme. The pathways provide a guideline for adaptation possibilities of a rubble mound breakwater to reduce wave overtopping and can be applied to different climate scenarios. The effects of the different adaptation measures on the overtopping discharge for the proposed academic cases are determined based on the empirical formulas elaborated in the literature review in Chapter 2. At the end of the chapter, the economically most attractive solutions are presented.

4.1. Selection of adaptation pathways

Because of the adaptive approach, different paths are created for which structures could be protected against a certain amount of sea level rise, each path corresponds to an adaptation strategy. For each unique path the costs are calculated to illustrate which combination of solutions is beneficial at larger predicted sea level rises. The four different adaptation possibilities to limit wave overtopping which are considered in this thesis are:

- The addition of a berm
- The addition of a crest-wall on top of the structure
- The addition of a low-crested structure in front
- Increasing the foreshore

Besides the previous described adaptations, in Chapter 1, also the option for the influence of oblique waves or an increased roughness is suggested as a solution for the rubble mound structure. The latter is not elaborated further as the roughness of a rubble mound structure depends on the stability of the structure. The correct influence of the oblique waves is indeed important but can not directly be coupled to implementation costs. In contrast to the correct influence of the oblique waves, the four options stated above can easily be compared to each other based on the costs.

A solution can be seen as sufficient if the wave overtopping remains smaller than 50 l/s/m, the point at which significant damage at vessels occurs (TAW 2002). When the sea level rise becomes too high to meet this requirement the so-called tipping point of a solution has been reached. At this point in time, other solutions are necessary to ensure enough safety. Theoretically, the solutions are always able to cope with the sea level rise if they are just made large enough. To prevent that the solutions become too large to be realistic, a few boundary values have been defined in the next section. Moreover, the dimensions of each adaptation determine the tipping points.

4.2. Tipping points different adaptations

4.2.1. Hydraulic conditions adaptive approach

Each possible adaptation measure has a boundary for which the adaptation is reasonable regarding the economical and constructability aspect. In the next sections, these conditions are defined. The dimensions of the considered solutions determine the tipping points in the pathway scheme. The maximum sea level rise considered in the adaptive pathway approach is 1.7 meters. Due to the initial crest level of 2.1 or 2.85 meters depending on the academic case investigated, multiple adaptations are required to prevent a severe amount of overtopping. Also, more than 1.7 meters sea level rise only occurs for the most extreme scenario published by the IPCC at the end of this century as can be seen in Figure 1.2. The 1.7 meter sea level rise corresponds to the upper limit of the RCP4.5 scenario adopted by the IPCC. In Figure 4.1, the ultimate scenario is presented for the case study based on the TAW equations without any adaptation measures.

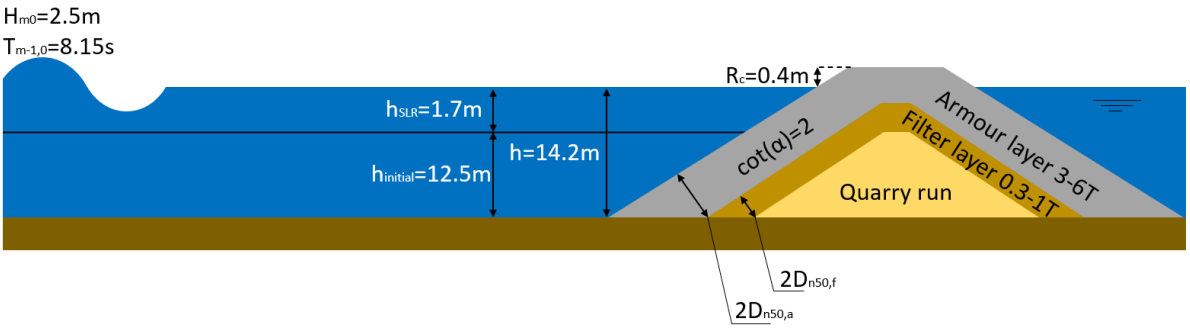

Figure 4.1: Maximum sea level rise considered (Academic case based on TAW overtopping equations)

The wave height (H_{m0}) and spectral wave period ($T_{m-1,0}$) are assumed as constant for an increasing sea level Therefore, the wave steepness remains constant. It is known that due to wave breaking the wave period changes, for example when waves travel over a low-crested structure. This fact is investigated in more detail for the final solution if this phenomenon is important to give a conclusion about the accuracy. Only for the solution in which the foreshore increases, a reduction in wave height is assumed. Therefore, with the same wave period, the waves become less steep. For the situation in which a foreshore is implemented at first, following with a berm or low-crested structure as second or third, it is assumed that these two adaptations are placed directly on the bottom of the situation without increased foreshore to remain enough space to implement a low-crested structure or berm with an armour and core layer.

4.2.2. Tipping point of a Berm

In Section 2.4.5 the optimal berm width according to the TAW (TAW 2002) has been elaborated. If the berm width is 40% of the length ($B_{berm} = 0.4 \cdot L_{berm}$), along with a berm at still water level, the influence factor of a berm is 0.6. The maximum berm width is assumed as five meters with the crest level just above still water (≈ 0.5). Therefore, just after construction, the influence factor is a bit larger than the maximum. However, with the sea level rising in the years after, the influence of the berm becomes larger until the maximum of 0.6. Moreover, Krom (2012) proved that berms above mean sea water level in front of a rubble mound breakwater have more influence than berms below still water. The total berm height depends on the moment of implementation and the corresponding sea level rise at that moment.

In Section 2.4.5 it is mentioned that waves should be breaking for the berm to become influential in the TAW overtopping equations. This is the case when the Iribarren number is lower than approximately 2.5 ($\xi_{m-1,0} \leq 2.5$). According to these equations, the berm will not influence the overtopping rate for larger Iribarren numbers. Figure 4.2 presents a sketch of the berm at the moment op implementation.

4.2.3. Tipping point of a Crest Wall

A crest wall is often used to limit wave overtopping or serve as a road for construction and maintenance operations. Therefore, a minimum width is applied to make it possible for machines to pass safely.

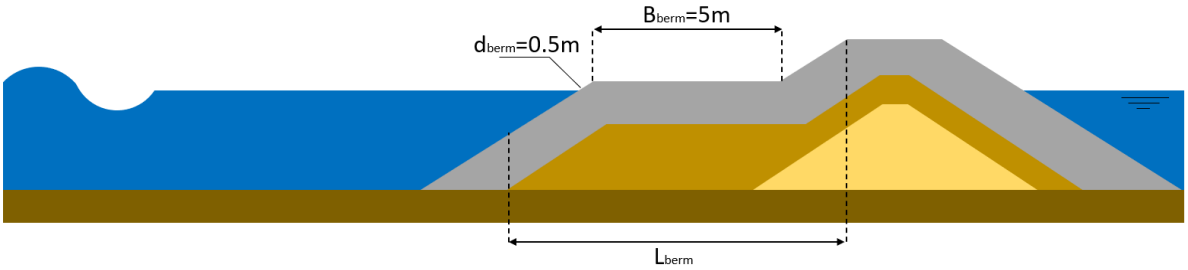

Figure 4.2: Berm in front of a rubble mound structure (NTS)

The height of the crest wall should not be too high as the wave load increases for higher crest walls. Therefore, the maximum height of a crest wall above the armour layer is assumed to be limited to 0.5 meters in this thesis. In Figure 4.3 the location of the crown wall is shown, it is placed directly on the core. Because of the size of the wall above the initial crest height, it is cheaper to increase the crest with 0.5 meters of rocks. First, a trench should be dug to create enough space to implement a wall. Whilst for the increased crest only rocks are dumped. However, the accuracy of the guidelines for combinations of solutions is investigated in this thesis and therefore a crest wall is relevant.

Figure 4.3: Crest wall on top of a rubble mound structure (NTS)

4.2.4. Tipping point of a Foreshore

A length of one deepwater wavelength is proposed for a foreshore in the TAW guideline (TAW 2002). Within this length, most waves will break if the foreshore is shallow or very shallow. One of the biggest disadvantages of nourishing the foreshore could be that erosion prevails at this part of the coast, for example, due to longshore transport. Due to this nourishing, the foreshore could be a frequently happening operation every few years, depending on the amount of erosion. The increase in foreshore level is approximately ten meters for this adaptation measure (Figure 4.4). From this point on, the influence of the foreshore becomes significant with the assumed rule of thumb ($H/d \approx 0.5$).

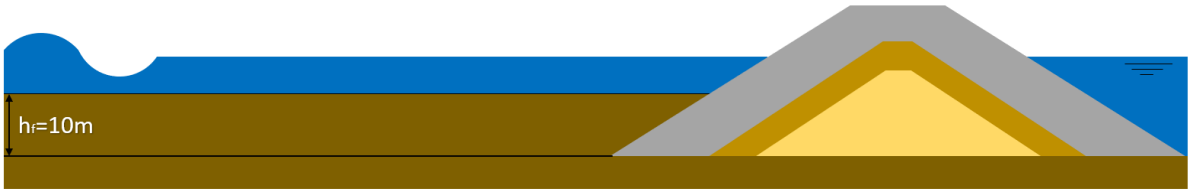

Figure 4.4: Increased foreshore (NTS)

4.2.5. Tipping point of a Low-Crested Structure

The crest width of the low-crested structure has been set to a maximum of 5 meters. The crest height is set below still water level at a minimum level of -1 meters relative to mean sea level. In Figure 4.5 an indication of the low crested structure is presented. The same slope and protection as for the rubble mound breakwater is used (1:2).

Figure 4.5: Low-crested structure in front of a rubble mound structure (NTS)

4.3. Cost estimation different solutions

4.3.1. Literature on price indications

For the cost estimation of the different adaptation measures only limited information is available in literature. In the past, several types of research compared the different costs of rubble mound breakwaters. First, Hauer (1995) presented some numbers for the construction of the different layers of a rubble mound breakwater. A few years later Tutuarima (1998) extended these costs and added transport and production costs of the different materials. As these costs are very outdated, in the master thesis by Van Rooijen (2005) a cost-estimation was made for the sea defence of Maasvlakte 2. In this research, some production and construction costs for different rock sizes and other materials are provided. These researches provide enough information to elaborate the economically most beneficial sequence from the adaptation pathways. Mainly, because the ratio of the cost-estimation between the different items is important and not the exact costs.

4.3.2. Cost indication of different materials

The costs of the different rock sizes are estimated based on the numbers in Table 4.1. Rocks are used to create a berm or a low-crested structure in front of the current structure determined in Chapter 3. Because the numbers in the thesis of Van Rooijen (2005) are based on a very large project more than fifteen years back, the costs are assumed as doubled due to inflation and the scale of this case study (larger orders of items are cheaper in general). Also, it has been assumed that these costs hold for The Netherlands and transport costs are already included in the unit price. The costs indication for the remaining materials are also provided in Table 4.1. The price of the crest wall is based on the unit price of concrete of 300€/m^3, which includes the transport and construction costs as well. Finally, the sand is used to increase the foreshore. In The Netherlands the price variate between 4 and 10 euros per cubic meter and for this case study a cost price of 6 euro per cubic meter has been chosen.

Material	Price indication	Unit
Rock	50	€/T
Sand	6	€/m^3
Concrete	300	€/m^3

Table 4.1: Production and construction costs

4.3.3. Pathway calculation method

The total costs per adaptation measure are calculated per meter length (i.e. width of the structure is 1 meter) by multiplying the volume of the adaptation measure with the costs per unit defined in the previous section. As rocks are ordered in tonnes at the quarry, the total weight of the layer is calculated based on Equation 4.1, in which information on the porosity (n_v) of the layer is necessary. Because this requires detailed information on the placement of the rocks, a porosity of 0.4 has been assumed for the rubble mound structure.

$$W = t \cdot A \cdot \rho_s \cdot (1 - n_v) \tag{4.1}$$

$W =$ Weight of the rock layer [kg/m]
$A =$ Area of the layer (plane parallel to the breakwater) [m^2]
$t =$ Thickness of the layer [m]
$\rho_s =$ Density rock layer=2650 [kg/m^3]
$n_v =$ Void porosity=0.4 [-]

The total costs are summed up according to Equation 4.2, for which the costs are zero if no adaptation at all is constructed. The first part of the equation describes the costs for the rock type of adaptation (i.e. a berm or a low-crested structure). The second part of the equation describes the two remaining adaptation types (i.e. increased foreshore or a crest wall).

$$C_{Total} = \sum_{i=1}^{2} \left(C_{c,p,i} \cdot W_i \right) + \sum_{j=1}^{2} \left(C_{c,p,j} \cdot V_j \right) \tag{4.2}$$

$C_{total} =$ Total costs per sequence of adaptation measures (per meter width) [€/m]
$i, j =$ Type of adaptation measure (Section 4.2) [-]
$C_{c,p,i} =$ Construction and production costs per adaptation measure i (Table 4.1) [€/T]
$C_{c,p,j} =$ Construction and production costs per adaptation measure j (Table 4.1) [€/m^3]
$W_i =$ Total weight of adaptation measure i [T/m]
$V_j =$ Total volume of adaptation measure j [m^3/m]

4.4. Results of the adaptation pathways

Based on the empirical formulas defined in Chapter 2, this section elaborates on the different pathways for the applied case studies. The empirical equations investigated can be found in the TAW/EurOtop 2007 manual (TAW, 2002) and in the master thesis of Krom (2012), who proposed an adapted TAW overtopping equation that includes the influence of a berm. For each theoretical guideline, a separate academic case study is proposed in Chapter 3. In both cases, the initial overtopping is 50 l/s/m at 0.6 meters sea level rise.

4.4.1. Possible pathways

A solution can be seen as sufficient until the so-called tipping point is reached, the dots in Figure 4.6. From these points on, a new adaptation measure is necessary to ensure the functionality of the breakwater. This process is repeated until the maximum sea level rise of 1.7 meters has been reached. All sequences of solutions together are put into one adaptation pathway scheme. Subsequently, the costs are used to estimate the economically best sequence of solutions. For all possible solutions holds the fact that the dimensions are of maximum size like defined at the beginning of the chapter. However, an exception can be made for the final solution. The last solution can be reduced in size if the limit of 1.7 meters sea level is exceeded by an adaptation measure (e.g. the adaptation measure decreases the overtopping rate more than 50 l/s/m). By doing so, the costs are significantly reduced. In Appendix A, the paths with the four different starting points are presented separately and give a more clear overview of the situation.

TAW and EurOtop 2007 (Case 1)

Figure 4.6 presents the adaptation pathway based on case study 1 (Chapter 3) and the TAW overtopping equations. A pathway is formed if the individual adaptations are combined. The tipping points of an individual adaptation depend on the empirical formulas stated in Chapter 2, but also on the dimensions defined previously. The vertical lines at the end of an individual solution mark the moment until

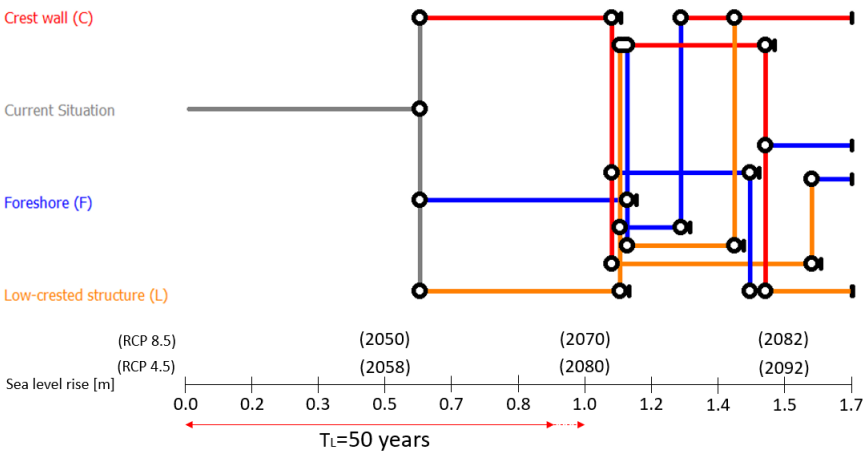

Figure 4.6: Adaptive pathways based on case 1 and the TAW overtopping equations

a solution ensures safety. Before this point is reached, the next adaptation measure should be implemented in the system. Therefore, the tipping points are used as a warning system. Due to the included safety of 0.6 meters defined in Chapter 3, the first adaptation measure is required after 0.6 meters of sea level rise. Different management strategies can be chosen based on the derived pathways. This strategy depends for example on the space available to implement solutions or the availability of different materials in the region.

Adapted TAW equation (Case 2)
The same steps are performed for case 2 and the empirical equation proposed by Krom. Because the influence of a berm is included in the adapted TAW overtopping equation for non-breaking waves, this solution is added in the pathway scheme (Figure 4.7).

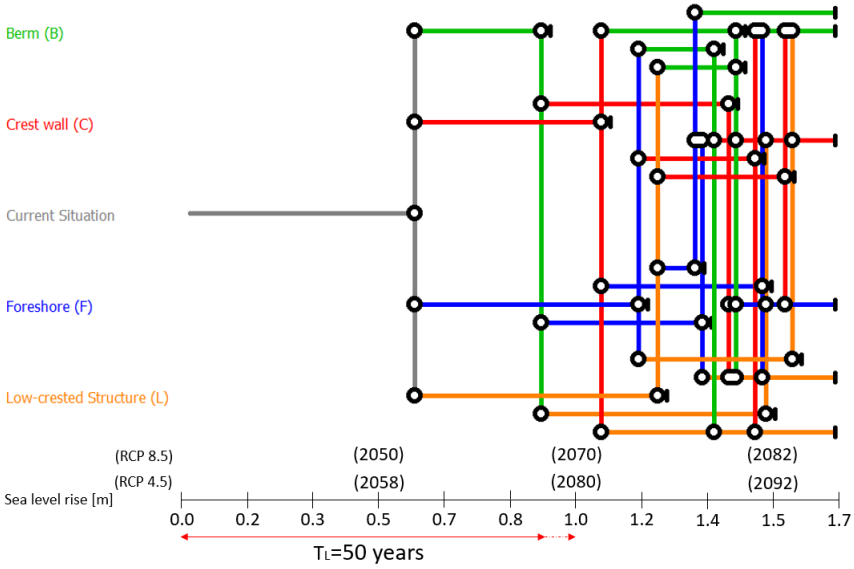

Figure 4.7: Adaptive pathways based on case 2 and the proposed equation by Krom

Lifetime of the structure in the adaptation paths
Currently, the adaptation paths are based on a maximum sea level rise of 1.7 meters. However, this sea level rise only occurs for the most extreme scenarios adopted by the IPCC (RCP 4.5 and 8.5) at the end of the century. With an average lifetime of 50 years, a breakwater constructed in the year 2020 only requires one or two adaptations. The average lifetime for both climate scenarios is also

highlighted in Figure 4.6 and Figure 4.7. However, if the lifetime of a structure is extended through the implementations of adaptations, the pathways schemes derived previously can be used.

4.4.2. Pathway costs

In the previous section two different adaptation pathway schemes were elaborated. Subsequently, the economically most attractive solutions are determined in this section, based on these pathway schemes. The different sequences are referred to according their first letter. Therefore: Foreshore (F), Crest wall (C), Berm (B) and Low-crested structure (L).

Case 1

In Table 4.2 the production and construction costs according to Tables 4.1 and 4.1 for each pathway are presented. As can be seen, the costs for each unique path are in the same order of magnitude. This is because each path contains the same three adaptations. After all, the berm is not included in the non-breaking overtopping equation. For the final sequence, the dimensions of the adaptation might be lower to limit the costs while the safety requirement is still met. Appendix A presents the reduced dimensions for the final solution in a sequence. Together with the the detailed costs and the individual paths. Again, the solutions implemented before the final solution in a path are always of maximum dimension. Those dimensions are defined in the first sections of this Chapter. For example, a crest wall is always 0.5 meters above the armour layer unless stated otherwise.

Sequence	Costs	Unit	Sequence	Costs	Unit
C-F-L	42 300	€/m	F-L-C	44 100	€/m
C-L-F	43 800	€/m	L-C-F	42 350	€/m
F-C-L	43 150	€/m	**L-F-C**	**42 000**	**€/m**

Table 4.2: Production and construction costs per solution (Case 1)

Case 2

The costs per path for the adapted overtopping equation are presented in Table 4.3. The economically most attractive and the economically least attractive combination are highlighted in bold. The implementation costs of a low-crested structure are quite expensive because of the relatively expensive costs in combination with a large water depth. In contrast to the low-crested structure, the implementation costs of a berm and mainly the crest wall are much lower. The implementation of a foreshore can also be beneficial due to the relatively low material costs of sand.

Sequence	Costs	Unit	Sequence	Costs	Unit
B-C-F	19 900	€/m	F-B-C	19 900	€/m
B-C-L	33 350	€/m	F-B-L	47 500	€/m
B-F-C	19 950	€/m	**F-C-B**	**18 150**	**€/m**
B-F-L	47 200	€/m	F-C-L	40 200	€/m
B-L-C	37 300	€/m	F-L-B	45 150	€/m
B-L-F	48 650	€/m	F-L-C	44 200	€/m
C-B-F	19 650	€/m	L-B-C	35 900	€/m
C-B-L	32 900	€/m	L-B-F	47 100	€/m
C-F-B	**17 400**	**€/m**	L-C-B	32 350	€/m
C-F-L	40 300	€/m	L-C-F	41 900	€/m
C-L	31 150	€/m	**L-F-B**	**57 500**	**€/m**
			L-F-C	41 900	€/m

Table 4.3: Production and construction costs per solution (Case 2)

4.4.3. Future value of adaptation paths

In the previous section, the pathway costs are elaborated based on the present value of the costs. Because the moment in time at which an individual adaptation measure should be implemented depends on the rate of sea level rise, the costs might differ. As this is a largely uncertain prediction, see Figure

1.2, the moment of implementation is also uncertain. Therefore, the costs of each path are compared for different climate scenarios according to their future value (FV). Due to inflation, the costs of an individual adaptation increase over time, the future value is calculated based on Equation 4.3.

$$FV = PV(1+r)^n \tag{4.3}$$

$FV =$	Future Value	[€/m]
$PV =$	Present Value	[€/m]
$r =$	Interest rate	[-]
$n =$	Number of years included	[-]

The present value (PV) is calculated and presented in Table 4.2 and 4.3. When the annual inflation rate (r) is included, the costs of an investment in n years can be calculated. The average Dutch inflation rate or consumer price index (CPI) was approximately 2.1% in the past 30 years (1990-2020) (CBS 2020). Due to the interest rate and year of implementation (n), a certain path can become more or less attractive. Expected is that the most expensive adaptation (e.g. low-crested structure) becomes relatively more attractive if constructed earlier in time compared to the cheaper adaptations.

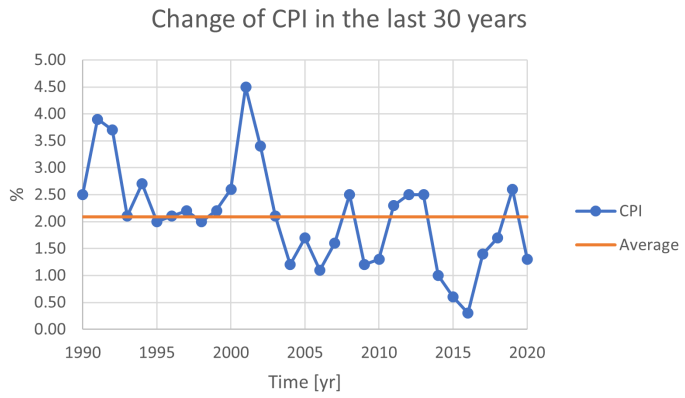

Figure 4.8: Average CPI or inflation rate of the Netherlands in the past 30 years

Because of the large uncertainty in sea level rise, increasing over time, a relatively conservative level (upper limit) is chosen for the calculation of the future value of an investment. The two climate scenarios evaluated are the two scenarios depending on the IPCC emission rates (Deltares 2018).

1.) RCP 4.5 scenario
First, the IPCC scenario in which the increase in emissions requires to stop in 2050 is evaluated and applied to the costs of the adaptation pathways. Previously, it was found that the present value costs of the solutions derived for case 1 are of the same order. As expected if the future value is included, paths in which a low-crested structure is constructed at first become more relevant (Table 4.4).

Sequence	Costs	Unit	Sequence	Costs	Unit
C-F-L	167 150	€/m	F-L-C	148 500	€/m
C-L-F	161 600	€/m	L-C-F	127 950	€/m
F-C-L	160 550	€/m	**L-F-C**	**119 100**	**€/m**

Table 4.4: Future value of solutions based on the RCP 4.5 scenario (Case 1)

Likewise, the low-crested structure constructed at first also becomes more relevant for case 2. However, paths including a berm, crest wall and foreshore remain more attractive due to the lower implementation costs. Compared to the present value analysis, the combination F-C-B becomes the most relevant one. Again, the most expensive solution should be implemented at first in this sequence (foreshore). In Table 4.5 the results of the future value calculation for case 2 are presented.

Sequence	Costs	Unit	Sequence	Costs	Unit
B-C-F	70 200	€/m	F-B-C	56 600	€/m
B-C-L	126 300	€/m	F-B-L	165 000	€/m
B-F-C	59 900	€/m	**F-C-B**	**54 100**	**€/m**
B-F-L	169 000	€/m	F-C-L	149 500	€/m
B-L-C	115 100	€/m	F-L-B	142 700	€/m
B-L-F	164.200	€/m	F-L-C	138 600	€/m
C-B-F	75 000	€/m	L-B-C	98 600	€/m
C-B-L	130 000	€/m	L-B-F	145 100	€/m
C-F-B	**62 600**	**€/m**	L-C-B	86 200	€/m
C-F-L	161 900	€/m	L-C-F	128 200	€/m
C-L	108 700	€/m	L-F-B	183 200	€/m
			L-F-C	120 800	€/m

Table 4.5: Future value of solutions based on the RCP 4.5 scenario (Case 2)

2.) RCP 8.5 scenario

The second and most extreme scenario evaluated on future value includes the fact that emission rates do not stop rising before 2100 (IPCC 2014). Compared to the milder RCP 4.5 scenario the same paths are economically more attractive for both case 1 and case 2 (Table 4.6 and 4.7). Notably, the total costs decrease because the year of implementation is a few years earlier.

Sequence	Costs	Unit	Sequence	Costs	Unit
C-F-L	132 750	€/m	F-L-C	119 000	€/m
C-L-F	128 600	€/m	L-C-F	105 200	€/m
F-C-L	128 500	€/m	**L-F-C**	**97 900**	**€/m**

Table 4.6: Future value of solutions based on the RCP 8.5 scenario (Case 1)

Sequence	Costs	Unit	Sequence	Costs	Unit
B-C-F	56 500	€/m	F-B-C	48 900	€/m
B-C-L	100 700	€/m	F-B-L	139 600	€/m
B-F-C	49 500	€/m	**F-C-B**	**44 900**	**€/m**
B-F-L	135 400	€/m	F-C-L	118 600	€/m
B-L-C	94 700	€/m	F-L-B	124 700	€/m
B-L-F	133 400	€/m	F-L-C	121 400	€/m
C-B-F	59 400	€/m	L-B-C	82 600	€/m
C-B-L	102 800	€/m	L-B-F	119 200	€/m
C-F-B	**49 400**	**€/m**	L-C-B	72 500	€/m
C-F-L	126 100	€/m	L-C-F	105 600	€/m
C-L	86 000	€/m	L-F-B	149 600	€/m
			L-F-C	98 000	€/m

Table 4.7: Future value of solutions based on the RCP 8.5 scenario (Case 2)

4.4.4. Conclusion on the future value calculations

As expected does the moment of implementation influences the different costs of paths. If a certain climate scenario with a large sea level rise is expected to occur in the next century, the more expensive solutions like a low-crested structure or a foreshore should be implemented earlier in time. However, not all solutions of a path might be required due to the large uncertainty of the predictions. Therefore, the costs are much larger than necessary if a more expensive solution is constructed as first instead of the economically more attractive solutions (e.g. berm or crest-wall).

The costs could be evaluated in a better way if the probability of occurrence would be available for each climate scenario adopted by the IPCC. Based on the probability of occurrence, the expected

pathways to ensure safety during the expected lifetime of a structure are computed. Subsequently, the costs are estimated. However, these probabilities are not known at the moment. Therefore, a large uncertainty about the cost estimation remains.

A berm and crest wall seem to be interesting solutions at the moment due to their large influence and low implementation costs. Together, these solutions ensure safety until approximately one meter of sea level rise. In none of the IPCC predictions this sea level rise is exceeded for the adopted lifetime in this thesis.

4.4.5. Costs for expected lifetime

In section 4.4.1 the expected lifetime of a rubble mound breakwater is defined as 50 years. After 50 years the predicted sea level rise for the RCP4.5 and 8.5 scenarios is approximately 1 meter. If this is the case, one adaptation would be sufficient to limit wave overtopping during the expected lifetime. The costs for each adaptation are presented in Table 4.8. As can be seen, is the crest wall economically more attractive compared to the other solutions. However, as this research focuses on the combination of solutions it is assumed that the lifetime of the structure is not normative.

Solution	Costs	Unit
Berm	8 500	€/m
Crest wall	1 700	€/m
Foreshore	11 300	€/m
Low-crested structure	23 600	€/m

Table 4.8: Costs per adaptation measure to ensure safety during the lifetime of 50 years

4.5. Application of a machine learning tool

Besides the empirical equations in the current guidelines, machine learning has become more relevant as well. With the XGB tool developed by Deltares, the case study derived in this thesis can be evaluated easily with corresponding adaptation measures. In recent research (den Bieman et al., 2020) this tool was already proven to be more accurate than the TAW and EurOtop 2018. By computing a path in XGB, a conclusion to the accuracy of current guidelines compared to a machine learning tool could be given.

Within the XGB tool, the mean value of the overtopping is calculated. Because the results are based on large data sets, there is a possibility that the derived adaptation paths in this chapter are out of range. If this happens, the results might not represent the correct physical processes. This is more likely to occur for combinations of solutions as there is a lack of data for combinations in the overtopping data set used in the XGB overtopping tool.

The influence of a berm is currently not included in the TAW overtopping equation for non-breaking waves, while a berm is expected to have an influence. The XGB results present that a berm indeed reduces the overtopping discharge. The reduction of a berm is even larger than computed with the adapted overtopping equations and could ensure safety for at least 1 meter of sea level rise. However, when the crest wall was added, the overtopping discharge became larger than for the situation with only 1 solution. As is expected that for a larger crest height the overtopping discharge should be lower, this combination is probably out of range in the data set. Therefore, it is impossible to compare the accuracy of the current guidelines for the proposed combinations with the machine learning tool. Moreover, it is not possible to derive accurate adaptation pathways at the moment.

4.6. Conclusion on the adaptation pathways

All the aspects described previously are used to answer the first research question. In Chapter 1 this question is stated as:

What sequence of solutions is economically beneficial according to the adaptation pathways by limiting wave overtopping of rubble mound breakwaters against sea level rise?

For now, the economically best sequences are considered as the most relevant solutions. Each of the four possible adaptations meets the functionality requirement until the overtopping rate exceeds 50 l/s/m. From this point on, an extra adaptation should be implemented to meet the functional requirements. Each solution is referred to their first letter: Berm (B), Crest wall (C), Foreshore (F) and the Low-crested structure (L). Later on, for the computations in the numerical model, the most relevant solution depends on the combination which is not validated or tested within current guidelines. If the numerical model gives a better insight into the effect of certain adaptations, a path can become more or less economically attractive.

TAW and EurOtop 2007 (Case 1)
The economically most attractive solution based on the present value analysis consists of a low-crested structure, foreshore and a crest wall (L-F-C). However, the costs of each solution are of the same order as the same adaptations are used in each path. If the future value is included for a certain climate scenario (e.g. RCP 4.5 or RCP 8.5), the paths in which a low-crested structure is implemented at first becomes more relevant as costs for expensive solutions increase relatively more over time. As for rubble mound breakwaters, the non-breaking overtopping equation is normative, the influence of a berm is not included. Therefore, only a limited number of paths are possible, all with the same adaptations. However, in recent research, it was already concluded that a berm influences the overtopping rate (e.g. Krom, 2012). In Chapter 6 the influence of a berm is investigated in more detail.

Adapted TAW equation (Case 2)
The solutions without a low-crested structure are the most attractive in the adaptation pathway for case 2 (C-F-B). Due to the relatively high water level and resource price, the costs of such a low-crested structure are more expensive. The crest wall and berm are more attractive to implement due to the smaller dimensions. Also, the foreshore is more attractive to implement than the low-crested structure due to the low costs of sand. If it is required to implement only two solutions during the lifetime of the rubble mound breakwater it is possible to combine a crest wall and a low-crested structure (C-L). The economically most attractive solution based on the future value consists of a foreshore, a crest wall and a berm (F-C-B).

Future value remarks
The future value makes certain paths more attractive compared to the situation in which the present value is included. Especially the more expensive paths with a low-crested structure or a foreshore as first become more attractive. In contrast, the paths in which these are constructed as latest become much more expensive. Because of the large uncertainty for the prediction of sea level rise, two climate scenarios were evaluated. Logically, the most extreme scenario (RCP 8.5) has lower costs than the less extreme scenario (RCP 4.5). However, this is compensated by the longer expected lifetime for the milder scenario.

The costs could be evaluated in a better way if the probability of occurrence would be available for each climate scenario adopted by the IPCC. Based on the probability of occurrence, the expected pathways to ensure safety during the expected lifetime of a structure are computed. Subsequently, the costs are estimated. However, these probabilities are not known at the moment. Therefore, a large uncertainty about the cost estimation remains. Solutions with a berm and crest wall seem to be interesting solutions to implement. Both adaptations have low construction costs and are relatively easy to implement.

General aspects
The negative side of the increased foreshore is the fact that detailed information on longshore transport is required and nourishment should happen regularly if this effect prevails. Moreover, the minimum length for a foreshore of one wavelength is used to calculate the volume of the nourishment. In reality there is a transition between the foreshore and the deeper water. The previous two effects are not taken into account for the calculation of the costs. Therefore, the costs can increase significantly.

Currently, the crest wall is 0.5 meters above the armour layer. However, in reality it might be cheaper to increase the crest with 0.5 meters of rocks. At first a trench should be dug to create enough space to implement the crest wall. Whilst for the increased crest only rocks are dumped. However, the accuracy of the guidelines for combinations of solutions is investigated in this thesis. Therefore, a crest wall is relevant.

The currently defined costs are corresponding to pathways until the maximum sea level rise of 1.7 meters. Depending on the climate predictions, smaller sea level rises might become more relevant if later in this century the RCP4.5 scenario would appear to overestimate the reality. In this case, the same pathways in Figure 4.6 and Figure 4.7 can be used but the costs should be calculated again if fewer solutions of the paths are implemented. If the most extreme case (RCP8.5) becomes more likely to happen, the crest height of the rubble mound structure should increase to ensure the functionality requirements. At 1.7 meters sea level rise, the crest height is relatively low and small waves would already overtop the breakwater.

Besides the different climate scenarios, the lifetime of a structure also determines the number of required adaptations. In the derived case studies a lifetime of approximately 50 years was assumed. The maximum sea level rise of 1.7 meters is exceeded in none of the climate scenarios adopted by the IPCC within the expected lifetime. Therefore, only 1 or 2 solutions are required to reduce the overtopping during the lifetime of a breakwater. However, if the lifetime of a structure is extended through the implementations of adaptations, the pathways schemes derived previously can be used.

Eventually, the economically most attractive sequences based on the future value are highlighted in Figure 4.9 and Figure 4.10 for both the original TAW overtopping equation and the adapted one (see next page). In both figures the expected lifetime is highlighted as well. The economically most attractive solution for case 1 consists of a low-crested structure, foreshore and a crest wall (L-F-C). The most attractive solution for case 2 consists of a foreshore, crest wall and a berm (F-C-B).

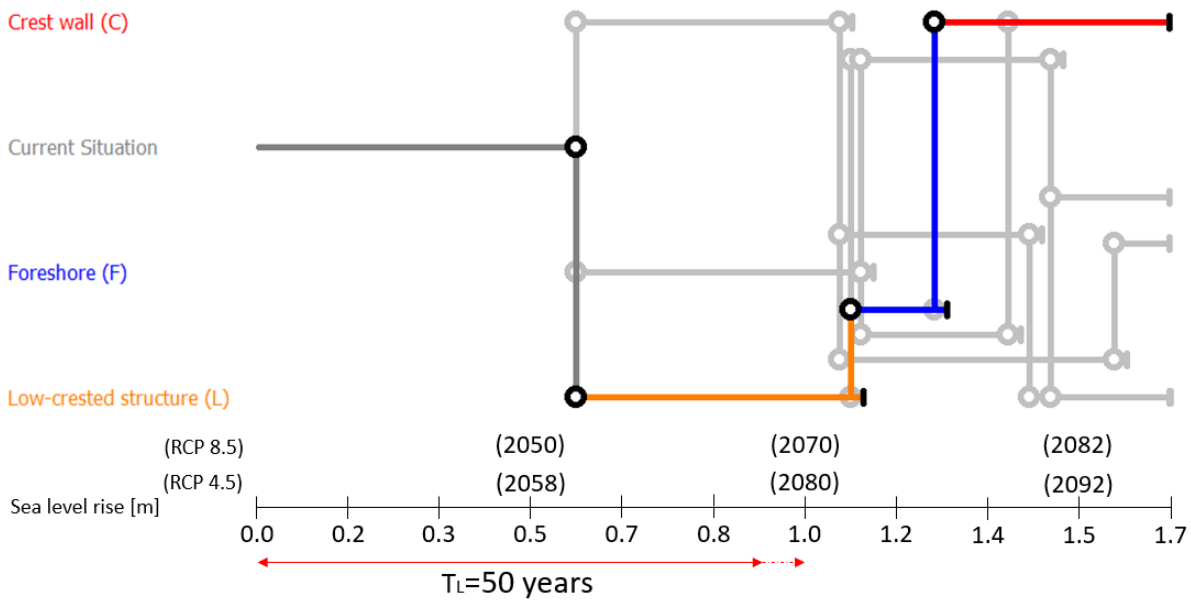

Figure 4.9: The economically most attractive adaptation paths based on the TAW overtopping equation

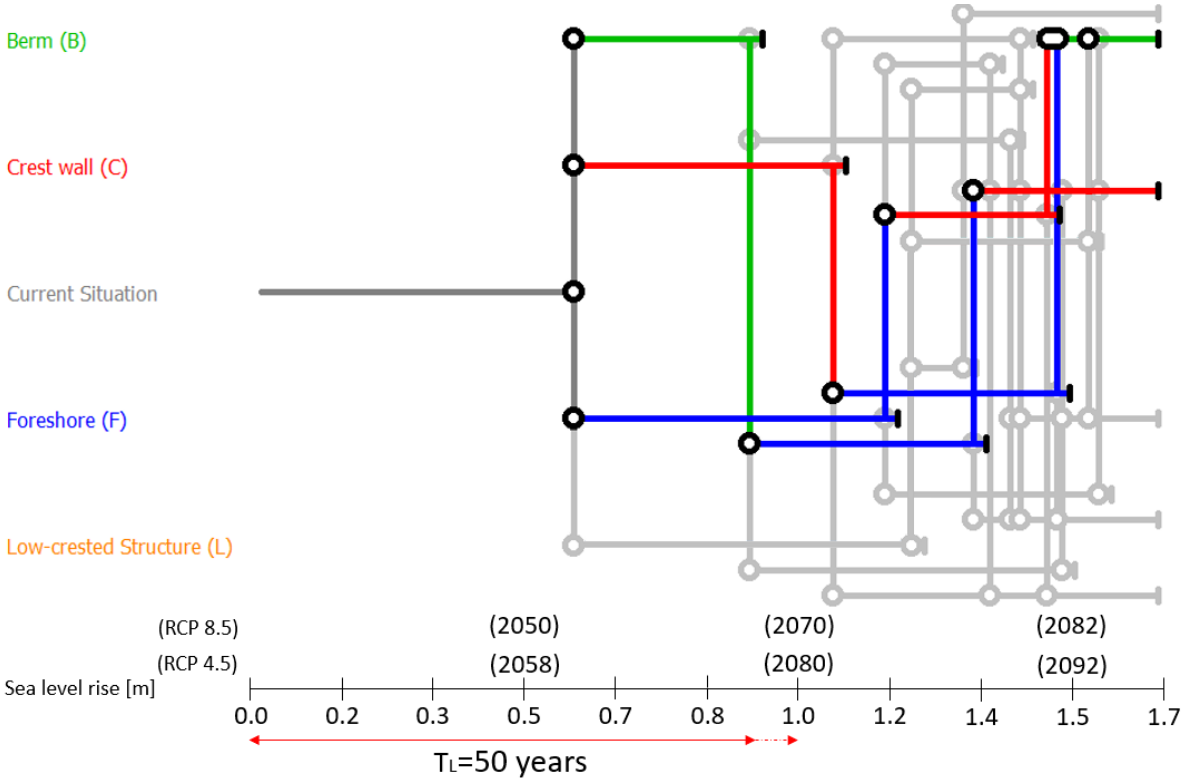

Figure 4.10: The economically most attractive adaptation paths based on the adapted TAW overtopping equation

5

Set-up OpenFOAM model

A numerical model is used to test the accuracy of current guidelines for combinations of solutions that limit wave overtopping. The model is configured for a base case without implementations before the combinations are implemented in the model. This chapter starts with the theoretical aspects necessary to set-up the model. Subsequently, the process of configuration is described. In the end, the model is evaluated against the theoretical outcomes. All the previous, describe the fourth methodological step.

5.1. Description of the OpenFOAM model

5.1.1. Background of numerical models for coastal structures

In the previous days, many physical models were applied for the assessment of a coastal structure, nowadays in addition to the physical models, a numerical model is used as well to optimize the initial design. Partly because physical models are expensive. Many of the formulas used in the initial design are based on empirical formulas, though it is not clear if the extrapolation of these formulas is always correct (Jacobsen et al., 2015). Often, these equations are used outside the validation range or are used in combinations that have not been tested in the experiments. Numerical models can remove much of the uncertainties following from this extrapolation of formulas. However, validation data is required for these models to be reliable.

For the application of breakwater structures, various models have been made in the past and included the interaction of irregular waves with these coastal structures. Jensen (2014) investigated overtopping and forces on crest elements because of irregular waves in OpenFOAM. OpenFOAM is a so-called open-source Computational Fluid Dynamics (CFD) software that can solve complex fluid flows, because it is a phase-resolving model the actual waves and set-up are described in detail. The OpenFOAM software is operated with the C++ programming library that allows using a lot of solvers and applications. The Navier-Stokes equation is most often used to solve these complex fluid flows. To account for permeable structures like the rubble mound breakwater, the Darcy-Forchheimer approximation is used (van Gent, 1995). Within the OpenFOAM software, the toolbox Waves2Foam (Jacobsen, 2012) can generate and absorb free surface waves and can deal with the interaction between the free surface waves and the permeable structure (Jensen, Jacobsen, et al., 2014). The waves are generated and absorbed in the relaxation zones in the model, the relaxation zones prevent reflecting waves from entering the model again.

5.1.2. Application of the OpenFOAM model

To investigate the uncertainties of empirical formulas for overtopping, the OpenFOAM software has been applied in this thesis. The choice to use OpenFOAM for this thesis is because many tools are available at the moment to describe the physical processes of waves in big detail. Based on the costs for combinations of solutions elaborated in Chapter 4 and combinations that are not validated in current guidelines, the solutions are computed in a numerical model to give more insight into the accuracy of empirical formulas.

In studies from Chen (2020) and van Gent (2019) it was already concluded that for a combination of solutions the current guidelines are not always accurate or validated for such combinations. Chen (2020) looked into the combination for increased roughness with a berm and proposed new equations for both. Also, for a combination of oblique waves with or without increased roughness, the empirical formulas in TAW (2002) and EurOtop (2007) seem inaccurate (van Gent, 2019). Accurate guidelines are very important to design coastal structures and adapt these if sea level rise becomes larger than currently designed for. The sequence of solutions that require extra research concerning the empirical formulas is computed in the OpenFOAM model. The results that follow from the model are used to compare them with the results from the current guidelines to give some more insight into the accuracy of those empirical formulas. If these empirical formulas indeed seem inaccurate, a certain path can become more or less economically attractive.

5.2. Theoretical aspects of the OpenFOAM model

This section describes the theoretical aspects that are included in the applied OpenFOAM model. Based on the theoretical aspects it is possible to use the model correctly. As stated in the section above, in recent years, a lot of research has been performed regarding porous media in OpenFOAM. These studies are studied in detail and are referred to where necessary in the remaining of this section.

5.2.1. Reynolds Averaged Navier-Stokes Equation

In OpenFOAM, the fluid flow is described by computing the Navier-Stokes equation. The Navier-Stokes (NS) equation consists of coupled differential equations, including the conservation of mass and conservation of momentum. This requires detailed information on the microscopic level, which is not desirable regarding computation time (Rusche, 2002). In OpenFOAM, often the Reynolds Averaged Navier-Stokes equations (RANS) are used, in which the influence of turbulence is included in the resistance term. The Reynolds stresses are modeled by the use of a turbulence model, e.g. an eddy-viscosity model ($\omega - k$) (Liu et al., 1999). If these equations are volume averaged, the influence of porous media like a breakwater is included. Because of this, the media can be seen as continuous and eliminates the need for detailed information about the geometry of the porous structure (van Gent, 1995, Losada et al., 2016). In Hsu (2002) this volume averaging approach was adopted and the turbulence inside the porous structure was included in the Darcy-Forcheimer equations. Jensen (2014) investigated the Volume-Averaged/Reynolds Averaged Navier-Stokes equations further and implemented the above in OpenFOAM as part of the waves2Foam toolbox. The final momentum equation is stated as (Jacobsen et al., 2015):

$$(1 + C_m)\frac{\delta}{\delta t}\frac{\rho \mathbf{u}}{n} + \frac{1}{n}\nabla \cdot \frac{\rho}{n}\mathbf{u}\mathbf{u}^T = -\nabla p^* + \mathbf{g} \cdot \mathbf{x}\nabla\rho + \frac{1}{n}\nabla \cdot (\mu + \mu_t)\nabla \mathbf{u} - \mathbf{F}_p \tag{5.1}$$

With:

$C_m =$ Added mass coefficient
$\mathbf{F}_p =$ Flow resistance, see section 5.2.2
$\rho =$ Density of the fluid
$p^* =$ Excess pressure ($p^* = p - \rho \mathbf{g} \cdot \mathbf{x}$)
$g =$ Gravitational acceleration
$n =$ Porosity
$\mathbf{x} =$ Cartesian coordinate vector (x,y,z)
$\mathbf{u} =$ Velocity field in Cartesian coordinates (u, v, w)
$\mu =$ Dynamic molecular viscosity
$\mu_t =$ Dynamic turbulent viscosity
$\nabla =$ Differential operator nabla:$(\delta/\delta x, \delta/\delta y, \delta/\delta z)^T$

Assuming incompressible flow, the continuity equation is defined as:

$$\nabla \cdot \mathbf{u} = 0 \tag{5.2}$$

For permeable structures the velocity field in Equation 5.2 is described as $\mathbf{u}_p = \mathbf{u}/n$, in which n is the porosity and $\mathbf{u}_p$ is the pore velocity (Jensen et al.,2014).

5.2.2. Resistance and turbulence terms

The influence of a structure inside the computational mesh is included via the Darcy-Forchheimer equation as a flow resistance term. Also, an extra term accounting for the inertia caused by the flow through the porous media is included as the added mass(C_m). The added mass is defined as:

$$C_m = \gamma_p \frac{1-n}{n} \tag{5.3}$$

Often, the empirical constant (γ_p) is set to 0.34 and was found as an average value in van Gent (1995). In Jacobsen (2015) almost no difference in outcome was observed when this parameter was set to 0.

The Darcy-Forcheimer flow resistance equation is divided into a laminar and a turbulent part, if only the laminar part is considered, the equation reduces to Darcy's equation. As the flow through porous media is considered, this is not the case in this thesis and can the Darcy-Forcheimer equation be described as:

$$\mathbf{F}_p = a\mathbf{u} + b\rho||\mathbf{u}||_2\mathbf{u} \tag{5.4}$$

The first term represents the laminar part and the second the turbulent part of the flow. Both include a resistance coefficient based on the dissertation research concluded by van Gent (1995). These coefficients are defined as:

$$\begin{aligned} a &= \alpha \frac{(1-n)^2}{n^3} \cdot \frac{\nu}{\rho \cdot d_{50}^2} \\ b &= \beta\left(1 + \frac{7.5}{KC}\right)\frac{1-n}{n^3} \cdot \frac{1}{d_{50}} \end{aligned} \tag{5.5}$$

With:

$\alpha, \beta =$ Closure coefficients based on the type and shape of grading
$d_{50} =$ Nominal grain size
$KC =$ Keulegan-Carpenter number
$\nu =$ Kinematic viscosity

Different values for the closure coefficients are found in the literature (Losada et al., 2016), but the results are all of the same order (Jensen, Jacobsen, et al., 2014). Therefore, the coefficients are assumed as recommended by van Gent (1995) with a value of: $\alpha = 1000$ and $\beta = 1.1$. As these values are found from measurements, the turbulence is already included. For this reason, Jensen (2014) concluded that the turbulence model (e.g. k, ω) is not necessary to compute the correct hydrodynamics at a porous structure. When one includes a turbulence model, these closure coefficients can no longer be used without overestimating the turbulence. However, as discussed in Losada (2016), when one wants to know the exact turbulence in a structure and not on a macroscopic level, a turbulence model should be included.

The Keulegan-Carpenter (KC) number describes the dimensionless ratio between the turbulence and the inertia because of oscillatory flow through the porous media (van Gent, 1995). For higher KC numbers, the turbulence becomes more important than the inertia. In Jacobsen (2015) the KC number was described as a hard parameter to estimate because of the rapid damping of the waves within the breakwater structure. However, the KC number is estimated based on the shallow water wave theory as:

$$KC = \frac{H_{m0}}{2}\sqrt{\frac{g}{h}}\frac{1.1T_{m-1,0}}{d_{50}} \tag{5.6}$$

5.2.3. Volume of Fluid method

In OpenFOAM, the free surface is tracked by the Volume of Fluid (VOF) method. The VOF method allows capturing detailed information on propagating and breaking waves. The amount of water and air in an individual computational cell is calculated according to the advection Equation 5.7 (Berberović et al., 2009). In OpenFOAM, the *IsoAdvection* solver is used to track the free surface.

$$\frac{\delta F}{\delta t} + \frac{1}{n}\nabla \cdot (\mathbf{u}F) + \frac{1}{n}\nabla \cdot [\mathbf{u}_r F(1-F)] = 0 \tag{5.7}$$

Where $\mathbf{u}_r$ is the vector of relative velocity and F represents the indicator function and can express the spatial variation properties in the fluid (e.g. ρ and μ). To include the porous structure in the VOF scheme, the velocity term in equation 5.7 is divided by the porosity. The indicator function is set to 1 if the computational cell is filled with water and 0 when filled with air. Therefore, the last term in the equation ($F(1-F)$) is zero for cells completely filled with water. Likewise, the density and viscosities are calculated according to this weighting (Jacobsen et al., 2015):

$$\begin{aligned} \rho &= F\rho_1 + (1-F)\rho_0 \\ \mu &= F\mu_1 + (1-F)\mu_0 \end{aligned} \tag{5.8}$$

In which the indices refer to the properties of air and water. In Figure 5.1 an example of such a computational cell is shown. As the VOF method can not exactly calculate where the water or air is located in the cell and only the fraction of both, it is clear that a finer mesh around the water line would predict the actual wave in a better way.

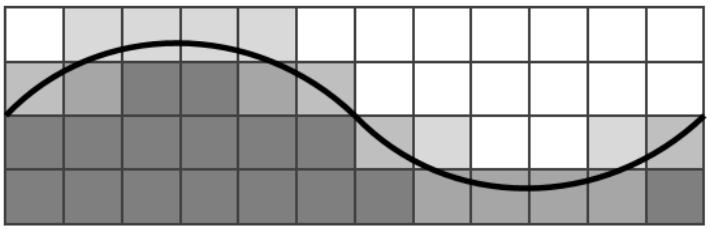

Figure 5.1: Volume of Fluid method, the darker the color the more water is captured in the computational cell

5.2.4. Relaxation zones

Waves can be generated and absorbed in different manners in a computational model and play an important role in the correct prediction of waves at the structure. For example, the generation and absorption of waves could be implemented in the model via wave peddles. Like the wave paddles in the flume, the paddle is corrected for reflection and other disturbances. However, in Jacobsen (2012) another possibility has been elaborated. At both the inlet and outlet of the computational mesh, a relaxation zone is implemented to avoid reflection of waves at the boundaries.

One advantage of this method is that there is no volume build-up as the target water level is retained in the relaxation zones. Also, this method is relatively easy to implement compared to wave paddles. A disadvantage of the relaxation zones is the required minimum length to correctly generate and absorb the waves. Therefore, the computational mesh increases in size. Consequently, the computation time also increases. The process of wave generation in the relaxation zone is described according to Equation 5.9.

$$\phi = \alpha_R \phi_{computed} + (1-\alpha_R)\phi_{target} \tag{5.9}$$

Where the relaxation function (α_R) is defined as:

$$\alpha_R(\chi_R) = 1 - \frac{\exp(\chi_R^{3.5}) - 1}{\exp(1) - 1} \quad \text{for: } \chi_R \in [0;1] \tag{5.10}$$

In which χ_R is the uniformly scaled x-coordinate and increases linearly from 0 at the left (or right at the outlet) boundary to 1 at the interface between the relaxation zone and the computational domain.

The weighting of ϕ is performed on either the **u** or the indicator function F. The relaxation function is such that at the interface between the relaxation zone and the main computational grid, the α_R is 1. Therefore, the target value vanishes at the interface and only the computed value remains. Figure 5.2 shows a sketch of the relaxation zones. As a first estimation is the length of the inlet is approximately one wavelength long and the length of the outlet is half of this.

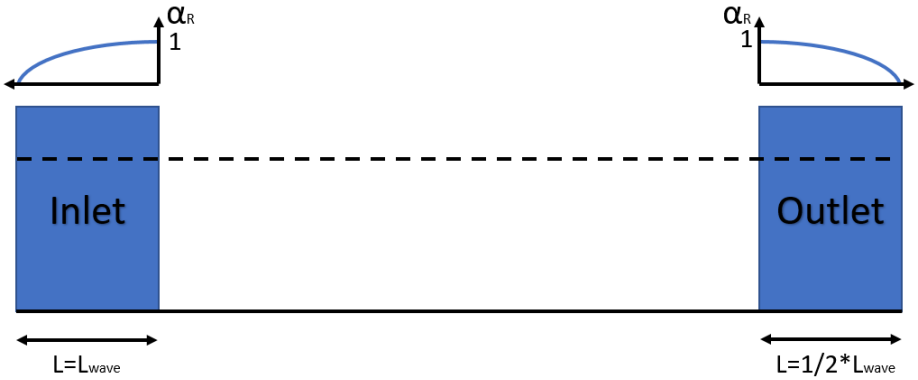

Figure 5.2: Relaxation zones, including the distribution of the weight

5.2.5. Irregular waves

The applied wave component in this thesis is irregular, with a JONSWAP spectrum and a peak enhancement factor of 3.3. This wave component is divided into an incident component and a reflective component because of the breakwater and is discussed in more detail in Section 5.5.2, in which the wave signal is configured. At the free surface, the wave component is described according to the first-order Stokes theory as (Jacobsen, 2017):

$$\eta = \sum_{i}^{N} a_i \cos\left(\omega_i - \mathbf{k}_i \cdot \mathbf{x} + \phi\right) \tag{5.11}$$

With:

$\eta =$ Surface elevation
$N =$ Number of wave components
$a_i =$ Amplitude of the i'th wave component
$\omega =$ Wave Frequency
$\mathbf{k} =$ Wave number vector
$\phi =$ Phase

Where both the amplitude and frequency depend on the spectral shape. To get a good representation of the wave, 100-500 wave components are often used. Within the *waveInput* file in OpenFOAM, the wave signal is cosine stretched, therefore the discretization of the spectrum close to the peak is finer and better described (Jacobsen, 2017). As described in Chapter 2, the corresponding wave height and period are determined based on the wave spectrum. This allows calibrating the wave spectrum at the toe of the structure in OpenFOAM with the used empirical parameters to determine the adaptation paths in Chapter 4.

5.2.6. Wave overtopping

In OpenFOAM, it is possible to track the overtopping as a run-time sample. Therefore, detailed information about the overtopping rate is available after the computation. To do so, a cell face at the crest of the breakwater is marked as the location to compute the wave overtopping output. Within the wave2Foam toolbox, three types of fluxes are available at the cell face (Jacobsen, 2017). However,

only one flux is interesting for the prediction of overtopping. This is the flux of water across the face multiplied with the indicator function (F=1 for water). The function of all cell faces together which are necessary to determine the complete overtopping is defined as:

$$\mathbf{q} = \sum \phi_{F,f} \frac{\mathbf{S}_f}{||\mathbf{S}_f||_2} \tag{5.12}$$

Where ϕ_F, f is defined as the flux of water through the cell face as defined in Figure 5.3. The flux is positive in the direction of the normal vector $\mathbf{S}_f$. The sum of each time step together gives the total overtopping volume.

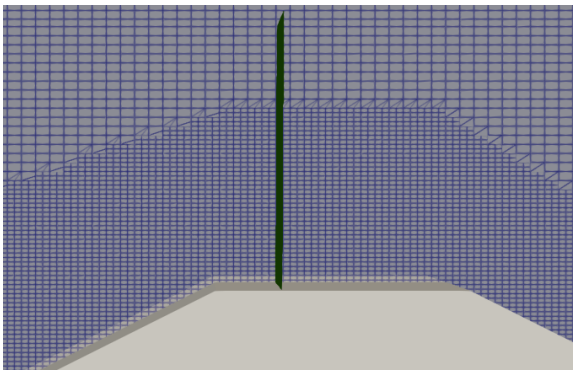

Figure 5.3: Side view: overtopping face on top of the crest

5.2.7. Courant number

The Courant Friedrich-Lewy (CFL) condition is necessary to accomplish convergence of a finite difference scheme (Zijlema, 2015). If this condition is not met, divergence could occur for the solution. For explicit methods, the CFL conditions should always be smaller than 1 to ensure stability and accuracy. The CFL condition for 1D is defined as:

$$C = \frac{u\Delta t}{\Delta x} \leq C_{max} \tag{5.13}$$

In which u is the magnitude of the velocity, Δt the time step and Δx the length interval. As can be seen, is the maximum time step limited by this condition. Because OpenFOAM solves implicit (solving with the next time step, e.g. Euler scheme), the maximum courant number can be higher than 1 to ensure stability. However, if the courant number is much larger than 1 the accuracy decreases significantly as a larger time step misses out much of the information. For this reason, the maximum courant number is taken as 0.8 in this thesis.

5.3. Model set-up

5.3.1. Properties computational mesh

The total size of the mesh, including the inlet and outlet, is 210 meters in length and twenty meters in height (210m x 20m). Within the mesh, about 98762 cells are included with each a length and height depending on the location in the mesh. The cell size should not be too big because important information about the physical processes occurring in the model could be under- or over- estimated. The ideal aspect ratio ($\Delta x/\Delta y$) of each cell is one. However, if the cell size is very small, the computation time significantly increases and therefore the ratio is slightly lower than 1 in this thesis. The individual grid size is shown in Table 5.1 (Without refinement). In Section 5.5.5 the influence of different grid sizes on the wave spectrum and the overtopping rate is evaluated. Depending on the results, the applied grid might change. To predict the behavior of the waves as accurately as possible with the VOF method (Section 5.2.3), the mesh around the still water line has been refined two times with the *snappyHexMesh* tool (Mesh tool OpenFOAM). Additionally, the mesh is refined across the crest of the breakwater. To correctly simulate the interaction between structure and wave. The mesh defined in *blockMesh* (mesh tool OpenFOAM) is divided into three blocks on top of each other in which the water

surface part is the middle block and contains approximately the area between the highest crest and lowest trough of the wave. Because this area is important to predict the physical processes, the cells are finer compared to the atmospheric and wet block (Below the waves). Also, the mesh is divided into three blocks because different refinements are applied depending on the area of interest. In Figure 5.4 the used mesh refinement is shown around the rubble mound structure. Figure 5.5 shows the grid in total size. The refinement area starts after the inlet relaxation and reaches just after the crest of the breakwater. The axes are orientated such that the Z-direction is pointed into the mesh.

Refinement	**Δx [m]**	**Δy [m]**	**Δz [m]**	**# Cells**
Wet block	0.25	0.53	0.020	15 120
Surface block	0.25	0.12	0.020	48 720
Atmospheric block	0.25	0.57	0.020	5 040

Table 5.1: Numerical discretisation of the OpenFOAM model

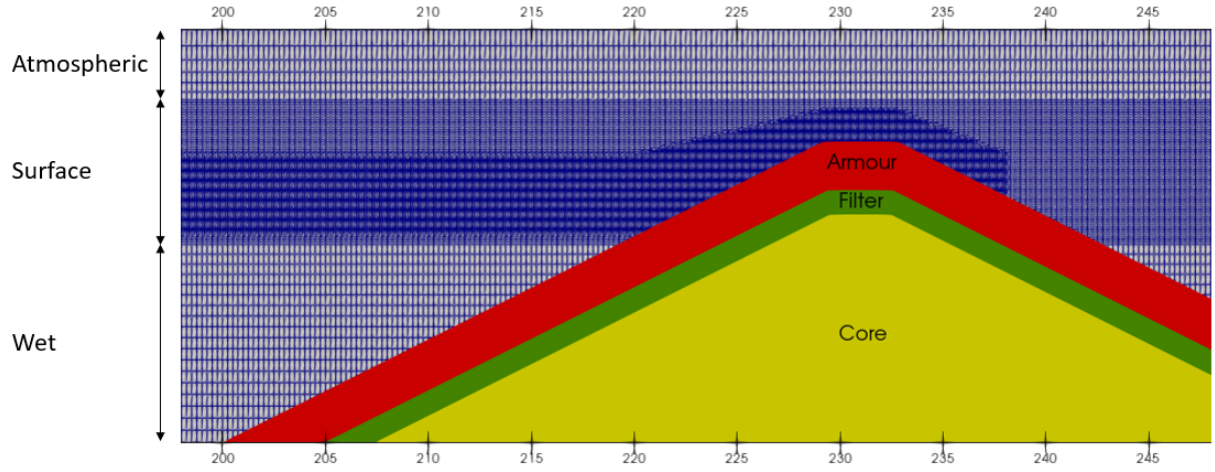

Figure 5.4: Overview mesh around the structure

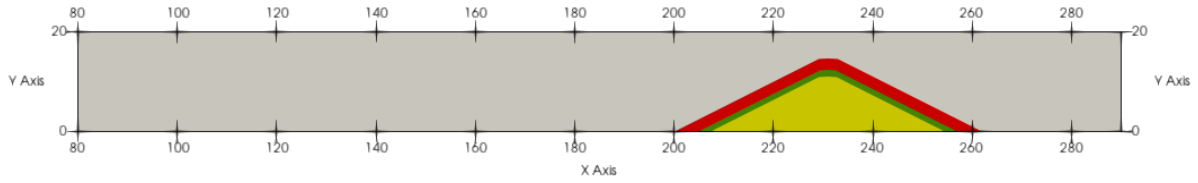

Figure 5.5: Configuration of the grid in OpenFOAM

5.3.2. Properties of the Rubble mound breakwater

Some properties are already discussed in short in the previous sections but are summarized again in this section in a table. The rubble mound breakwater consists of three different layers, i.e. the armour- and filter layer and the core. The porosity (n) of each layer is defined as 0.4. As stated in Section 5.2.2, the closure coefficients (α, β) adopted by van Gent (1995) proved to be a good estimation for different ranges of data sets Jacobsen (2018). As such, the same closure coefficients are used in this thesis. Also, because of the lack of experimental data for this thesis, these parameters can not be calibrated in detail. The rock sizes used in the different layers are the same as derived in the assessment of the academic case in Chapter 3. All parameters used as the starting point for the computations and configuration of the academic case are summed in Table 5.2. Additionally, the added mass term required for the resistance term of the averaged Navier-Stokes equation is set to 0.34.

	α [-]	β [-]	n [-]	KC [-]	Dn50a	Dn50f	Dn50c
Rubble mound breakwater	1000	1.1	0.4	1000	1.18	0.59	0.21

Table 5.2: Parameters applied on the breakwater in the OpenFOAM model

5.3.3. Boundary conditions

In OpenFOAM, three types of boundary conditions are specified to describe the flow; the phase, the velocity and the pressure. For each patch, a condition is applied, where the patches are specified in the *blockMesh* file in OpenFOAM. The irregular waves are generated and absorbed in the relaxations zones as discussed in Section 5.2.4. In the inlet relaxation, 500-1000 waves are generally generated to simulate an irregular wave spectrum. The applied boundary condition for flow at the bottom and contact with the crest wall is the slip (symmetry) condition. The atmospheric boundary condition allows water and air to flow out of the numerical mesh, but only air can flow back in again (Jacobsen et al., 2018).

If a wave wall is implemented in the model an extra condition is included to prevent that air becomes trapped between the water and the wall. Because of this entrapment, the wave forces are much bigger compared to a situation in which air is allowed to escape. In Jacobsen (2018) this entrapment was investigated and a ventilated boundary condition was suggested for the validation of wave forces. This allows air to flow in and out between the water and the impermeable wave wall. The new boundary condition included an openness of the structural element and a loss coefficient. In Jacobsen (2018) an openness of 3% proved to be the most accurate for the tested data sets. As no data sets are available for this thesis, the openness of 3% is also applied if a wave wall is implemented in the solution.

5.4. Set-up adaptation measures

As discussed in Chapter 4 a total of four different adaptation measures are evaluated. For the berm and crest wall, the computational grid remains the same and is computed as shown in Figure 5.6.

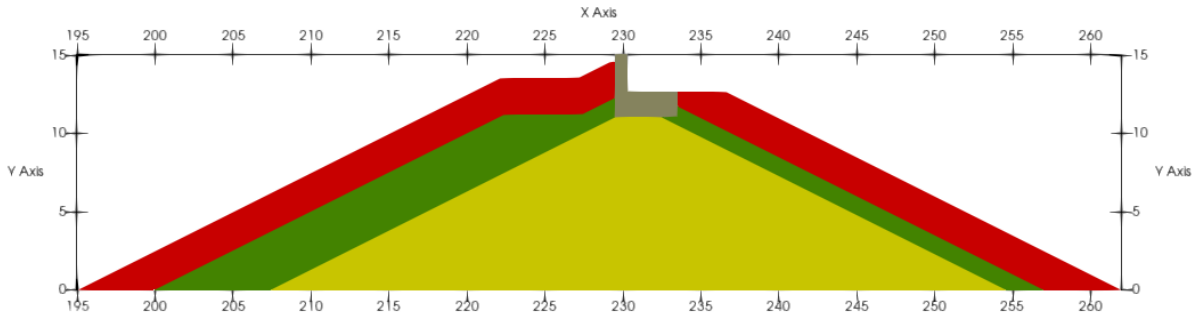

Figure 5.6: Configuration of a berm and crest wall in OpenFOAM

For both the low-crested structure and the increased foreshore, the computational grid as determined in Section 5.3.1 should be increased. If the low-crested structure is implemented, the grid increases by 80 meters. Because of the increase, there is enough space to compute the waves in the inlet and to adapt to the new situation in which the wave height is reduced. In Figure 5.7 this situation is shown, including a crest wall and berm at the original breakwater.

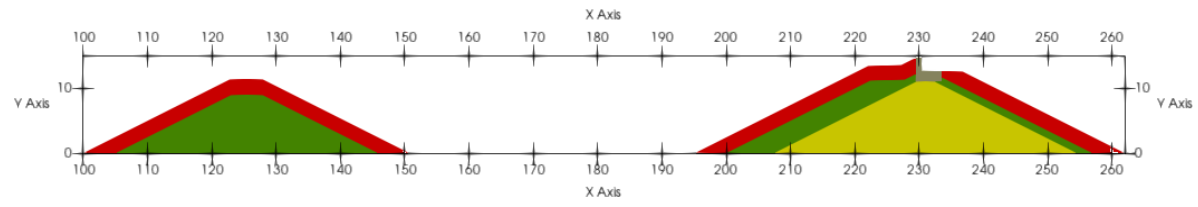

Figure 5.7: Configuration of a Low-crested structure in OpenFOAM

If the foreshore increases, the grid increases also because of the required gradual change from the deeper water (12.5 meters) to the new water depth. With a water depth of 5 meters and an assumed foreshore slope of 1:50, the minimal required increase in grid is 375 meters, which is almost 200% of the current grid length (210 meters).

5.5. Calibration of the numerical model

Often, a numerical model is calibrated to experimental data executed in the wave flume for example. If this is the case, the model can be calibrated for wave height and reflection at the toe of the structure. However, for this thesis, no experimental data is available and an academic case study is applied. Therefore, the calibration process is limited to the wave parameters used for the calculation of the overtopping with the empirical equations. The configuration process consists of four steps:

- Configure the wave spectrum at the toe of the structure
- Evaluate number of simulated waves
- Evaluate overtopping rate
- Evaluate change of cell size

5.5.1. Approach for configuration

For the set-up of the adaptation pathways in Chapter 4 a JONSWAP (developing wind sea) spectrum with a spectral wave height (H_{m0}) of 2.5 meters and a spectral period ($T_{m-1,0}$) of 8.15 seconds is applied. The configuration process is done such that the spectrum initiated in the inlet generates the same wave characteristics at the toe of the structure as applied in Chapter 4. To do so, the waves should not break as this will alter the spectrum. The initiated JONSWAP spectrum is shown in Figure 5.8. In the OpenFOAM model, a constant wave seed is used such that the same phase and wave train are reproduced for each unique computation.

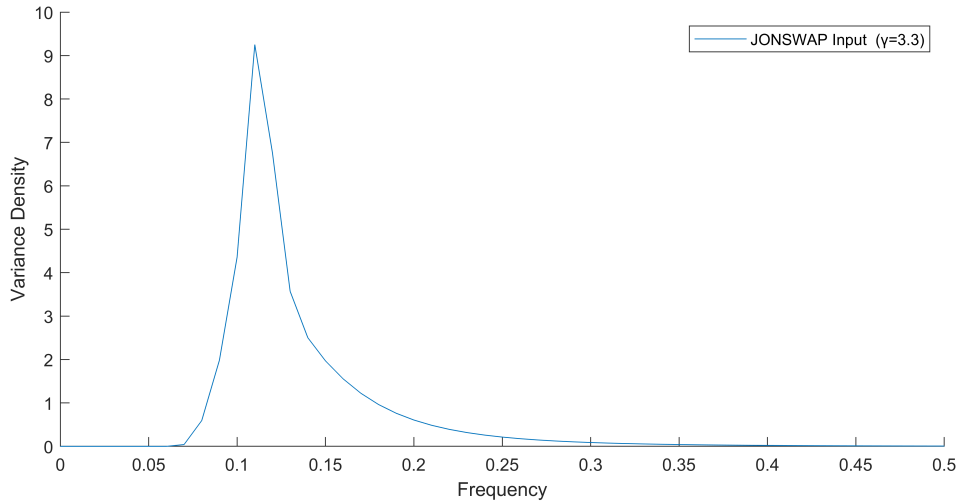

Figure 5.8: Initiated JONSWAP spectrum with a peak enhancement factor (γ) of 3.3

5.5.2. Configuration of the wave height

The objective of the configuration process is to get the same wave spectrum at the toe of the structure as used in the assessment of the adaptation paths in Chapter 4. As stated, the waves should not break too much as this will alter the spectrum. Because the spectrum at the toe consists of both incoming and reflected waves, the spectrum is significantly different. Zelt investigated this process and derived a set of equations to separate the incoming and reflective waves (Zelt and Skjelbreia, 1992). This theory is based on the surface elevation simulated at three locations or more. When only three wave gauges are evaluated, this theory is the same as investigated by Mansard (1980) who applied a least-squares approach with uniform weighting to solve wave direction. Also, the wave gauges should not be evaluated

at the half wavelength of each other ($|x_2 - x_1| \neq n\lambda_j/2$). This criterion should be taken into account when choosing the locations of the wave gauges and for the correct prediction of the frequencies.

Based on Zelts equations, the waves in the OpenFOAM model are divided into an incident wave and a reflective wave. Subsequently, only the incident wave is of importance for the correct configuration. In OpenFOAM, 30 non-equidistant wave gauges are placed between 0 and 20 meters offshore of the rubble mound structure (See Figure 5.9). By doing so, different sets can easily be checked on the correct configuration of the spectrum. Below the overview of the computational domain, the idea of configuration is shown, for which both spectra are almost the same. It may not possible to have identical spectra just after the inlet and at the toe of the breakwater because of some small wave breaking. Therefore, the spectral parameters including steepness at the toe of the structure, are compared with the theoretical parameters. If these parameters are of the same order, the configuration can be seen as successful.

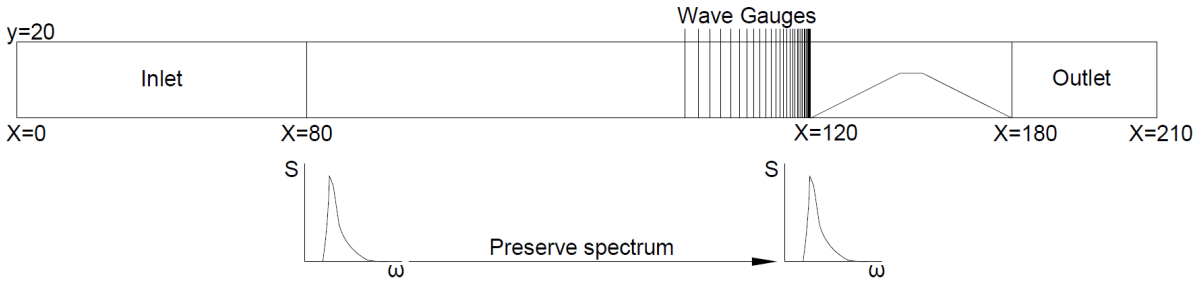

Figure 5.9: Overview computational mesh including the Wave Gauges

The applied JONSWAP spectrum in the academic case (Chapter 3) has a spectral wave height (H_{m0}) and spectral mean period ($T_{m-1,0}$) of 2.5 meter and 8.15 seconds. This theoretical spectrum is also defined in Table 5.3, together with the first configuration steps. As can be seen, when in the OpenFOAM model a spectrum with the same parameters has been applied, as in the academic case, the final spectrum differs a lot because of small wave breaking. For example, because of the superposition of the initial and reflective wave, the maximum steepness is exceeded and therefore waves start to break a bit. To preserve almost the same spectral parameters at the toe of the structure as applied in the academic case study, the initial spectral wave height at the end of the relaxation zone is increased by a certain percentage. Because of the small amount of energy dissipating out of the spectrum, the same spectrum occurs at the toe of the breakwater. Initially, the spectral wave height is increased with relatively big steps of 13, 14 and 15% (See Table 5.3 for the results).

	H_{m0} input [m]	H_{m0} [m]	%	$T_{m-1,0}$ [s]	%	T_p [s]	%	s [-]	%
Theoretical JONSWAP	2.50	2.50	-	8.150	-	8.965	-	0.0311	-
H250T082+0%	2.50	2.42	-3.34	8.163	0.16	8.901	-0.72	0.0300	-3.54
H250T082+13%	2.90	2.75	11.27	8.168	0.22	8.906	-0.66	0.0342	9.97
H250T082+14%	2.93	2.78	11.94	8.151	0.02	8.907	-0.64	0.0346	11.25
H250T082+15%	2.95	2.82	12.82	8.157	0.08	8.906	-0.66	0.0348	12.86

Table 5.3: Configuration steps to the correct spectral parameters

The wave parameters for the initial increase in wave height seem not to be sufficiently accurate, therefore a lower percentage is initiated at the inlet. The final configuration results are shown in Table 5.4. If the wave height has an initial increase of 4%, the final wave parameters at the toe of the structure are approximately of the same order as applied in the academic case study. With the 4 percent increase in spectral wave height at the inlet of the OpenFOAM model, all the important parameters are within 1% of the theoretical spectrum. The number of simulated waves might alter the wave spectrum. Therefore, the effect of the number of generated waves is evaluated in the next section. In general, 500-1000 waves should be enough to correctly represent the spectrum.

	H_{m0} input [m]	H_{m0} [m]	%	$T_{m-1,0}$ [s]	%	T_p [s]	%	s [-]	%
Theoretical JONSWAP	2.50	2.50	-	8.150	-	8.965	-	0.0311	-
H250T082+3%	2.58	2.48	-0.79	8.158	0.10	8.902	-0.70	0.0309	-0.79
H250T082+4%	2.60	2.51	0.20	8.158	0.10	8.903	-0.69	0.0311	0.20
H250T082+5%	2.63	2.52	0.95	8.155	0.06	8.902	-0.71	0.0314	0.95
H250T082+6%	2.65	2.54	1.77	8.163	0.16	8.902	-0.70	0.0316	1.77

Table 5.4: Further configuration of the correct spectral parameters

Figure 5.10 shows the incident wave spectrum as computed in the OpenFOAM model using the Zelt & Skjelbreia (1992) method to separate the incident and reflective wave. As can be seen in the figure are the peaks for both the computed and theoretical JONSWAP of the same order. The computed spectrum has a small tail at higher frequency waves compared to the original JONSWAP, with a peak enhancement factor of 3.3. It should be noted that the waves might be less affected by dissipation for higher sea levels and therefore, the spectrum can slightly differ if the model is computed with a larger water depth. If this difference becomes too large, the configuration step should be performed again.

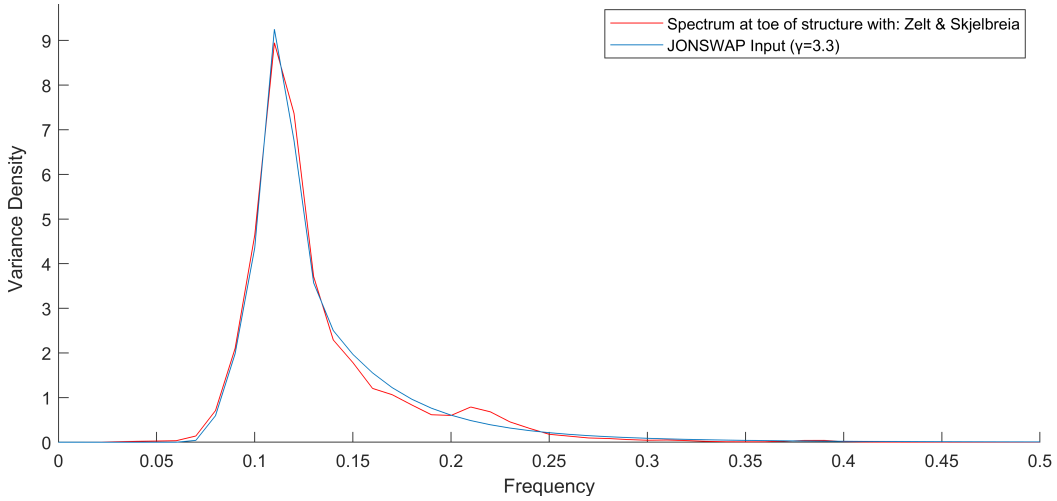

Figure 5.10: Comparison of the computed and theoretical spectrum at the toe of the breakwater

5.5.3. Evaluate number of simulated waves

In this section, the influence of the number of simulated waves is evaluated. To get a good representation of the spectrum, at least 500-1000 waves should be simulated. If this is less, the bigger waves may not have occurred yet and the spectrum is underestimated. However, the number of waves simulated determines the computation time. The total time simulated is defined approximately as (not the actual computation time):

$$T_{total} = T_{m-1,0} \cdot N_{waves} \tag{5.14}$$

Thus, if 500 waves are evaluated with a mean period of 6 seconds, the total time simulated is 3000 seconds. In Williams et al., 2014 a large number (5000) of simulated waves was compared to smaller numbers (500) and was concluded that for numbers larger than 500-1000 there was almost no difference in results. To verify this, a simulation of 750 and 1000 waves is compared to a simulation of 500 waves. For the simulation with 750 or 1000 waves, the spectral wave height (H_{m0}) is slightly lower

	H_{m0} input [m]	H_{m0} [m]	%	$T_{m-1,0}$ [s]	%	T_p [s]	%	s [-]	%
Theoretical JONSWAP	2.50	2.50	-	8.150	-	8.965	-	0.0311	-
H250T082 500 waves	2.60	2.51	0.20	8.158	0.10	8.903	-0.69	0.0311	0.20
H250T082 750 waves	2.60	2.49	-0.49	8.159	0.11	8.878	-0.97	0.0309	-0.64
H250T082 1000 waves	2.60	2.48	-0.68	8.141	-0.11	8.849	-1.30	0.0310	-0.32

Table 5.5: Difference in number of simulated waves

than the required spectral wave height of 2.5 meters (Table 5.5). For the seed used (generated phases

and wave trains) the higher waves are generated within the first 500 waves. In the second half, the generated waves are slightly lower, causing the decrease in spectral wave height. Therefore, it is also expected that the simulated average wave overtopping is lower in the second half of the computation (563 l/s/m over 610 l/s/m). However, as all the important parameters in the table are of the same order it can be assumed that 500 waves give a good representation of the wave spectrum.

5.5.4. Evaluate overtopping

Because the wave spectrum at the toe of the structure is configured, the overtopping rate can be evaluated. As the accuracy of current guidelines is checked in this thesis, the overtopping rate can differ from what is being expected. Also, because of the lack of experimental validation data, the different applied theoretical guidelines and OpenFOAM can not be calibrated further at the moment and certain assumptions regarding the parameters are made (Section 5.3.2).

In Figures 5.11 and 5.12 the evaluation of the overtopping rate in OpenFOAM compared to current guidelines is computed. The confidence intervals are plotted with the standard deviation given in the applied guidelines (TAW 2002 and Krom, 2012). As can be seen, the computed overtopping rate differs a factor of 7 to 12 times the theoretical overtopping. This is quite a big difference and almost continuous overtopping is present for the base case with no implementations. As stated, this can be because of multiple assumptions made in Section 5.3.2 regarding the structural properties. Because of the lack of experimental data, it is not possible to calibrate the model further. However, it is possible for the remainder of this thesis to evaluate the influence of different adaptations on the overtopping rate. Therefore, it is evaluated if the overtopping difference becomes larger or smaller when one of the four possible adaptions is implemented in the model.

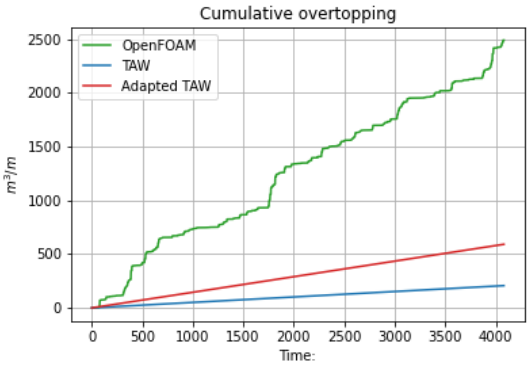

Figure 5.11: Cumulative overtopping OpenFOAM versus current guidelines

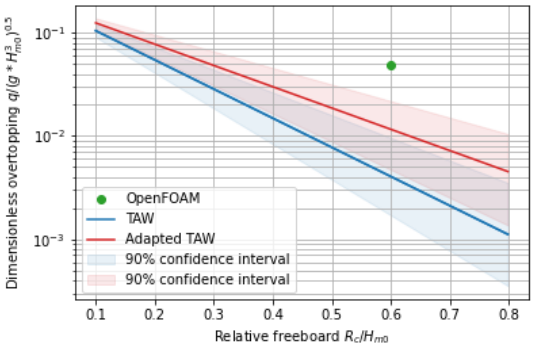

Figure 5.12: Comparison dimensionless overtopping OpenFOAM versus current guidelines

In Table 5.6 the calculated average overtopping rates according to the guidelines and OpenFOAM are presented. As was already concluded in the figures above does the average overtopping rate differs for the theoretical and computed case. In the table also the conditions applied for the overtopping calculations in both the theoretical guidelines and OpenFOAM model are presented.

	R_c [m]	SLR [m]	h [m]	H_{m0} [m]	q [l/s/m]	$q_{OpenFOAM}/q_{theoretical}$ [-]
TAW	1.5	0.6	13.1	2.505	50.67	12.04
Adapted TAW	1.5	0.6	13.1	2.505	84.15	7.25
OpenFOAM	1.5	0.6	13.1	2.505	610.04	-

Table 5.6: Comparison between the applied guidelines and OpenFOAM

5.5.5. Evaluate change of cell size

Not only the number of simulated waves has an influence on the wave spectrum at the toe. Also, different cell sizes can alter the output of the spectrum. The limitation of smaller cell sizes is the number of extra iterations during the computation of the model. As a consequence does the simulation time

increase. Contrastingly, the cell size should not be too big, as important physical processes are not correctly included in the model.

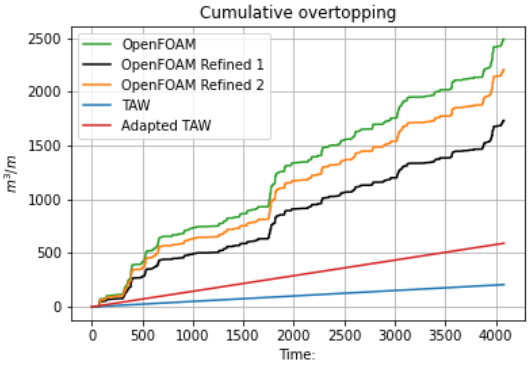

Figure 5.13: Cumulative overtopping OpenFOAM versus current guidelines

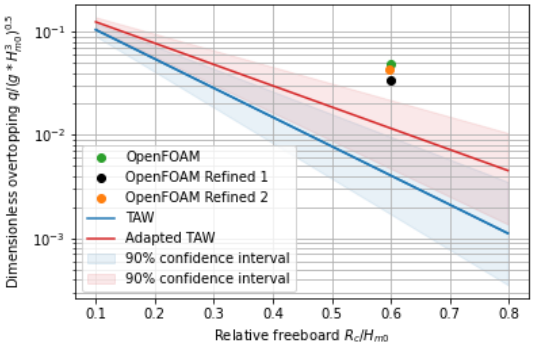

Figure 5.14: Comparison dimensionless overtopping OpenFOAM versus current guidelines

In Figure 5.13 and 5.14 can be seen that for a refined mesh with approximately 127.000 cells, the overtopping rate is slightly lower ($\approx$ 70 l/s/m) compared to the original mesh. In Table 5.7 the different refinement details are presented. With the applied grid sizes, there are approximately 300-400 cells per wavelength. As no experimental data is available, it is impossible to determine the best cell size in the OpenFOAM model. However, for an aspect ratio of 1 (dy/dx) the physical processes are often better captured. The most refined case gave no significant change in output compared to *Refined 1* and therefore the refined grid with a cell size of 0.25 will be used in the remaining of this thesis. This cell size also decreases the simulation ($T_{simulation}$) time by almost 14 hours. For the refined cases, it was verified that the wave spectrum remains constant.

	# Cells	Δy [m]	Δx [m]	AR [-]	$T_{simulation}$ [hr]	q [l/s/m]
H250T082 Configured	98762	0.12	0.25	0.5	46	610.04
H250T082 Refined 1	80862	0.25	0.25	1	32.5	424.63
H250T082 Refined 2	126982	0.2	0.2	1	70	540.44

Table 5.7: Comparison between the different cell sizes

5.6. Conclusions on the applied and configured OpenFOAM model

To analyze the accuracy of current guidelines in a numerical model, the model should first be configured. This chapter is used to describe the setup of the OpenFOAM model. In Figure 5.15 the final set-up is presented. The inlet and outlet are used to generate and absorb waves and do also prevent reflecting waves within the model.

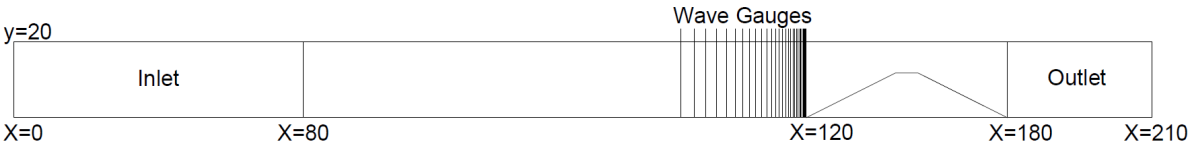

Figure 5.15: Overview computational mesh including the Wave Gauges

Subsequently, the model as derived based on the performed checks is summarized in this section. Again, the performed steps are:

- Configure the wave spectrum at the toe of the structure
- Evaluate number of simulated waves

- Evaluate overtopping rate
- Evaluate change of cell size

The configuration step applied in Section 5.5.2 shows that the wave height initiated at the inlet should be increased by 4% to preserve the same spectrum at the toe of the structure as applied for the adaptation paths in Chapter 4 ($H_{m0} = 2.5m$ and $T_{m-1,0} = 8.15s$). Therefore, the wave height at the inlet is 2.60 meters with a mean wave period of 8.15 seconds. As no validation data is available for this thesis, the previous is the only calibration step executed for the OpenFOAM model.

Besides the configuration of the wave hydrodynamics, three evaluation steps were performed. In Section 5.5.3 is found that a simulation of 500 waves gave a good representation of the wave spectrum and a simulation with more generated waves (750 or 1000) is not necessary.

Next, based on the evaluated and configured wave spectrum at the toe of the structure, the wave overtopping was evaluated at the top of the crest (Section 5.5.4). For both applied theoretical guidelines (TAW 2002 and Krom, 2012) the overtopping rate is underestimated compared to the OpenFOAM simulation with a factor between 7 and 12. Because the accuracy of current guidelines is tested in this thesis, there is a possibility that the current guidelines are indeed not accurate enough. However, because of the lack of validation data, the model is not calibrated for the structural parameters. The lack of this data could also cause the difference in the overtopping rate. Therefore, in Chapter 6 the influence of an adaptation in OpenFOAM has been compared relative to the influence in current guidelines.

The final evaluation step performed is the influence of the cell size in Section 5.5.5. The physical process of a wave is best captured with an aspect ratio ($\Delta y/\Delta x$) of 1. Again, because of the lack of validation data, it is hard to determine the best cell size. However, the computations with a cell size of 0.25 meters in width and height gave the lowest overtopping rate and computation time. Also, the discrepancy with the other refinement which uses an aspect ratio of one was negligible. Table 5.8 presents the final numerical discretization applied in OpenFOAM. Because different refinements are applied depending on the important areas (e.g. water surface), the mesh is divided into three blocks. See Section 5.3.1 and Figure 5.4 for the exact definition of the different blocks.

Refinement	**Δx [m]**	**Δy [m]**	**Δz [m]**	**# Cells**
Wet block	0.25	0.26	0.020	31 920
Surface block	0.25	0.25	0.020	23 520
Atmospheric block	0.25	0.26	0.020	10 920

Table 5.8: Final numerical discretization applied in the OpenFOAM model

The remaining parameters which are applied in the OpenFOAM model are presented in Table 5.9. These structural parameters are used to simulate the flow through porous media and are not calibrated further in this research because of the lack of validation data. The closure coefficients (α, β) are investigated in more depth in van Gent (1995) together with the applied added mass (C_m) term of 0.34. The applied rock sizes are elaborated in the academic case study in Chapter 3.

	α **[-]**	β **[-]**	**n [-]**	**KC [-]**	$\mathbf{D_{n50a}}$	$\mathbf{D_{n50f}}$	$\mathbf{D_{n50c}}$
Rubble mound breakwater	1000	1.1	0.4	1000	1.18	0.59	0.21

Table 5.9: Parameters applied on the breakwater in the OpenFOAM model

6

Application of adaptive pathways in OpenFOAM

This chapter describes the final and fifth methodological step. The accuracy of current guidelines is tested in the OpenFOAM model. In Chapter 5, the model set-up and configuration is presented. First, the equation proposed by the TAW (2002) is evaluated against the OpenFOAM computations. Next, the adapted overtopping equation proposed by Krom (2012) is evaluated. At the end of this chapter, a conclusion about the accuracy of both methods for the evaluated path is presented. Moreover, the conclusion answers the second research question.

6.1. OpenFOAM

6.1.1. Different OpenFOAM simulations

The adaptive approach performed in Chapter 4, analyses two case studies. The case studies are based either on the original TAW overtopping equation or on the adapted TAW overtopping equation. The biggest difference between both of the case studies is the crest height. The analyzed path is computed for both case studies. Subsequently, the effects compared to guidelines are presented. Again, the case studies are referred to as Case 1 or Case 2. The corresponding sea level rise (in centimeters) and adaptation is referred to as: Case X-Adaptation+Sea level rise (e.g. Case1-B060), where the adaptation is expressed with the first letter of a solution: Berm(B), Crest wall(C), Foreshore(F) and Low-crested structure(L).

6.1.2. OpenFOAM without adaptation measures

As reported in Chapter 3, there is an initial safety of 0.6 meters included in the crest height before the first adaptation measure is constructed. This section evaluates the OpenFOAM results for the situation without a berm, crest wall, foreshore or low-crested structure.

Figure 6.1 presents the difference between the results in OpenFOAM and the theoretical guidelines. The terms TAW and Adapted TAW (ATAW) represent the different theoretical guidelines. In Table 6.1, the differences between the computed and predicted values for the two different scenarios are presented. Both the predicted values based on the theoretical guidelines are underestimating compared to the OpenFOAM results. The adapted equation predicts higher overtopping rates for the same crest height compared to the overtopping equation proposed by the TAW (2002). This difference in overtopping rate is caused by the different influence of roughness. As the OpenFOAM model computes higher overtopping rates, the discrepancy with the adapted TAW equations is smaller compared to the original TAW equations.

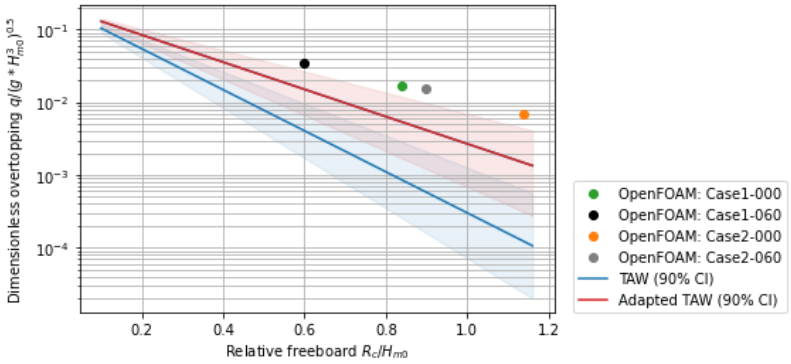

Figure 6.1: OpenFOAM versus theoretical guidelines for the situation without adaptation measures

SLR [m]	h [m]	$R_{c,1}$ [m]	$q_{TAW,1}$ [l/s/m]	$q_{OF,1}$ [l/s/m]	$q_{OF,1}/q_{TAW,1}$ [-]	$R_{c,2}$ [m]	$q_{ATAW,2}$ [l/s/m]	$q_{OF,2}$ [l/s/m]	$q_{OF,2}/q_{ATAW,1}$ [-]
0.0	12.5	2.1	10.53	205.22	19.5	2.85	18.14	63.43	3.50
0.6	13.1	1.5	50.12	424.63	8.5	2.25	51.07	148.22	2.90

Table 6.1: Comparison of the overtopping rates for both case studies and the situation without adaptation measures (SLR 0-0.6m)

6.2. Evaluated combination of solutions in OpenFOAM

At first, only one unique path is computed in the OpenFOAM model to evaluate the accuracy of the current guidelines. By doing this thoroughly, a conclusion about current guidelines is presented. Based on the conclusions it is decided whether an extra path is computed or if a certain combination requires more research later on in this chapter. For each different adaptation measure, the effects compared to the OpenFOAM results are discussed. The two applied methods are first separated in the original and adapted TAW overtopping equations. At the end of this chapter, a conclusion for both theories combined is presented.

The path evaluated is the solution in which a berm, a crest wall and a low-crested structure are constructed. This path is not the economically most attractive solution (Chapter 4) but is interesting to compute as the TAW overtopping equation for non-breaking waves described in Section 2.4.1 not includes the effect of a berm. Because it is expected that a berm influences the average overtopping rate, in Section 2.4.2 an adapted TAW overtopping equation proposed by Krom (2012) is described as well. The latter method is applied to include the berm in the pathway scheme.

The influence of a foreshore is not evaluated further in this thesis because of time limitations. The grid should increase with a few wavelengths to gradually increase the bottom to the final height of the foreshore. The extra grid space significantly increases the computational time compared to the current computation time of approximately 1.5 days. To decrease the computation time, OceanWave3D could be used (Ensig-Karup et al., 2009) as extension of the current model. However, this model cannot deal with breaking waves.

6.3. Solution: Berm - Crest wall - Low-crested structure

Figure 6.2 highlights the evaluated path. The overtopping events are evaluated at the start of each adaptation (the circles) and at the end of an adaptation (|). Therefore, a total of six evaluation moments per path and two per individual adaptation measure are analyzed. By doing so, the effects on the overtopping rate of an adaptation are compared to the current guidelines. In Chapter 5 it is concluded that the current guidelines are under-estimating the average overtopping discharges compared to the OpenFOAM results.

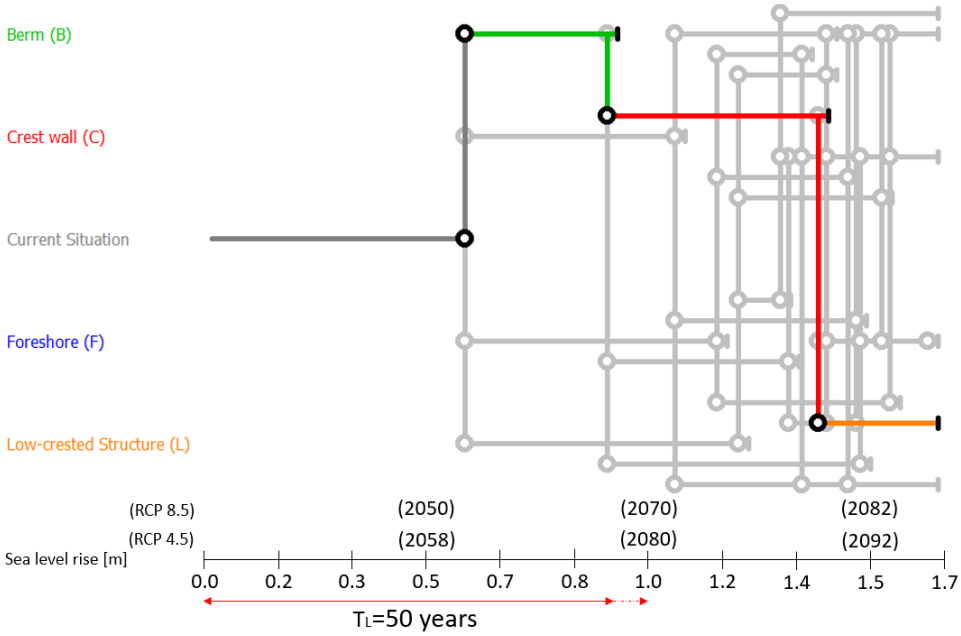

Figure 6.2: Path evaluated in OpenFOAM based on the Adapted TAW equations (Case 2)

6.3.1. Adaptation 1: Berm

The first evaluated solution is the construction of a berm at 0.6 meters sea level rise. As the influence of a berm is not included into the original TAW overtopping equation, the adapted TAW equations are used to determine the tipping point of this adaptation measure. The next adaptation measure should be implemented at 0.94 meters sea level rise to ensure safety according to the adapted TAW equations. See also Figure 6.2. At the moment of implementation, the berm height is 0.5 meters above the water. The berm height above water becomes lower for a rising sea level.

Accuracy TAW (Case 1)

The influence of a berm is currently not included in the maximum overtopping equation proposed in the TAW (2002). As can be seen in Figure 6.3, a berm decreases the overtopping rate compared to the situation without this implementation. Thus, in contrast to the theoretical guideline does a berm influences the overtopping rate. In Figure 6.3, the range at which a berm ensures safety according to the evaluated path is presented and compared to the TAW overtopping equation. Notably, the computed overtopping rate is still overestimating compared to the TAW equation for the implementation of a berm. However, the difference between OpenFOAM and the overtopping equation becomes less.

The previous also follows from the results in Table 6.2, in which a clear reduction in overtopping discharge is found for implementing a berm in OpenFOAM. The reduction ($q_{reduction}$) in overtopping discharge (%) is caused by implementing an adaptation measure (i.e. $q_{reduction} = (q_{i+1} - q_i)/(q_i)$, with i represents the current situation and i+1 the next situation with an extra adaptation). The effect of a berm is 30% when implemented at 0.6 meter sea level rise and increases to 43 % at 0.94 meters sea level rise. Therefore, the berm becomes more influential closer to still water level as the initial height of the berm was 0.5 meters above still water level at construction. The discrepancy between the computed and predicted overtopping rate is calculated as the difference between a solution with and without adaptation at a certain sea level rise for both the OpenFOAM and theoretical calculated situation ($\Delta q_{OF}/\Delta q_{TAW}$). If this value is smaller than 1, the theory predicts a larger influence of the adaptation. For a value larger than 1, the OpenFOAM model computes a larger influence. The influence of a berm is not accounted for in the overtopping equation proposed by the TAW (2002). Therefore, the ratio can not be computed for the current situation.

Adaptation	SLR [m]	h [m]	$R_{c,1}$ [m]	$q_{TAW,1}$[l/s/m]	$q_{reduction}$ [%]	$q_{OF,1}$ [l/s/m]	$q_{reduction}$ [%]	$q_{OF,1}$ / $q_{TAW,1}$	$\Delta q_{OF,1}$ / $\Delta q_{TAW,1}$
-	0.6	13.1	1.5	50.12	-	424.63	-	8.5	-
	0.94	13.44	1.16	121.32	-	887.23	-	7.31	-
+ Berm	0.6	13.1	1.5	50.12	-	295.16	-30.49	5.88	-
	0.94	13.44	1.16	121.32	-	503.56	-43.24	4.15	-

Table 6.2: Influence of a berm compared to the TAW overtopping equations.

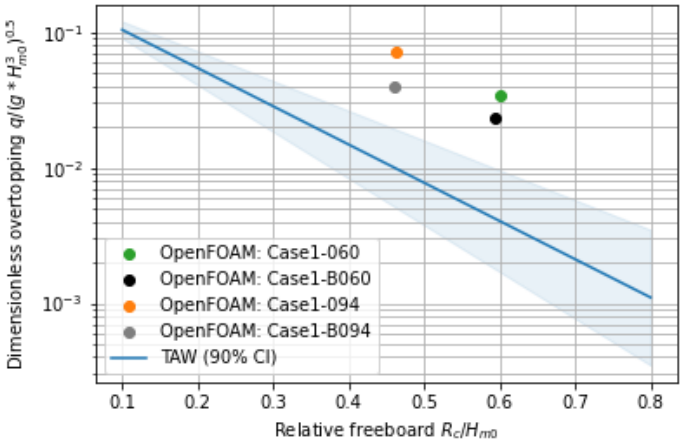

Figure 6.3: Comparison of the dimensionless overtopping in OpenFOAM to the TAW overtopping equation

6.3.2. Adaptation 2: Crest wall

The second adaptation measure is the implementation of a crest wall at 0.94 meters sea level rise. According to the adapted TAW overtopping equation, this ensures safety until 1.44 meters sea level rise (Figure 6.2).

Accuracy TAW (Case 1)

In contrast to the influence of a berm, the crest wall is included in the overtopping equations by simply increasing the crest height (R_c). Figure 6.4 presents the influence of a crest wall at a sea level rise of 0.94 and 1.44 meters.

Table 6.3 presents the results from the figure. The reduction ($q_{reduction}$) represents the reduction in the overtopping rate compared to the previous situation. The influence of a crest wall remains constant (72.75%) in the TAW overtopping equation. The influence of a crest wall slightly decreases in OpenFOAM for a higher sea level rise. Finally, the OpenFOAM model reduces the wave overtopping with a larger value compared to the theory (Factor 2.5).

Adaptation	SLR [m]	h [m]	$R_{c,1}$ [m]	$q_{TAW,1}$[l/s/m]	$q_{reduction}$ [%]	$q_{OF,1}$ [l/s/m]	$q_{reduction}$ [%]	$q_{OF,1}$ / $q_{TAW,1}$	$\Delta q_{OF,1}$ / $\Delta q_{TAW,1}$
Berm	0.94	13.44	1.16	121.32	-	503.56	-	4.15	-
	1.44	13.94	0.66	445.17	-	918.00	-	2.06	-
+ Crest wall	0.94	13.44	1.66	33.06	-72.75	281.28	-44.14	8.51	2.52
	1.44	13.94	1.16	121.32	-72.75	584.93	-36.28	4.82	2.36

Table 6.3: Influence of a crest wall compared to the TAW overtopping equations

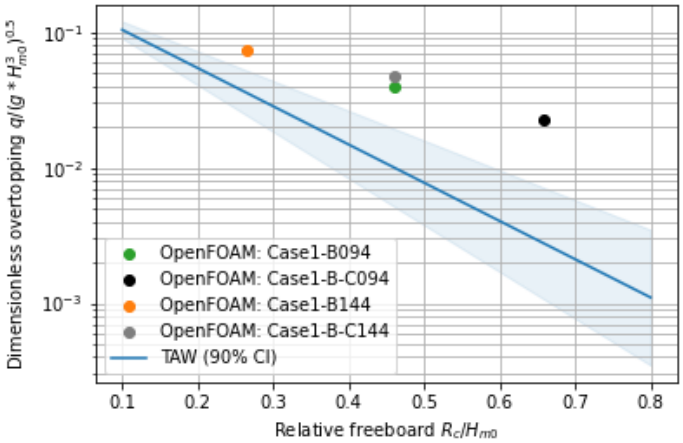

Figure 6.4: Comparison of the dimensionless overtopping in OpenFOAM to the TAW overtopping equation

6.3.3. Adaptation 3: Low-crested structure

The final and third adaptation includes the construction of a low-crested structure. The grid increases by approximately 80 meters (Section 5.4) to ensure enough space for the adaptation measure. The low-crested structure decreases the wave height and thus the average overtopping rate. In Figure 6.2 can be seen that the low-crested structure ensures safety until 1.70 meters sea level rise if the adapted TAW equation is applied on case 2.

Accuracy TAW (Case 1)

The implementation of a low-crested structure in OpenFOAM causes a significant reduction in overtopping discharge (Figure 6.5). Figure 6.5 and Table 6.4 show that the computed overtopping values are larger than what is being expected from theory. The absolute reduction caused by the low-crested structure is a factor 6-7 larger in OpenFOAM than the reduction based on the applied theory.

An important side note is the fact that the hydrodynamics are not configured again at the toe of the breakwater for the increased grid. Therefore, the waves at the toe might be reduced too much over the length. However, the hydrodynamics at the toe of the low-crested structure are of the same order. As the exact wave height is not known, the model can not be configured for this effect. Also, the transmission coefficient computed in OpenFOAM is lower than the applied transmission coefficient in the theoretical part (Section 2.4.8). The transmission coefficient computed in OpenFOAM is 74% compared to 82% calculated based on the Briganti equations (Briganti et al., 2003).

Adaptation	SLR [m]	h [m]	$R_{c,1}$ [m]	$q_{TAW,1}$[l/s/m]	$q_{reduction}$ [%]	$q_{OF,1}$ [l/s/m]	$q_{reduction}$ [%]	$q_{OF,1}$ / $q_{TAW,1}$	$\Delta q_{OF,1}$ / $\Delta q_{TAW,1}$
Berm +	1.44	13.94	1.16	121.32	-	584.93	-	4.82	-
Crest wall	1.70	14.2	0.9	238.52	-	847.99	-	3.56	-
+ Low-crested	1.44	13.94	1.16	44.46	-63.35	116.31	-80.12	2.62	6.10
Structure	1.70	14.2	0.9	154.38	-35.28	275.41	-67.52	1.78	6.81

Table 6.4: Influence of a Low-crested structure compared to the TAW overtopping equations

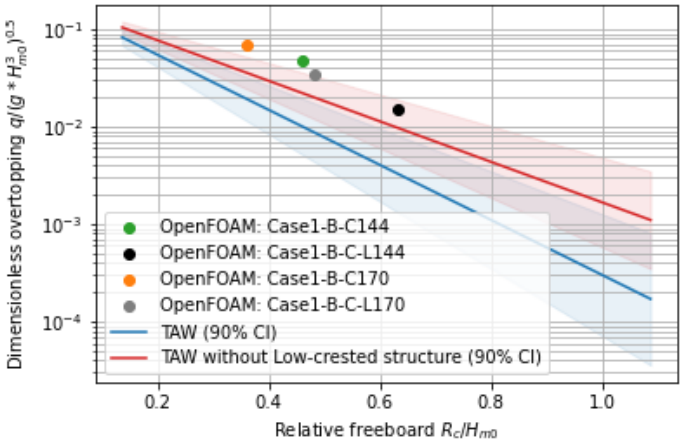

Figure 6.5: Comparison of the dimensionless overtopping in OpenFOAM to the TAW overtopping equation

6.3.4. Conclusions on the computed path

The path evaluated in OpenFOAM consists of a berm, crest wall and a low-crested structure. This path is evaluated against the results from the theoretical predictions of overtopping proposed by the TAW (2002). Furthermore, case study 1 is evaluated to determine the discrepancy between theory and OpenFOAM. Figure 6.6 presents the difference in mean overtopping rate between the calculated (empirical formula) and simulated (OpenFOAM). The black line represents the maximum allowed wave overtopping of 50 l/s/m as applied for the adaptation paths in Chapter 4.

The berm reduces the overtopping rate for the applied case study in contrast to the equation proposed by the TAW (2002). Moreover, both the crest wall and low-crested structure have a larger reduction in OpenFOAM than based on the empirical equation. Regarding the low-crested structure, two aspects should be considered. The first aspect is the increased grid to include the low-crested structure in OpenFOAM. This new situation is not configured and therefore the waves are possibly decreased too much over the extra length. The second aspect is the extra reduction compared to the applied theory for transmitted waves. In OpenFOAM 74% of the original wave height traveled across the low-crested structure compared to 82% in the pathway analysis. If the lower wave height is applied to the theory, the difference between both calculation methods becomes smaller.

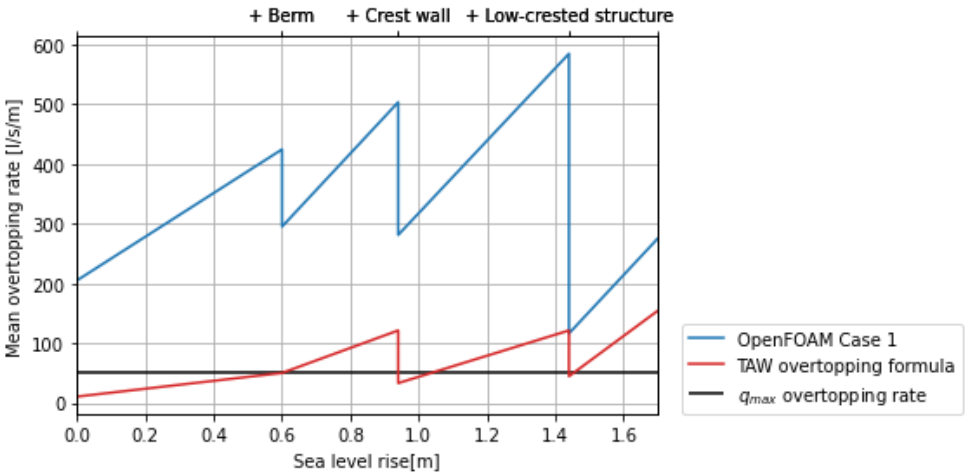

Figure 6.6: Overtopping rate in OpenFOAM compared to the TAW (2002) overtopping formula

6.4. Effect of adaptations

In the previous sections, the applied crest heights at the tipping points for both the theory and OpenFOAM calculations were equal. As observed, the overtopping rate in OpenFOAM differs from what is to be expected based on the empirical overtopping equations. Because the calculated overtopping rates for the model and theory are in a different regime, the effect of an adaptation can be different as well. Therefore, this section compares the effect of an adaptation for an equal overtopping rate at the start. In other words, the applied crest height in the theoretical part is lowered. By doing so, the overtopping rate will be approximately the same ($q_{OF}/q_{TAW} \approx 1$) at the start of an adaptation.

6.4.1. Effect without adaptations

At first, the difference in overtopping rate for the situation without implementations is computed again. Therefore, the overtopping rate in both the theory and OpenFOAM is equal at zero meters sea level rise ($q_{OF}/q_{TAW} \approx 1$). As can be seen in Table 6.5, the discrepancy between theory and model increases for a larger sea level. The original TAW equation predicts almost twice the overtopping rate simulated in OpenFOAM (subscript 1). For the adapted case (ATAW,subscript 2), the discrepancy is smaller.

SLR [m]	h [m]	$R_{c,1}$ [m]	$q_{TAW,1}$ [l/s/m]	$q_{OF,1}$ [l/s/m]	$q_{OF,1}/q_{TAW,1}$ [-]	$R_{c,2}$ [m]	$q_{ATAW,2}$ [l/s/m]	$q_{OF,2}$ [l/s/m]	$q_{OF,2}/q_{ATAW,2}$ [-]
0.0	12.5	0.96	204.07	205.22	1.01	2.12	63.91	63.43	0.99
0.6	13.1	0.36	971.12	424.63	0.44	1.63	179.92	148.22	0.82

Table 6.5: Comparison of the overtopping rates for both case studies and the situation without adaptation measures (SLR 0-0.6m)

6.4.2. Effect of adaptations in OpenFOAM compared to the TAW equations

The overtopping equation proposed by the TAW (2002) lacks the influence of a berm as mentioned in Chapter 2. In other words, the reduction of a berm is zero percentage. In Section 6.3.1 the reduction of a berm for case study 1 was found as approximately 40% in OpenFOAM. The discrepancy in reduction of a crest wall or low-crested structure between OpenFOAM and theory has been elaborated in the remaining of this section. Again, the ratio q_{OF}/q_{TAW} is equal to one at the start of an adaptation. The starting point is the situation just before the adaptation is implemented. In Table 6.6 and Table 6.7 the results are presented.

Adaptation: Crest wall

Compared to the situation with equal crest height, the reduction percentage in theory remains the same. Obviously, the difference in overtopping rate between OpenFOAM and the applied empirical equation is smaller for the new situation. The biggest difference is the fact that for the same overtopping rate as starting point, the absolute reduction based on the empirical equation is larger than in OpenFOAM($\Delta q_{OF} / \Delta q_{TAW} < 1$).

Adaptation	SLR [m]	h [m]	$R_{c,TAW}$ [m]	q_{TAW}[l/s/m]	$q_{reduction}$ [%]	$q_{OF,1}$ [l/s/m]	$q_{reduction}$ [%]	$q_{OF,1} / q_{TAW}$	$\Delta q_{OF,1} / \Delta q_{TAW}$
Berm	0.94	13.44	0.61	506.97	-	503.56	-	0.99	-
	1.44	13.94	0.11	1860.23	-	918.00	-	0.49	-
+ Crest wall	0.94	13.44	1.11	138.17	-72.75	281.28	-44.14	2.04	0.60
	1.44	13.94	0.61	506.97	-72.75	584.93	-36.28	1.15	0.25

Table 6.6: Influence of a crest wall compared to the TAW overtopping equations with equal starting point ($q \approx 504$ l/s/m)

Adaptation: Low-crested structure

The reduction (%) according to the theory is smaller compared to the situation with equal crest height. The ratio between OpenFOAM and theory becomes smaller as the calculated overtopping rate is larger for the situation with lower crest height. However, the absolute reduction in OpenFOAM remains larger than the reduction based on the empirical equations. Therefore, the ratio ($\Delta q_{OF} / \Delta q_{TAW}$) is larger than one. But again, this is partly because of the larger reduction of wave height in OpenFOAM (i.e. lower wave height computes a lower overtopping rate).

Adaptation	SLR [m]	h [m]	$R_{c,TAW}$ [m]	q_{TAW} [l/s/m]	$q_{reduction}$ [%]	$q_{OF,1}$ [l/s/m]	$q_{reduction}$ [%]	$q_{OF,1}$ / q_{TAW}	$\Delta q_{OF,1}$ / Δq_{TAW}
Berm +	1.44	13.94	0.55	592.56	-	584.93	-	0.99	-
Crest wall	1.70	14.2	0.29	1164.97	-	847.99	-	0.73	-
+ Low-crested	1.44	13.94	0.55	312.72	-47.23	116.31	-80.12	0.37	1.67
Structure	1.70	14.2	0.29	905.91	-22.24	275.41	-67.52	0.30	2.21

Table 6.7: Influence of a Low-crested structure compared to the TAW overtopping equations with equal starting point ($q \approx 590$ l/s/m)

6.4.3. Conclusions on equal overtopping rate

The previous can be summarized in Figure 6.7. The figure presents the *average* reduction of an adaptation in both OpenFOAM and based on the empirical formula. The current design formula proposed by the TAW (2002) lacks the influence of a berm. Therefore, the reduction is zero percent. However, for the applied case study, the berm reduces the overtopping rate by approximately 40%. In contrast to the berm, the crest wall is included in the design formula. The reduction based on the formula is larger than the simulated overtopping rate. Finally, when the low-crested structure is included, the reduction in OpenFOAM is larger than the calculated overtopping rate.

Summarizing, the berm and low-crested structure are underestimated in the applied theory. Therefore, both adaptations have a larger influence on the adaptation pathway analysis than determined in Chapter 4. On the flip side, the crest wall is overestimated in current theory. This means that the crest wall becomes less effective in the adaptation pathways.

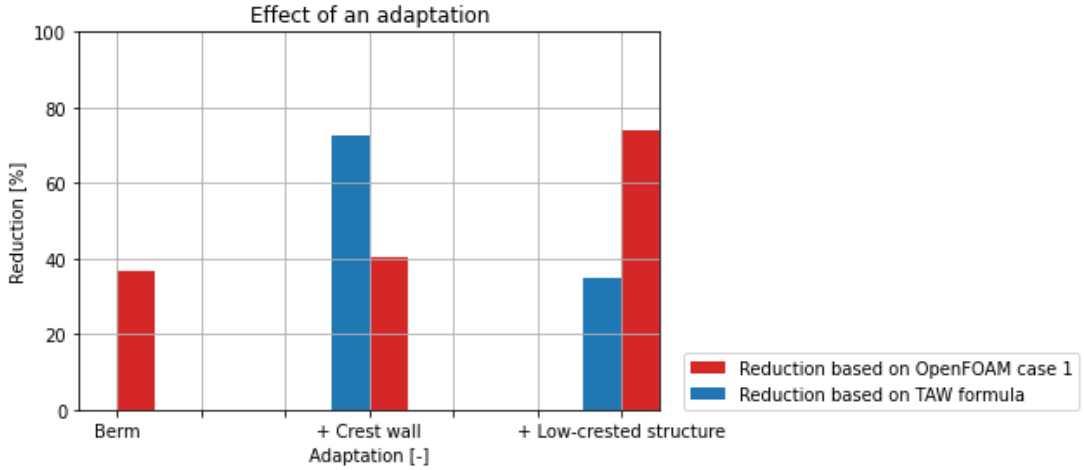

Figure 6.7: Reduction per adaptation in OpenFOAM compared to the TAW overtopping formula

6.5. Accuracy Adapted TAW

Besides the overtopping equation proposed in the TAW, an adapted overtopping equation (Krom, 2012) is applied as well in this thesis. This section evaluates the accuracy of the formula which includes the effect of a berm. Therefore, the same procedure is followed as for the TAW overtopping formula (Section 6.3 and Section 6.4). Apart from the different formula, *Case 2* is now computed in OpenFOAM. Case 2 is derived in Chapter 3 based on the Adapted overtopping formula and has the same overtopping rate as Case 1 at first.

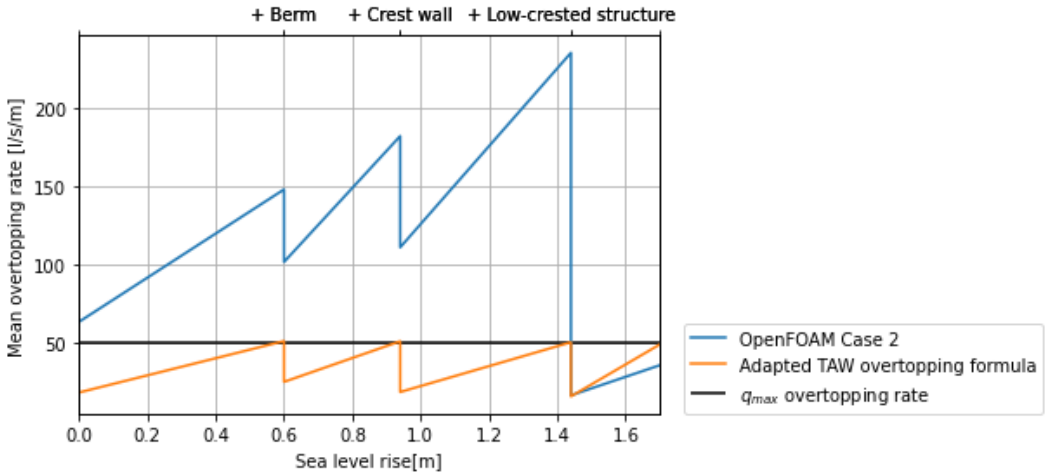

Figure 6.8: Overtopping rate in OpenFOAM compared to the Adapted TAW (2012) overtopping formula

Figure 6.8 presents the difference between the simulated (OpenFOAM) and calculated (empirical formula) overtopping rate for the computed path (berm, crest wall, low-crested structure). In contrast to the simulated overtopping rate, the calculated overtopping rate is much lower. Moreover, the reduction of an adaptation in OpenFOAM is larger than calculated with the Adapted TAW formula. The previous makes the reductions be underestimated in the empirical equation. However, the initial discrepancy in the overtopping rate is already significant.

Next, the crest height is lowered in the empirical equation. By doing so, the calculated overtopping rate is equal to the simulated overtopping rate at the start of an adaptation. Therefore, the reduction in OpenFOAM is better comparable to the reduction based on the empirical formula. Figure 6.9 presents the discrepancy between the simulated and calculated reduction. In the proposed case study, the empirical equation is overestimating the reduction for a berm and a crest wall. Because of the overestimation, a solution is less effective than determined in the adaptation pathway analysis. If a low-crested structure is implemented last, the current theory is underestimating the reduction. In contrast to a berm in combination with a crest wall, the solution is more effective than determined in the pathway analysis.

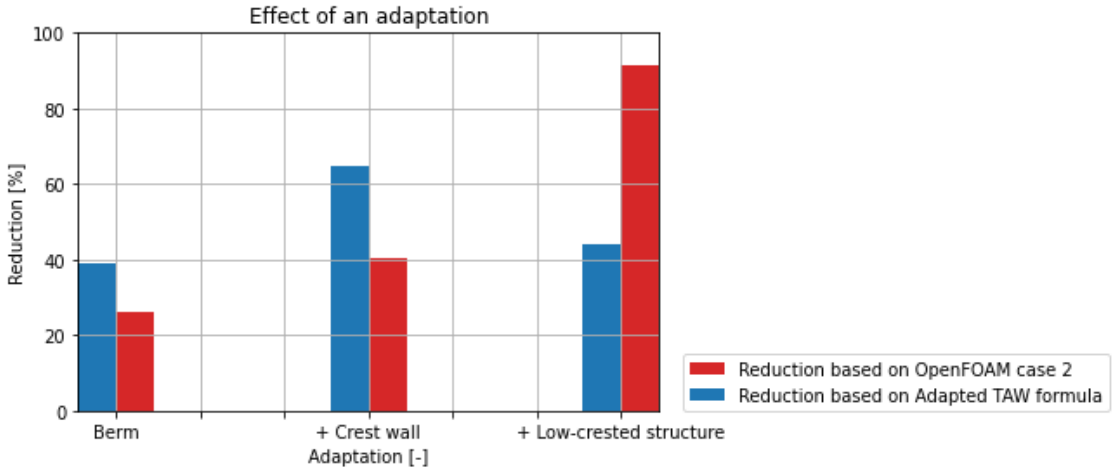

Figure 6.9: Reduction per adaptation in OpenFOAM compared to the Adapted TAW overtopping formula

See Appendix B for more details on the exact reduction and discrepancy between calculated and simulated overtopping rates. Within the Appendix, the same tables and figures are presented as derived for the comparison between OpenFOAM and the TAW overtopping formula at the start of this chapter.

6.6. Conclusion on the OpenFOAM computations

All the aspects described previously are used to answer the second research question. This question is defined in Chapter 1 as:

How do the relevant combinations of solutions perform in the numerical model if the outcome is compared to the current guidelines?

First, the most interesting adaptation path is computed and compared to the empirical equation proposed by the TAW (2002). Next, because of the large discrepancy in the overtopping rate between theory and model, the crest height in the empirical equation is lowered. By doing so, the overtopping rate in model and theory is equal at the start of an adaptation. Therefore, the effect of an adaptation in the model is better comparable to the effect according to the theory. Finally, the same procedure has been performed for the adapted TAW overtopping equation proposed by Krom (2012).

The computed path consists of a berm, a crest wall and a low-crested structure (derived with the Adapted TAW equations). In contrast to the results from Chapter 4 this is not the economically most attractive solution. However, the solution is relevant to compute in OpenFOAM and compare with the economically most attractive solution. The solution is interesting because the overtopping formula proposed by the TAW (2002) lacks the influence of a berm. Also, the influence of a crest wall is rather crude by simply increasing the crest height. The influence of an increased foreshore is not considered as the computation time significantly increases for this.

Accuracy TAW compared to the OpenFOAM results

A large discrepancy between model and theory is observed for the situation with equal crest height. The average wave overtopping is much larger in the model. Moreover, the absolute reduction per adaptation is also much larger compared to the theory. Therefore, the applied theory is underestimating for the applied case study. However, because of the initial difference in overtopping rate, the effect of each adaptation could be different as well.

Next, the crest height in the theoretical part is lowered. Such that at the start of an adaptation the overtopping rate in both the model and empirical formula is equal. The current theory lacks the influence of a berm. Therefore, the effect is underestimated compared to the OpenFOAM results (40% reduction). On the flip side, the effect of a crest wall is overestimated. Furthermore, the effect of a low-crested structure is underestimated by almost 50%. However, two possibilities could explain the large difference between theory and model. First, because of the increase in grid length, the waves could decrease extra over the length. Second, the simulated transmission coefficient in OpenFOAM is smaller compared to the applied transmission equation (74% in OpenFOAM compared to 82% for the theoretical part).

At the moment, a berm and low-crested structure seem to be less effective in the derived adaptation pathways than simulated in OpenFOAM. Further, the crest wall is currently more effective in the adaptation pathways than simulated in OpenFOAM. In other words, the berm and low-crested structure are underestimated and the crest wall is overestimated in applied theory.

Accuracy Adapted TAW compared to the OpenFOAM results

The discrepancy in overtopping rate between the Adapted TAW formula and OpenFOAM is smaller compared to the original TAW overtopping formula. However, the difference is still significant. Again, the theory is underestimating the overtopping rate for the applied case study.

Next, the crest height is lowered in the empirical equation. By doing so, the calculated overtopping rate is equal to the simulated overtopping rate at the start of an adaptation. Therefore, the reduction in OpenFOAM is better comparable to the reduction based on the empirical formula. The reduction of a berm and crest wall is overestimating compared to the OpenFOAM results. On the other hand, the effect of a low-crested structure is underestimated in the applied theory. Therefore, the berm and crest wall are less effective in the adaptation pathway scheme than currently designed for. Furthermore, the low-crested structure becomes more effective in the adaptation pathway scheme.

General conclusion
Based on the performed computations it is concluded that a berm influences the overtopping rate. It can also be concluded that the current method of increasing the crest height with the height of the wall overestimates the reduction. Therefore, one should carefully test the effect of a crest wall. Finally, implementing a low-crested structure underestimates the effect on the wave height. It is found that the transmitted wave height in OpenFOAM is decreased by 10% more than calculated with the empirical equation for transmitted waves. However, the increased grid is not configured again for the applied hydrodynamics at the toe. Therefore, the wave height at the toe is slightly lower.

Thus, comparing the OpenFOAM results with the TAW (2002) equations, shows that adaptation pathways that include a berm are relatively more attractive than if these pathways are calculated based on the TAW (2002). Pathways including a crest wall could be slightly less attractive than those pathways calculated with TAW (2002) would suggest. The (limited) computations with a low-crested structure indicate that an adaptation pathway with a low-crested structure could be more relevant than expected based on the TAW (2002).

Overall, the performance of combinations of solutions can be computed with OpenFOAM. Adaptation pathways including a berm and a crest wall seem to be relevant pathways, either in combination with a shallow foreshore or with a low-crested structure. Nevertheless, these results need to be validated based on data from experiments.

Also, the computations indicate it is likely that the original TAW (2002) equations are not suitable to account for the effects of berms in the seaward slope of breakwaters. Thus, adaptation pathways including a berm are highly relevant but cannot be computed accurately with the original TAW (2002) equation. Until a sufficiently validated empirical method is available, the adapted TAW formula as proposed by Krom (2012) is likely to lead to more realistic adaptation pathways than using the original TAW equations.

7

Discussion

This chapter focuses on the climate adaptation of rubble mound breakwaters. Because of climate change, these structures possibly need one or more adaptations to fulfill their function. Accurate design formulas are required to create multiple adaptation paths with a combination of solutions. Currently, the design formulas to calculate the wave overtopping do not seem to be accurate enough. Therefore, existing prediction methods for wave overtopping discharges are discussed in this chapter.

7.1. Applied theory

Two empirical equations are applied to calculate the overtopping rate of a rubble mound breakwater in this thesis. Either the equation presented by the TAW, or the adapted TAW equation derived by Krom. One of the disadvantages of the original TAW overtopping equation is that the influence of a berm or wave steepness is not included. Therefore, the current theory is overestimating the overtopping rate for rubble mound structures with a berm. The wave steepness, on the other side, can decrease or increase the occurring wave overtopping. The wave overtopping decreases for steeper waves because of the faster wave damping and vice versa.

Consequently, a second empirical equation is applied: the adapted TAW equation derived by Krom (2012). This equation includes the effect of wave steepness and a berm. However, this equation is valid for a limited data range. It is unsure whether the equation is well-founded outside the data range. Also, the proposed equation is validated for a situation with a berm. Therefore, it is unclear how accurate the equation is for configurations without a berm.

Besides the influence of wave steepness and a berm, the influence of a crest wall is implemented in the TAW (2002) in a rather crudely way. The TAW proposes to increase the crest height (R_c) with the height of the crest wall above the current armour layer level. The results in OpenFOAM show that the reduction is about a factor 5 smaller than calculated with the empirical equations for the applied case study. In van Doorslaer (2015), it also seems that the method applied in the TAW is overestimating the reduction in overtopping. In the same research, a new formula for the influence of a crest wall is presented.

7.2. Hydraulic and structural assumptions

Some assumptions are made in the applied theory. One of the assumptions is that the wave period ($T_{m-1,0}$) remains constant in all conditions. The results of the hydrodynamics in OpenFOAM show that the wave steepness slightly lowers for a rising sea level. At the maximum sea level adopted in this thesis, the wave steepness is approximately 5% lower than applied in the empirical equations. The lower steepness causes more wave overtopping at rubble mound structures. However, as the difference is negligible it is not expected that the extra overtopping is significant. The assumption of a constant wave period also applies to waves traveling over a low-crested structure. One should account for the fact that the wave spectrum alters because of energy dissipation at the porous low-crested structure.

To include the increased foreshore within the adaptation pathway scheme, a rule of thumb of H/d = 0.5 is applied. This rule should only be used in a preliminary design phase. For a more detailed research, a wave model like SWAN or OceanWave3D can be used to determine the exact wave transformation. Besides the applied rule of thumb, possible erosion of the foreshore is not accounted for in the design. Therefore, costs could significantly increase due to frequently occurring maintenance.

The TAW proposes to apply a roughness coefficient (γ_f) of 0.40 for a two-layer rubble mound structure with a porous core. In recent research, it is concluded that this value could be higher (Molines and Medina, 2015). Consequently, the overtopping rate increases and matches more with the simulated overtopping rate in OpenFOAM. For example, a roughness coefficient of 0.53 decreases the gap between OpenFOAM and theory by approximately 20%.

Regarding the stability of the structure, two assumptions are made. Both the crest wall and the rubble mound structure are assumed to be stable. The stability of the rubble mound breakwater is calculated in the setup of the academic case study to give some representative values. For a larger water depth, however, the wave height could increase. The stability of the structure will therefore decrease. In addition, the wave impact increases for higher crest walls. Therefore, the stability of a crest wall should be verified. One is advised to carefully consider those aspects.

7.3. Applied case study

The case study examined in this thesis uses constant parameters for both the hydraulic and structural conditions. The hydraulic conditions applied are representative for the Dutch coast. The most important parameter which influences the overtopping rate and corresponding adaptation measures is the wave period. As discussed, the overtopping rate increases for a lower wave steepness. Subsequently, because of the lower wave steepness, all adaptations become less effective. Therefore, the applied adaptation should increase in width to overcome the larger wavelength. Consequently, a low-crested structure becomes too expensive compared to other adaptations, in projects with a budget cap for example.

If the slope of the structure is smaller than the applied 1:2 slope, the TAW formula for breaking waves might become normative. However, breakwaters generally have slopes between 1:2 and 1:1.5. Thus, this does not apply to this research.

7.4. Applied data

This research is based on certain assumptions regarding the applied literature. The hydrodynamics derived for this thesis are based on governing conditions for the Dutch coast with a certain return period. Based on the wave height and period, the structural parameters were determined. As no physical data is available to verify the accuracy of the computations during this research, the discrepancy between model and theory can be different. Therefore, a conclusion about the accuracy is not presented in this research.

7.5. Applicability adaptation pathways

Adaptation pathways increase the capability to manage structures during a largely uncertain sea level rise. The tipping points in such a scheme determine the moment at which the next solution should be implemented to ensure safety. The adaptation pathways derived in this thesis depend on the fact that all resources are available at the location. However, the outcome of these pathways depends on local conditions and resources available at that moment. Also, the costs included are relative and based on outdated projects. One should carefully investigate the local conditions and local market to determine the economically most attractive solution. Furthermore, costs like labor, preparation of the site, maintenance and many more are not included in the current cost estimation.

Besides the derived pathways and estimated costs, the expected lifetime of structures also determines the outcome. If the most extreme climate scenario occurs, it is best to implement the most expensive solution at first. On the flip side, if a milder scenario occurs and the most expensive solution is

already implemented, the costs are unnecessarily high. Moreover, the required lifetime of a structure can become larger than expected initially. The most likely climate scenario could be determined if the probabilities of occurrence are available for each climate scenario. However, these are not available at the moment.

In the this research, the adaptation pathways are derived based on empirical equations. However, for a realistic project, it is possible to derive these pathways with OpenFOAM. The possibility to do so depends on the data available to calibrate the model. Furthermore, on the number of simulations computed simultaneously. The project time significantly increases if a limited number of simulations are performed at the same time. In the tender phase of a project, the applicability of OpenFOAM depends on the funds available for the project. For projects with a limited budget, the current guidelines can be applied to derive the adaptation pathways at first. The adapted TAW equation can be used as a first estimation of the impact of a berm.

7.6. Applicability on different structures

This research focuses on rubble mound breakwaters. However, there are many more coastal structures that protect the hinterland. Dikes, for example, apply the same empirical equations to determine the overtopping rate. Dikes are often less steep and therefore the equation for ”breaking” waves is used instead of the maximum for ”non-breaking” waves, as applied in this thesis. Furthermore, the equation for breaking waves includes the influence factor of the berm.

The framework of this research can also be applied on vertical walls. The equations used are slightly different, but the principle remains the same. Besides the equations, other adaptation possibilities can be applied as well (e.g. a bullnose). Adding a berm in front of a vertical wall may be less realistic since a berm can significantly increase the wave impacts on vertical walls. Also, the water depth decreases for a berm. This water depth may be necessary for shipping.

Summarizing, one can apply the adaptation pathways on many structures if the different equations and conditions are taken carefully into account. Moreover, the previously described structures are computable in the OpenFOAM model.

8

Conclusions and Recommendations

This chapter presents the conclusions on the proposed research questions and objective. Based on the performed research, recommendations for further investigation are given.

8.1. Conclusions

In Section 1.3, the objective of this thesis was defined as:

> ”The objective of this research is to elaborate several relevant combinations of adaptation solutions that limit wave overtopping at rubble mound breakwaters, where the sequence of solutions with lack of validation in current guidelines is computed in a numerical model to enhance insight into the accuracy of those combinations.”

Based on the objective and the findings of the two proposed research questions, a final conclusion is given.

Conclusions on performed research

In this research it is concluded that for a large sea level rise (>1 meter) during the lifetime of a structure, multiple solutions are required to ensure safety against wave overtopping. These combinations of solutions were derived based on the applied theoretical guidelines (i.e. TAW and the adapted TAW). As the influence of a berm is not included in the original overtopping equation proposed by the TAW (2002), this solution is further investigated in OpenFOAM. From the OpenFOAM results, it can be concluded that a berm, in contrast to the TAW overtopping equation for ”non-breaking” waves, has a significant influence on the wave overtopping. Furthermore, the effect of a crest wall in combination with a berm seems to be overestimated in the TAW (2002). Additionally, a low-crested structure is implemented in the solution. A low-crested structure in front of the rubble mound breakwater in combination with a berm and a crest wall seems to underestimate the reduction in wave overtopping.

In conclusion, the berm and low-crested structure are relatively more effective in the adaptation paths than currently presented in the TAW (2002). On the flip side, the pathways which include a crest wall seem to be less effective. Overall, the performance of combinations of solutions can be computed with OpenFOAM. Adaptation pathways including a berm and a crest wall seem to be relevant pathways, either in combination with a shallow foreshore or with a low-crested structure. Nevertheless, these results need to be validated based on data from experiments.

Also, the computations indicate that it is likely that the original TAW (2002) equations are not suitable to account for the effects of berms in the seaward slope of breakwaters. Thus, adaptation pathways including a berm are highly relevant but cannot be computed accurately with the original TAW (2002) equation. Until a sufficient empirical validation method is available, the adapted TAW formula as proposed by Krom (2012) is likely to lead to more realistic adaptation pathways than the original TAW equations.

Conclusions on research questions
The findings in this report are based on two research questions which are elaborated in Chapter 1. The answers to these research questions are summarized below.

1.) What sequence of solutions is economically beneficial according to the adaptation pathways by limiting the wave overtopping of rubble mound breakwaters against sea level rise?
The performed research shows that the economically most attractive solution depends on multiple factors. The number of adaptations required depends on the occurring climate scenario and the lifetime of a structure. In this thesis, the lifetime of a rubble mound structure was approximately 50 years. Two climate scenarios were applied in the adaptation pathways, the RCP 4.5 and RCP 8.5. For both climate scenarios, a single adaptation is sufficient to ensure safety during the lifetime of the breakwater. However, because the influence of a combination of solutions is investigated, the maximum sea level rise is set to 1.70 meters, the maximum sea level rise at the end of the century predicted in the RCP4.5 scenario. Therefore, multiple solutions are required to ensure safety ($q_{max} < 50$ l/s/m).

The adaptation pathways based on the overtopping equation proposed in the TAW (2002) consist of a crest wall, increased foreshore and a low-crested structure. Three adaptations are required at the maximum sea level rise adopted in this thesis. Therefore, the order of construction is not of importance if the present value is evaluated. However, if the future value is included, the most expensive solution should be implemented first.

Furthermore, this thesis presents the adaptation pathways based on the adapted TAW overtopping formula proposed by Krom (2012). In total four solutions were applied: a berm, a crest wall, an increased foreshore or a low-crested structure. The solutions without a low-crested structure are economically more attractive due to the lower investment costs. The economically most attractive solution if the future value is included consists of a foreshore followed by a crest wall and a berm.

The research conducted shows that it is difficult to directly calculate the costs of an adaptation path because of the large uncertainty in climate scenarios. If the most extreme solution is constructed at first and a much milder climate scenario occurs, the project becomes unnecessarily expensive. Moreover, the lifetime of the structure will become longer than adopted during the construction phase. The probability of occurrence for each climate scenario should be determined in order to calculate the expected costs of a solution. However, these probabilities of occurrence are not available at the moment.

Solutions which include a berm or crest wall are economically more attractive compared to a foreshore and low-crested structure. A berm and crest wall together would cover almost one meter of sea level rise and are relatively easy to implement. During the adopted lifetime of the structure, none of the climate scenarios exceeds this sea level rise. Therefore, solutions with a berm and crest wall seem to be most interesting to add to a rubble mound breakwater at the moment.

2.) How do the relevant combinations of solutions perform in the numerical model if the outcome is compared to the current guidelines?
In this research, the accuracy of current guidelines is verified in a numerical model. The computed path, based on the adapted TAW equation, consists of a berm, a crest wall and a low-crested structure. It is found that in contrast to the overtopping equation proposed by the TAW (2002), the berm influences the overtopping rate. A berm reduces the overtopping rate by approximately 40%. The current theory proposes to increase the crest height (R_c) with the height of the crest wall. It is found that this approach is rather crude if a berm and crest wall are combined. Consequently, the reduction is overestimated. Furthermore, the low-crested structure as final adaptation underestimates the reduction in the overtopping rate.

Thus, comparing the OpenFOAM results with the TAW (2002) equations, shows that adaptation pathways that include a berm are relatively more attractive than when calculated based on the TAW (2002). Pathways including a crest wall could be slightly less attractive than TAW (2002) would suggest. The (limited) computations with a low-crested structure indicate that an adaptation pathway with a low-crested structure could be more relevant than expected based on TAW (2002).

8.2. Recommendations

Based on the performed research, the following recommendations for further research are advised. First, three recommendations about the adaptation criteria are given. Next, a recommendation for the applied data is presented. Furthermore, recommendations regarding the application of adaptation paths are given. Finally, two recommendations regarding the applicability in OpenFOAM are presented.

Adaptation criteria

- If one applies the adaptation pathways, it is advised to carefully investigate the local conditions and market prices to determine the economically most attractive path. Besides the applied costs in the performed research, there are many more possible costs that should be considered. Costs like labor, preparation of the site, maintenance and many more are not included in the current cost estimation.
- The cost-estimation in this thesis depends on the applied climate scenario. Currently, there are many different climate scenarios adopted by the IPCC, depending on the emission rates. One is advised to include the probability of occurrence of the different climate scenarios. By doing so, an expected cost-estimation can be made.
- Apart from the costs, one could also include aspects like the carbon footprint or constructability to determine the ”best” adaptation path. Just like a multi-criteria analysis, certain weighting can be assigned to the points of interest.

Data

- In the conducted research, no data was available and assumptions regarding the hydrodynamics were made. Therefore, it is advised to include physical data in the model and calibrate the structural parameters. This provides extra insight into how the overtopping performs when adaptations are included. If data is included, the effects of a low-crested structure and a foreshore can be investigated better as well. For these adaptations, the hydrodynamics at the toe of the structure were not configured.

Application

- The effect of each adaptation is based on one case study. As the pathways can differ for other adaptation dimensions or different wave conditions, it is advised to perform a sensitivity analysis. Within this sensitivity analysis, the dimensions of an adaptation can be optimized such that the effect is optimum (e.g. a berm above or below water level).
- The adaptation pathways derived in this thesis are based on the overtopping equation proposed by the TAW. According to the OpenFOAM results in this research, the berm influences the overtopping rate, in contrast to the predictions based on TAW (2002). Therefore, it is recommended to perform further research on how to implement a berm in the empirical equation. Although an adapted equation proposed by Krom (2012) is applied as well, no feedback about the accuracy of this equation can be given. The adapted TAW equation is validated for a small number of tests.
- The method proposed in the TAW to account for a crest wall seems to overestimate the reduction in wave overtopping compared to the results from OpenFOAM. If one includes a crest wall, it is advised to verify the accuracy of different literature (e.g. van Doorslaer et al., 2015) and apply this in the empirical equation.
- For the equation proposed by the TAW, it is advised to perform research on the influence of the roughness. The proposed influence factor (γ_f) is based on the average of different measurements. A smaller or larger value can make a big difference in the calculated overtopping rate.

- Based on the performed research, a realistic combination of the adaptation measures consists of a combination of a berm, a crest wall and a shallow foreshore. Therefore, it is advised to focus more on this combination of adaptation measures. It is necessary to improve the guidelines for combinations of these measures since the existing ones seem to be either incorrect (TAW, 2002) or require a better validation (Krom, 2012).

OpenFOAM

- Unlike the three other adaptation possibilities, the size of a crest wall is limited because of the wave force on this crest wall. For the berm and low-crested structure, the forces acting on it do not change and are already calculated in the stability assessment. The wave force acting on the wave wall can be calculated in OpenFOAM as well. This is elaborated in various studies (Jacobsen et al., 2018). If one wants to implement the crest wall as defined in this report, it is recommended to simulate the wave forces to make sure the wall has the right dimensions.
- When one applies the OpenFOAM model to determine adaptation pathways it is recommended to run simulations simultaneously to decrease the workload. If the adaptation paths are applied to a real project, data is also necessary to calibrate for a base case.

References

Battjes, J. A. (1974). *Computation of set-up, longshore currents, run-up and overtopping due to wind-generated waves* (Doctoral dissertation). TU Delft.

Berberović, E., van Hinsberg, N. P., Jakirlić, S., Roisman, I. V., & Tropea, C. (2009). Drop impact onto a liquid layer of finite thickness: Dynamics of the cavity evolution. *Physical Review E - Vol. 79*. https://doi.org/10.1103/physreve.79.036306

Briganti, R., van der Meer, J. W., M.Buccino, & Calabrese, M. (2003). Wave transmission behind low-crested structures. *ASCE 2003*. https://doi.org/10.1061/40733(147)48

Burcharth, H. . F., Kramer, M., Lamberti, A., & Zannutigh, B. (2006). Structural stability of detached low crested breakwaters. *Coastal Engineering 53*. https://doi.org/10.1016/j.coastaleng.2005.10.023

Centraal Bureau voor Statistiek (CBS). (2020). Jaarmutatie consumentenprijsindex.

CETMEF, C. C. (2007). *The Rock Manual. The use of rock in hydraulic engineering (2nd edition)*. CIRIA.

Chen, W., van Gent, M. R. A., Warmink, J. J., & Hulscher, S. J. M. H. (2020). The influence of a berm and roughness on the wave overtopping at dikes. *Coastal Engineering Volume 156*. https://doi.org/10.1016/j.coastaleng.2019.103613

d'Angremond, K., van der Meer, J. W., & de Jong, R. J. (1996). Wave transmission at low-crested structures. *ASCE - Chapter 187*. https://doi.org/10.1061/9780784402429.187

Deltares Report, Haasnoot, M., Bouwer, L., Diermanse, F., Kwadijk, J., van der Spek, A., Oude Essink, G., Delsman, J., Weiler, O., Mens, M., ter Maat, J., Huismans, Y., Sloff, K., & Mosselman, E. (2018). *Mogelijke gevolgen van versnelde zeespiegelstijging voor het Deltaprogramma* (tech. rep. 11205750-006-GEO-0002). Deltares.

Deltares Report, Zwanenburg, S., van der Werf, I., & van Gent, M. R. A. (2019). *Climate adaptive flood defences* (tech. rep.). Deltares.

den Bieman, J. P., van Gent, M. R. A., & van den Boogaard, H. F. P. (2020). Wave overtopping predictions using an advanced machine learning technique. *Coastal Engineering*. https://doi.org/ https://doi.org/10.1016/j.coastaleng.2020.103830

Ensig-Karup, A. P., Bingham, H. B., & Lindberg, O. (2009). An efficient flexible-order model for 3d nonlinear water waves. *Journal of Computational Physics 228 2100-2118*. https://doi.org/10.1016/j.jcp.2008.11.028

Eurotop (2007). wave overtopping of sea defences and related structures: Assessment manual. (2007).

Goda, Y. (2000). Random seas and design of maritime structures. *World Scientific Publishing Co. Pte. Ltd.* https://doi.org/10.1142/3587

Haasnoot, M., Kwakkel, J., Walker, W., & ter Maat, J. (2013). Dynamic adaptive policy pathways: A method for crafting robust decisions for adeeply uncertain world. *Global Environmental Change 23 (2013) 485–498*. https://doi.org/10.1016/j.gloenvcha.2012.12.006

Hauer, M., Op den Velde, W., Vrijling, J. K., & d'Angremond, K. (1995). *Comparison construction costs conventional rubblemound breakwaters/bermbreakwaters* (tech. rep.). Delft University of Technology.

Holthuijsen, L. H. (2007). *Waves in oceanic and coastal waters*. Cambridge University Press.

Hsu, T.-J., Sakakiyama, T., & Liu, P. L.-F. (2002). A numerical model for wave motions and turbulence flows in front of a composite breakwater. *Coastal Engineering 46, 25-50*. https://doi.org/10.1016/s0378-3839(02)00045-5

Hudson, R. Y. (1953). *Wave forces on breakwaters* (tech. rep.). ASCE. https://doi.org/10.1061/taceat.0006816

IPCC, R.K.Pachauri, & L.A.Meyer. (2014). *Climate Change 2014: Synthesis report* (tech. rep.). IPCC.

Jacobsen, N. G. (2017). *Waves2foam manual*.

Jacobsen, N. G., Fuhrman, D. R., & Fredsøe, J. (2012). A wave generation toolbox for the open-source cdf library openfoam. *International Journal For Numerical Methods in Fluids 70:1073-1088*.

Jacobsen, N. G., van Gent, M. R. A., Capel, A., & Borsboom, M. (2018). Numerical prediction of integrated wave loads on crest walls on top of rubble mound structures. *Coastal Engineering 142 (110-124)*. https://doi.org/10.1016/j.coastaleng.2018.10.004

Jacobsen, N. G., van Gent, M. R. A., & Wolters, G. (2015). Numerical analysis of the interaction of irregular waves with two dimensional permeable coastal structures. *Coastal Engineering 102*. https://doi.org/10.1016/j.coastaleng.2015.05.004

Jensen, B., Christensen, E. D., & Jacobsen, N. G. (2014). Simulation of extreme events of oblique wave interaction with porous breakwater structures. *Coastal Engineering 84*. https://doi.org/10.9753/icce.v34.structures.1

Jensen, B., Jacobsen, N. G., & Christensen, E. D. (2014). Investigations on the porous media equations and resistance coefficients for coastal structures. *Coastal Engineering 84*. https://doi.org/10.1016/j.coastaleng.2013.11.004

Kim, I.-C., & Suh, K.-D. (2018). Effect of sea level rise and offshore wave height change on nearshore waves and coastal structures. *Marine Science and Application 17:192-207*. https://doi.org/10.1007/s11804-018-0022-8

KNMI' 14 klimaatscenario' s voor nederland. (2015).

Krom, J. (2012). *Wave overtopping at rubble mound breakwaters with a non-reshaping berm* (Master's thesis). TU Delft.

Kwadijk, J. C. J., Haasnoot, M., Mulder, J. P. M., Hoogvliet, M. M. C., Jeuken, A. B. M., van der Krogt, R. A. A., van Oostrom, N. G. C., Schelfhout, H. A., van Velzen, E. H., van Waveren, H., & de Wit, M. J. M. (2010). Using adaptation tipping points to prepare for climate change and sea level rise: A case study in the netherlands. *WileyInterdisciplinary Reviews: Climate Change 1, 729–740*. https://doi.org/10.1002/wcc.64

Lioutas, A. C. (2010). *Experimental research on spatial distribution of overtopping* (Master's thesis). TU Delft.

Lioutas, A. C., Smith, G. M., & Verhagen, H.-J. (2012). Spatial distribution of overtopping. *Coastal Engineering No 33*. https://doi.org/10.9753/icce.v33.structures.63

Liu, P. L.-F., Lin, P., Chang, K.-A., & Sakakiyama, T. (1999). Numerical modeling of wave interaction with porous structures. *Journal of Waterway, Port, Coastal and Ocean Engineering - Vol. 125 No. 6*. https://doi.org/10.1061/(asce)0733-950x(1999)125:6(322)

Losada, I. J., Lara, J. L., & del Jesus, M. (2016). Modeling the interaction of water waves with porous coastal structures. *Journal of Waterway, Port, Coastal and Ocean Engineering 142(6)*. https://doi.org/10.1061/(asce)ww.1943-5460.0000361

Mansard, E. P. D., & Funke, E. R. (1980). The measurement of incident and reflected spectra using a least squares method. *Coastal Engineering 1980*. https://doi.org/10.1061/9780872622647.008

Molines, J., & Medina, J. R. (2015). Calibration of overtopping roughness factors for concrete armor units in non-breaking conditions using the clash database. *Coastal Engineering 96 62-70*. https://doi.org/10.1016/j.coastaleng.2014.11.008

NEN-EN 13383-1 Waterbouwsteen - deel 1: Specificatie. (2002). CEN.

Regeling veiligheid primaire waterkeringen 2017. (2017). Minister van Infrastructuur en Milieu.

Rusche, H. (2002). *Computational fluid dynamics of dispersed two-phase flows at high phase fractions* (Doctoral dissertation). Imperial College of Science, Technology and Medicine.

Steendam, G. J., van der Meer, J. W., Verhaeghe, H., Besley, P., Franco, L., & van Gent, M. R. A. (2005). The international database on wave overtopping. *Coastal Engineering 2004, pp. 4301-4314*. https://doi.org/10.1142/9789812701916_0347

TAW. (2002). *Technical report wave run-up and wave overtopping at dikes* (tech. rep.). Technical Advisory Committee for Flood Defence in the Netherlands(TAW).

Tutuarima, W., & d'Angremond, K. (1998). *Cost comparison of breakwater types* (tech. rep.). Delft University of Technology. https://doi.org/10.1061/9780784404119.145

van den Bos, J. P., & Verhagen, H. J. (2018). *Breakwater design lecture notes CIE5308*.

van der Meer, J. W. (1988). *Rock slopes and gravel beaches under wave attack* (Doctoral dissertation). Technische Universiteit Delft.

van der Meer, J. W. (1995). *Conceptual design of rubble mound breakwaters* (tech. rep.). https://doi.org/10.1142/9789812797582_0005

van Doorslaer, K., de Rouck, J., Audenaert, S., & Duquet, V. (2015). Crest modification to reduce wave overtopping of non-breaking waves over a smooth dike slope. *Coastal Engineering 101 69-88*. https://doi.org/10.1016/j.coastaleng.2015.02.004

van Gent, M. R. A. (1995). *Wave interaction with permeable coastal structures* (Doctoral dissertation). Delft University of Technology.

van Gent, M. R. A. Climate adaption of coastal structures. In: *International short course/conference of applied coastal research*. 2019.

van Gent, M. R. A., Kuiper, C., & Smale, A. Stability of rock slope with shallow foreshores. In: *Coastal structures 2003*. 2003. https://doi.org/10.1061/40733(147)9.

van Gent, M. R. A., van den Boogaard, H. F. P., Pozueta, B., & Medina, J. R. (2007). Neural network modelling of wave overtopping at coastal structures. *Coastal Engineering 54 (586-593)*. https://doi.org/10.1016/j.coastaleng.2006.12.001

van Rooijen, D. (2005). *The northern sea defence of maasvlakte 2* (Master's thesis). Delft University of Technology.

Walker, W. E., Rahman, S. A., & Cave, J. (2001). Adaptive policies, policy analysis and policy-making. *European Journal of Operational Research 128: 282-289*. https://doi.org/10.1016/s0377-2217(00)00071-0

Williams, H. E., Briganti, R., & Pullen, T. (2014). The role of offshore boundary conditions in the uncertainty of numerical prediction of wave overtopping using non-linear shallow water equations. *Coastal Engineering 89, 30-44*. https://doi.org/10.1016/j.coastaleng.2014.03.003

Zelt, J. A., & Skjelbreia, J. E. (1992). Estimating incident and reflected wave field using an arbitrary number of wave gauges. *Coastal Engineering 1992 No. 23*. https://doi.org/10.1061/9780872629332.058

Zijlema, M. (2015). *Computational modelling of flow and transport, lecture notes cie4340*.

Appendices

A

Individual Adaptation Pathways

In this Appendix the adaptive pathway generated in Chapter 4 is split into four individual pathways to give a more clear view on the solutions. Subsequently, the costs per solution are elaborated based on the defined costs per adaptation measure. The costs are defined in Table A.1. In the next sections

Material	Price indication	Unit
Rock	50	€/T
Sand	6	€/m^3
Concrete	300	€/m^3

Table A.1: Production and construction costs other materials

the different pathways and costs are elaborated. For the costs, the sequences are defined with the first letter representing the corresponding adaptation measure. Therefore: Foreshore (F), Crest wall (C), Berm (B) and Low-crested structure (L). Also, the reduced dimensions for the last chain in the sequence are defined to lower the costs if the adaptation measure is much safer than 50 l/s/m.

A.1. TAW: Crest wall

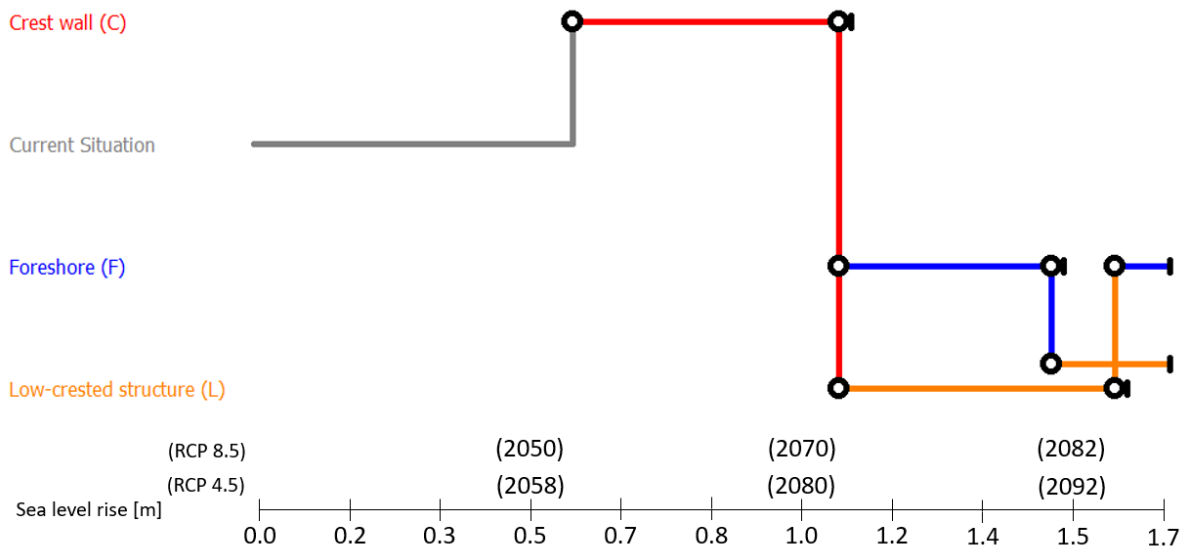

Figure A.1: Adaptive pathway TAW: Crest wall

Sequence	Costs	Unit	Reduced dimension	Unit
C-F-L	42 300	€/m	$B_{lc} = 5, R_{lc} = -1.8$	m
C-L-F	43 800	€/m	$h_f = 9.8$	m

Table A.2: Production and construction costs TAW: Crest wall

A.2. TAW: Increased foreshore

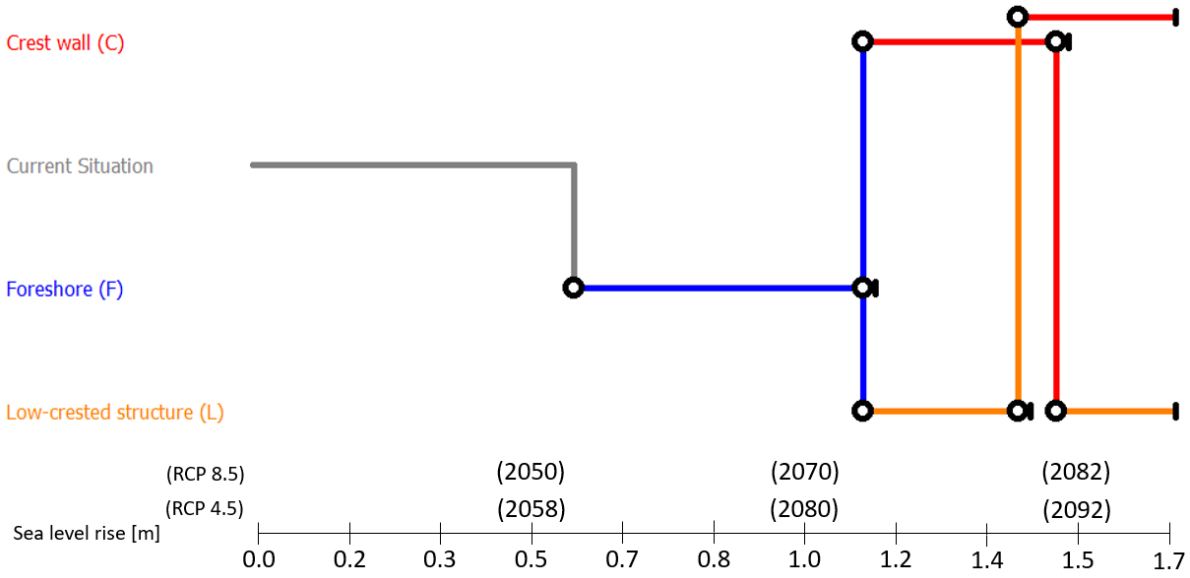

Figure A.2: Adaptive pathway TAW: Increase foreshore

Sequence	Costs	Unit	Reduced dimension	Unit
F-C-L	43 200	€/m	$B_{lc} = 5, R_{lc} = -1.8$	m
F-L	44 100	€/m	$h_c = 0.36$	m

Table A.3: Production and construction costs TAW: Increased foreshore

A.3. TAW: Low-crested structure

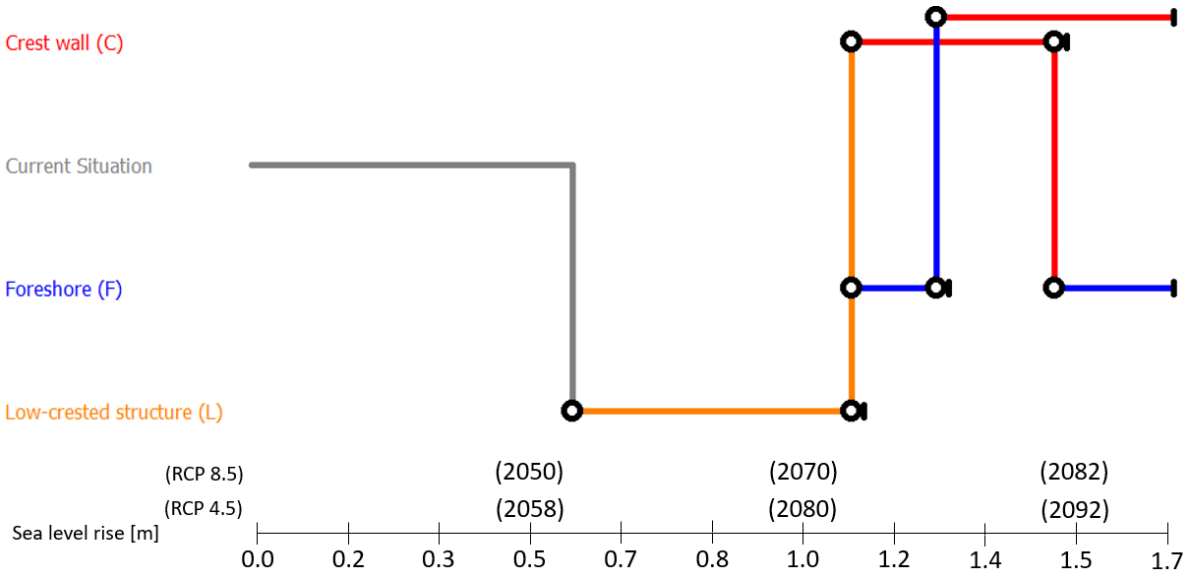

Figure A.3: Adaptive pathway TAW: Low-crested structure

Sequence	Costs	Unit	Reduced dimension	Unit
L-C-F	42 350	€/m	$h_f = 10.4$	m
L-F-C	42 000	€/m	$h_c = 0.62$	m

Table A.4: Production and construction costs TAW: Low-crested structure

A.4. Adapted TAW: Berm

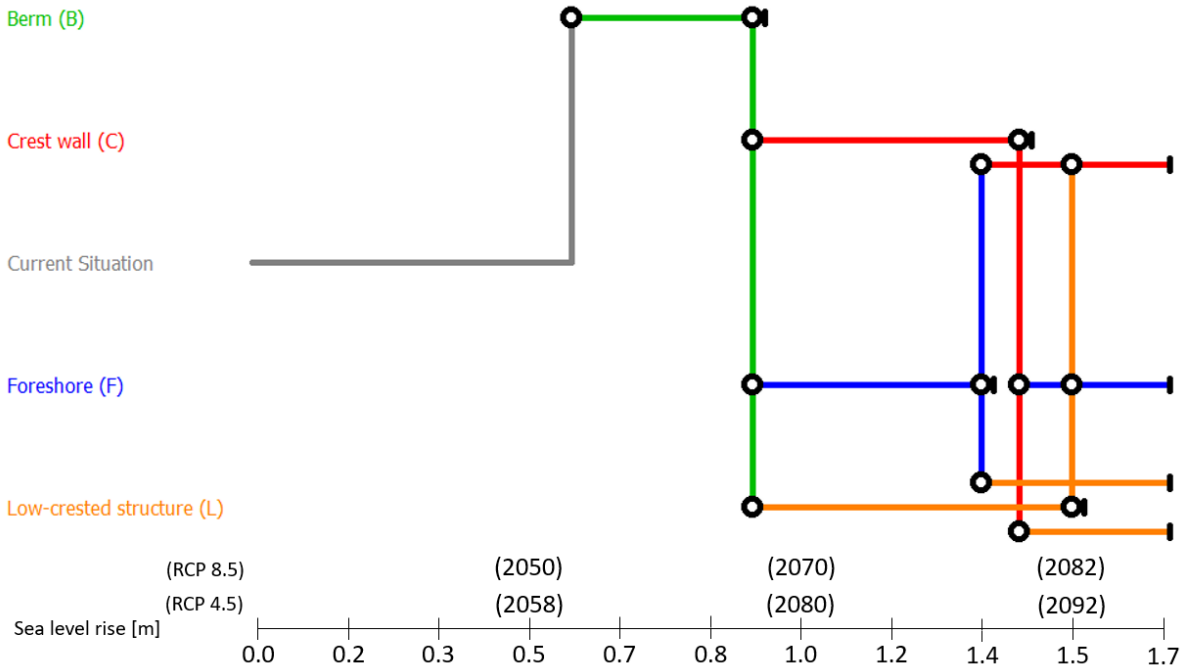

Figure A.4: Adaptive pathway adapted TAW: Berm

Sequence	Costs	Unit	Reduced dimension	Unit
B-C-F	19 900	€/m	$h_f = 9.9$	m
B-C-L	33 350	€/m	$R_{lc} = -2.5$	m
B-F-C	19 950	€/m	$h_c = 0.45$	m
B-F-L	47 200	€/m	$R_{lc} = -1.35$	m
B-L-C	37 300	€/m	$h_c = 0.23$	m
B-L-F	48 700	€/m	$h_f = 10.45$	m

Table A.5: Production and construction costs adapted TAW: Berm

A.5. Adapted TAW: Crest wall

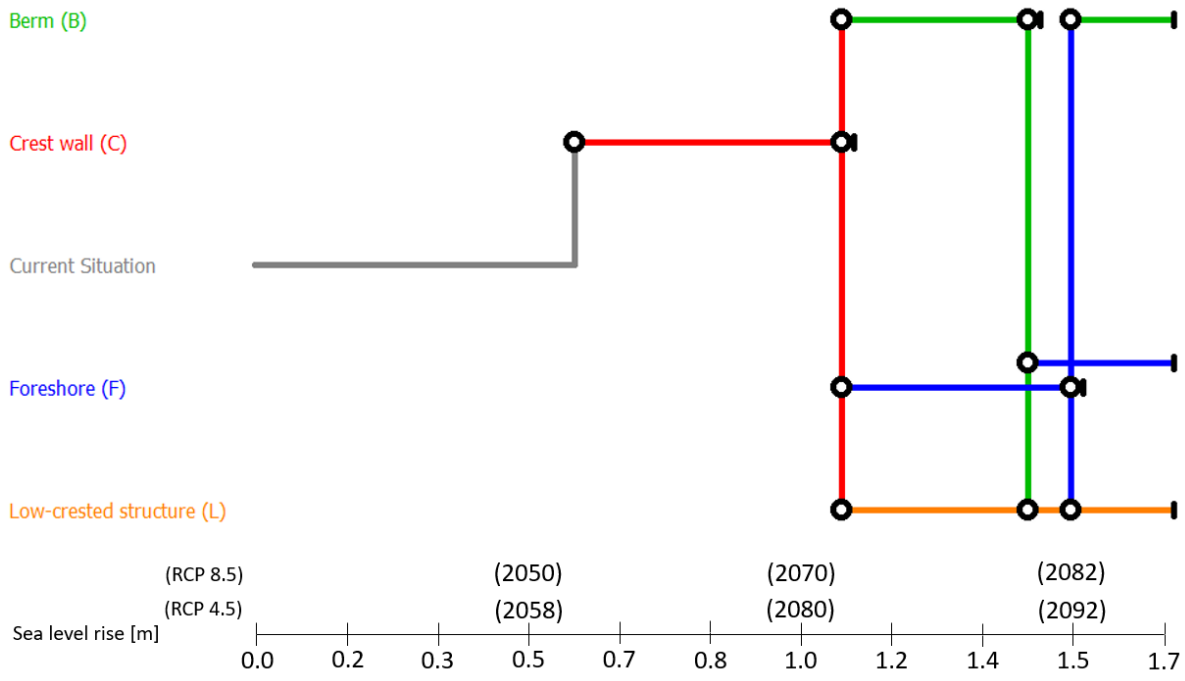

Figure A.5: Adaptive pathway adapted TAW: Crest wall

Sequence	Costs	Unit	Reduced dimension	Unit
C-B-F	19 600	€/m	$h_f = 9.8$	m
C-B-L	32 900	€/m	$R_{lc} = -2.6$	m
C-F-B	17 400	€/m	$B_{berm} = 3$	m
C-F-L	40 300	€/m	$R_{lc} = -2.3$	m
C-L	31 150	€/m	$R_{lc} = -1.2$	m

Table A.6: Production and construction costs adapted TAW: Crest wall

A.6. Adapted TAW: Increased foreshore

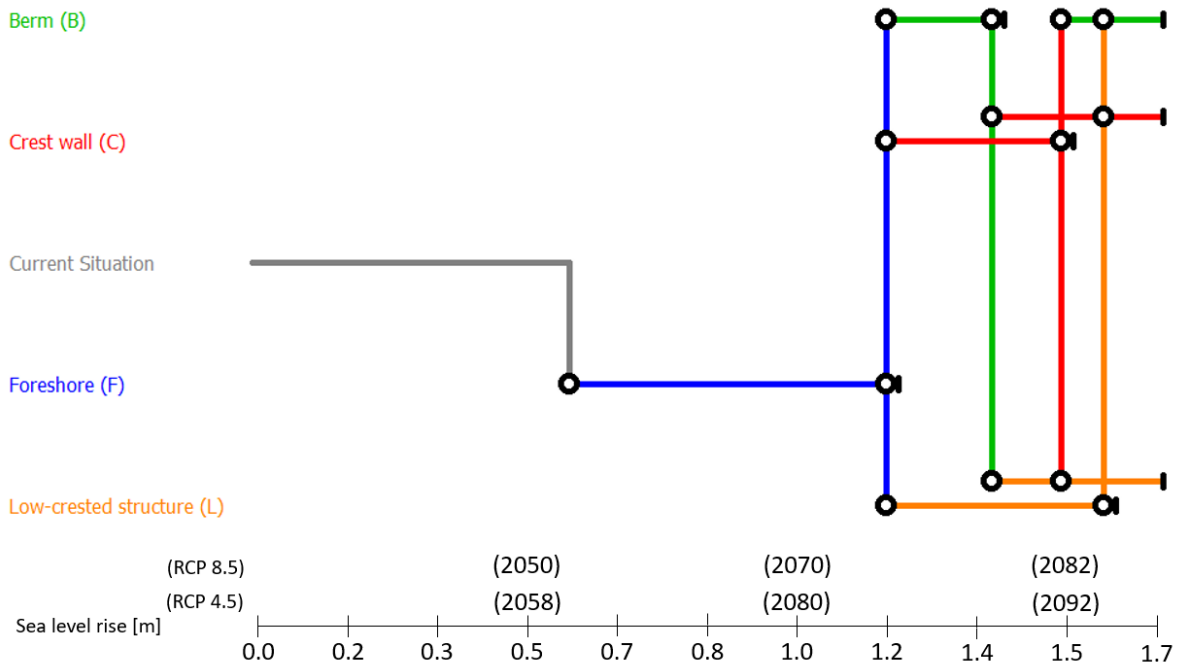

Figure A.6: Adaptive pathway adapted TAW: Increased foreshore

Sequence	Costs	Unit	Reduced dimension	Unit
F-B-C	19 900	€/m	$h_c = 0.44$	m
F-B-L	47 500	€/m	$R_{lc} = -1.5$	m
F-C-B	18 150	€/m	$B_{berm} = 3.5$	m
F-C-L	40 200	€/m	$B_{lc} = 3.54, R_{lc} = -2$	m
F-L-B	45 100	€/m	$B_{berm} = 2$	m
F-L-C	44 200	€/m	$h_c = 0.15$	m

Table A.7: Production and construction costs adapted TAW: Increased foreshore

A.7. Adapted TAW: Low-crested structure

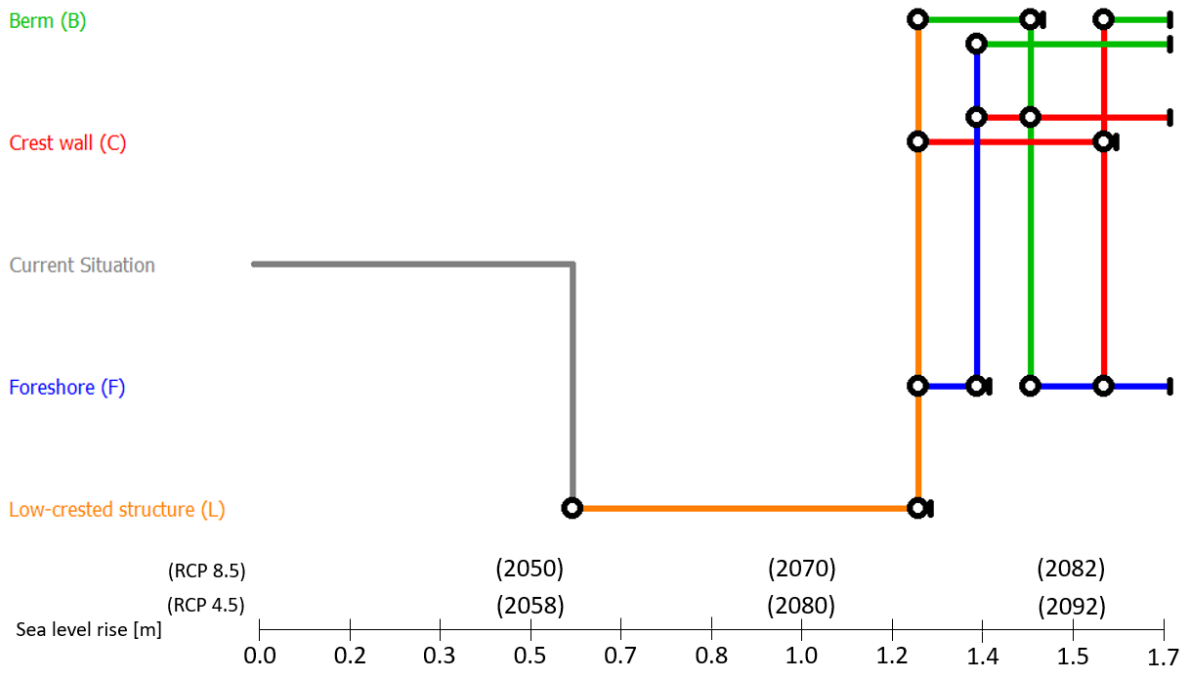

Figure A.7: Adaptive pathway adapted TAW: Low-crested structure

Sequence	Costs	Unit	Reduced dimension	Unit
L-B-C	35 900	€/m	$h_c = 0.36$	m
L-B-F	47 100	€/m	$h_f = 10.7$	m
L-C-B	32 350	€/m	$B_{berm} = 2,\ d_b = 0$	m
L-C-F	41 900	€/m	-	m
L-F-B	57 500	€/m	$B_{berm} = 14$	m
L-F-C	41 900	€/m	$h_c = 1.4$	m

Table A.8: Production and construction costs adapted TAW: Low-crested structure

B

OpenFOAM results case study 2

This Appendix elaborates on the OpenFOAM results for case study 2. This case study is derived based on the adapted TAW equation proposed by Krom (2012). First the computed path is evaluated. Subsequently, the effect of an adaptation is evaluated in more detail.

B.1. Computed path

As discussed in Chapter 6, the most relevant solution consists of a berm, a crest wall and a low-crested structure.

Adaptation 1: Berm

Adaptation	SLR [m]	h [m]	$R_{c,2}$ [m]	$q_{ATAW,2}$[l/s/m]	$q_{reduction}$ [%]	$q_{OF,2}$ [l/s/m]	$q_{reduction}$ [%]	$q_{OF,2}$ / $q_{ATAW,2}$	$\Delta q_{OF,2}$ / $\Delta q_{ATAW,2}$
-	0.60	13.10	2.25	51.07	-	148.22	-	2.90	-
	0.94	13.44	1.91	91.81	-	231.82	-	2.52	-
+ Berm	0.60	13.10	2.25	24.94	-51.17	101.74	-31.36	4.08	1.78
	0.94	13.44	1.91	50.94	-44.52	182.37	-21.33	3.58	1.21

Table B.1: Influence of a berm compared to the Adapted TAW overtopping equations.

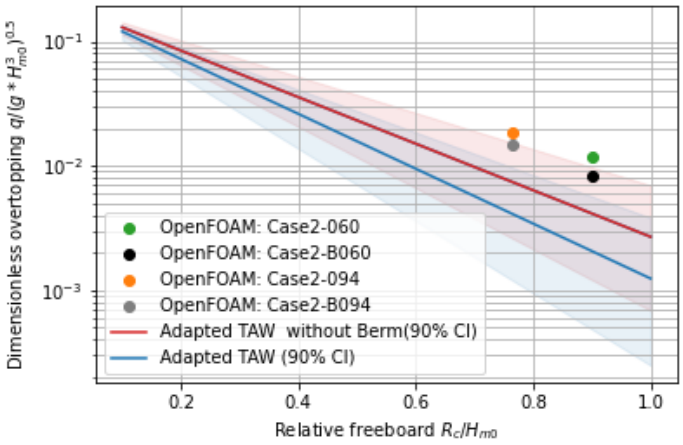

Figure B.1: Comparison of the dimensionless overtopping in OpenFOAM to the adapted TAW overtopping equation

Adaptation 2: Crest wall

Adaptation	SLR [m]	h [m]	$R_{c,2}$ [m]	$q_{ATAW,2}$[l/s/m]	$q_{reduction}$ [%]	$q_{OF,2}$ [l/s/m]	$q_{reduction}$ [%]	$q_{OF,2}$ / $q_{ATAW,2}$	$\Delta q_{OF,2}$ / $\Delta q_{ATAW,2}$
Berm	0.94	13.44	1.91	50.94	-	182.37	-	3.58	-
	1.44	13.94	1.41	139.59	-	406.86	-	2.91	-
+ Crest wall	0.94	13.44	2.41	18.43	-63.82	111.09	-39.09	6.03	2.19
	1.44	13.94	1.91	50.34	-63.94	235.76	-42.05	4.68	1.92

Table B.2: Influence of a crest wall compared to the Adapted TAW overtopping equations

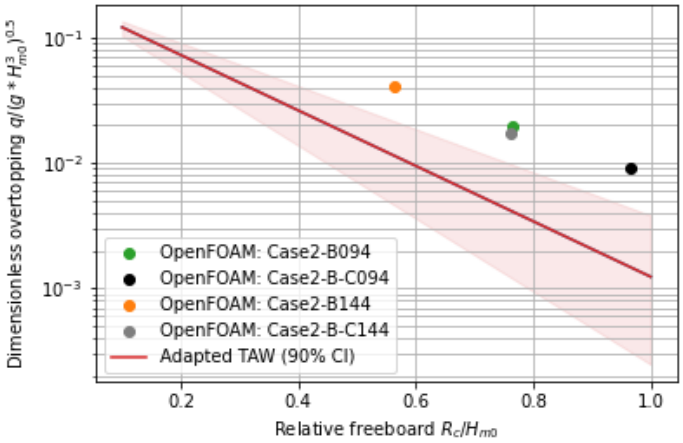

Figure B.2: Comparison of the dimensionless overtopping in OpenFOAM to the adapted TAW overtopping equation

Adaptation 3: Low-crested structure

Adaptation	SLR [m]	h [m]	$R_{c,2}$ [m]	$q_{ATAW,2}$[l/s/m]	$q_{reduction}$ [%]	$q_{OF,2}$ [l/s/m]	$q_{reduction}$ [%]	$q_{OF,2}$ / $q_{ATAW,2}$	$\Delta q_{OF,2}$ / $\Delta q_{ATAW,2}$
Berm +	1.44	13.94	1.91	50.34	-	235.76	-	4.68	-
Crest wall	1.70	14.2	1.65	84.66	-	342.33	-	4.04	-
+ Low-crested	1.44	13.94	1.91	15.63	-68.95	16.32	-93.08	1.04	6.32
Structure	1.70	14.2	1.65	48.90	-42.24	35.59	-89.60	0.73	8.58

Table B.3: Influence of a Low-crested structure compared to the Adapted TAW overtopping equations

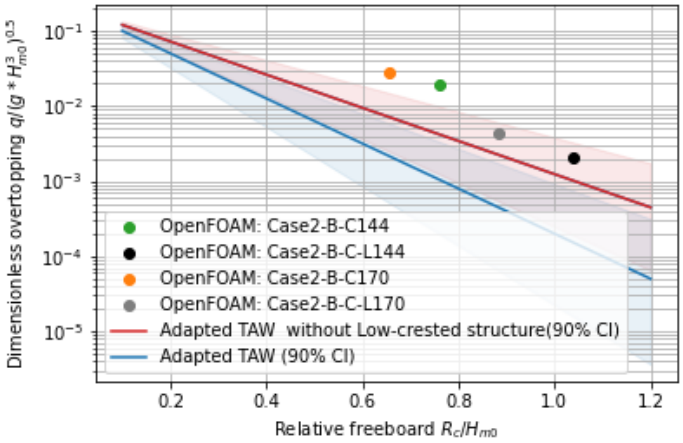

Figure B.3: Comparison of the dimensionless overtopping in OpenFOAM with the adapted TAW overtopping equation

B.2. Effect of adaptations

Next, the overtopping rate at the start of an adaptation is set equal in both the formula and OpenFOAM. Therefore, the crest height in the theory has been lowered.

Adaptation 1: Berm

Adaptation	SLR [m]	h [m]	$R_{c,ATAW}$ [m]	q_{ATAW} [l/s/m]	$q_{reduction}$ [%]	$q_{OF,2}$ [l/s/m]	$q_{reduction}$ [%]	$q_{OF,2}$ / q_{ATAW}	Δ $q_{OF,2}$ / Δ q_{ATAW}
-	0.60	13.10	1.63	148.82	-	148.22	-	1.00	-
	0.94	13.44	1.29	267.53	-	231.82	-	0.87	-
+ Berm	0.60	13.10	1.63	85.57	-42.50	101.74	-31.36	1.19	0.73
	0.94	13.44	1.29	172.69	-35.45	182.37	-21.33	1.06	0.52

Table B.4: Influence of a berm compared to the Adapted TAW overtopping equations with equal starting point ($q \approx 148$ l/s/m)

Adaptation 2: Crest wall

Adaptation	SLR [m]	h [m]	$R_{c,ATAW}$ [m]	q_{ATAW} [l/s/m]	$q_{reduction}$ [%]	$q_{OF,2}$ [l/s/m]	$q_{reduction}$ [%]	$q_{OF,2}$ / q_{ATAW}	Δ $q_{OF,2}$ / Δ q_{ATAW}
Berm	0.94	13.44	1.26	182.24	-	182.37	-	1.00	-
	1.44	13.94	0.76	505.61	-	406.86	-	0.80	-
+ Crest wall	0.94	13.44	1.76	64.87	-64.40	111.09	-39.09	1.71	0.61
	1.44	13.94	1.26	178.51	-64.69	235.76	-42.05	1.32	0.52

Table B.5: Influence of a crest wall compared to the Adapted TAW overtopping equations with equal starting point ($q \approx 182$ l/s/m)

Adaptation 3: Low-crested structure

Adaptation	SLR [m]	h [m]	$R_{c,ATAW}$ [m]	q_{ATAW} [l/s/m]	$q_{reduction}$ [%]	$q_{OF,2}$ [l/s/m]	$q_{reduction}$ [%]	$q_{OF,2}$ / q_{ATAW}	Δ $q_{OF,2}$ / Δ q_{ATAW}
Berm +	1.44	13.94	1.12	235.11	-	235.76	-	1.00	-
Crest wall	1.70	14.2	0.86	401.48	-	342.33	-	0.86	-
+ Low-crested	1.44	13.94	1.12	100.69	-57.17	16.32	-93.08	0.16	1.63
Structure	1.70	14.2	0.86	277.06	-30.99	35.59	-89.60	0.13	2.47

Table B.6: Influence of a low-crested structure compared to the Adapted TAW overtopping equations with equal starting point ($q \approx 235$ l/s/m)